NURA: a curated dataset of nuclear receptor modulators

Cecile Valsecchi[1], Francesca Grisoni[2]*, Stefano Motta[1], Laura Bonati[1], Davide Ballabio[1]

[1]Department of Earth and Environmental Sciences, University of Milano-Bicocca, P.za della Scienza 1-20126, Milano, Italy

[2]ETH Zurich, Department of Chemistry and Applied Biosciences, RETHINK, Vladimir-Prelog-Weg 4, 8049 Zurich, Switzerland

*corresponding author: francesca.grisoni@pharma.ethz.ch, francesca.grisoni@unimib.it

Abstract

Nuclear receptors (NRs) are key regulators of human health and constitute a relevant target for medicinal chemistry applications as well as for toxicological risk assessment. Several open databases dedicated to small molecules that modulate NRs exist; however, depending on their final aim (*i.e.,* adverse effect assessment or drug design), these databases contain a different amount and type of annotated molecules, along with a different distribution of experimental bioactivity values. Stemming from these considerations, in this work we aim to provide a unified dataset, NURA (NUclear Receptor Activity dataset), collecting curated information on small molecules that modulate NRs, to be intended for both pharmacological and toxicological applications. NURA contains bioactivity annotations for 15,206 molecules and 11 selected NRs, and it was obtained by integrating and curating data from toxicological and pharmacological databases (*i.e.,* Tox21, ChEMBL, NR-DBIND and BindingDB). Our results show that NURA dataset is a useful tool to bridge the gap between toxicology- and medicinal-chemistry-related databases, as it is enriched in terms of number of molecules, structural diversity and covered atomic scaffolds compared to the single sources. To the best of our knowledge, NURA dataset is the most exhaustive collection of small molecules annotated for their modulation of the chosen nuclear receptors. NURA dataset is intended to support decision-making in pharmacology and toxicology, as well as to contribute to data-driven applications, such as machine learning. The dataset and the data curation pipeline can be downloaded free of charge at the following URL: https://michem.unimib.it/download/data/nura/.

Keywords: Nuclear receptors, medicinal chemistry, toxicology, in vitro, in silico, NURA

1. Introduction

Nuclear receptors (NRs) are a superfamily of transcription factors that control cell growth, development, homeostasis and metabolism (Francis et al. 2003; Olefsky 2001; Huang et al. 2010; Pascussi et al. 2008; Rouiller-Fabre et al. 2015; Swedenborg et al. 2009). Due to their biological relevance, NRs have been the target of numerous computational projects for toxicological (Khandelwal et al., 2008; Kleinstreuer et al., 2017; Mansouri et al., 2020, 2016) and medicinal chemistry applications (Grisoni et al., 2018; Heitel et al., 2019; Merk et al., 2018; Motta et al., 2018; Niu et al., 2016; Park et al., 2010; Rupp et al., 2010). These computational projects are often based on machine learning approaches, which are "data-hungry" and require as many training data as possible to reach satisfying levels of predictivity and generalization ability (Halevy et al., 2009). Moreover, it is in general accepted that curated data constitute a precious resource for quantitative structure-activity relationship modeling and the corresponding decision-making in medicinal chemistry, toxicology and related fields (Cronin and Schultz, 2003; Griffen et al., 2018; Tropsha, 2010; Vangala et al., 2012). In this framework, it becomes fundamental to create datasets comprising as many experimental data as possible. Additionally, since public and commercial databases can contain up to 10% errors in structural and/or experimental annotations (Fourches et al., 2010; Olah et al., 2007; Young et al., 2008), data curation becomes a fundamental step to remove potential inconsistencies and ensure reliable molecular modeling research (Fourches et al., 2010; Olah et al., 2007; Young et al., 2008).

Several freely accessible databases containing information on nuclear receptor modulation for small molecules exist (Gaulton et al. 2017; Réau et al. 2018; Gilson et al. 2016; Tice et al. 2013; Nanduri et al. 2015). However, the amount and type of annotated chemical structures (and respective chemical scaffolds), and the proportion of biologically active or inactive molecules depend on the database purpose (Wassermann and Bajorath, 2011). In fact, depending on the database aims, each of the available repositories might contain different sets of compounds and

investigated targets, and may exhibit a different proportion of modulators and non-modulators (Wassermann and Bajorath, 2011). For instance, Tox21 (Toxicology in the 21st Century (NIH)) database – aimed to investigate the adverse effects of man-made chemicals – shows a predominance of inactive compounds (more than 80% considering nuclear receptors, Tice et al., 2013). On the contrary, repositories with a medicinal chemistry focus, *e.g.*, ChEMBL (Gaulton et al., 2017), NR-DBIND (Réau et al., 2018) and BindingDB (Gilson et al., 2016), mainly contain information on bioactive compounds. For example, in NR-DBIND – a database dedicated to NRs – 75% of compounds (computed as the average per target) have pK_i or pIC_{50} larger than 7 (Réau et al., 2018).

The curation of a comprehensive dataset on nuclear receptors can overcome the issue of "data fragmentation" among sources with different aims (*e.g.*, medicinal chemistry and toxicology) and thus be highly beneficial to the scientific community, in terms of proportion between annotated active and inactive molecules as well as covered chemotypes and scaffolds.

In this work, we describe the collection and curation of *in vitro* public bioactivity data (agonism, antagonism and binding), which resulted in a dataset of 15,206 molecules for 11 selected nuclear receptors (androgen receptor, estrogen receptor, progesterone receptor, glucocorticoid receptor, peroxisome proliferator-activated receptor, pregnane X receptor, retinoid X receptor, farnesoid X receptor. Data were collected and curated from four different open databases, namely: ChEMBL25 (Gaulton et al. 2017), BindingDB (Gilson et al., 2016), NR-DBIND (Réau et al., 2018), and Tox21 (NIH).

The resulting dataset, NURA (NUclear Receptor Activity dataset) can serve as a basis to develop machine learning methods for toxicological and/or medicinal chemistry applications, *e.g.,* to predict the modulation of a panel of receptors or the selectivity among the selected NRs (Ramsundar et al., 2015; Sadawi et al., 2019), and is intended to provide a support to decision-making in pharmacology and adverse effect assessment.

In what follows, after describing the chosen nuclear receptors and data sources, we introduce the data curation and analysis pipeline. Our post-hoc analysis on the curated NURA dataset highlights the benefits of data integration from multiple sources, in terms of expansion of the covered chemical and property space. NURA dataset and the data curation pipeline are accessible free of charge at the following URL: https://michem.unimib.it/download/data/nura/.

2. Materials and methods

2.1. Data collection and curation

2.1.1. Target selection

We collected and curated *in vitro* bioactivity data on eight nuclear receptors, selected based on their biological relevance and data availability in public databases:

- Androgen receptor (AR), which plays a key role in many sexual, somatic and behavioral functions critical to lifelong health, as well as in the development of several diseases such as prostate cancer and cardiovascular diseases (Davey and Grossmann, 2016).

- Estrogen receptor (ER), which is the main mediator of estrogen action in development and reproductive system as well as in brain function, bone maintenance, cardiovascular system and adipose tissue (Mueller and Korach, 2001). Several diseases are associated with this receptor, including osteoporosis, obesity and Alzheimer disease (Mueller and Korach, 2001).

- Progesterone receptor (PR), which mainly affects the female sexual development end pregnancy and it is a promising target for the treatment of breast cancer, cardiovascular disease, and central nervous system disorders (Huang et al., 2010; Schug et al., 2011).

- Glucocorticoid receptor (GR), which plays multiple roles in human physiology, *e.g.,* immune mediation, inflammation, glucose balance, the stress response, fat distribution, and normal growth and is involved in the development of several disorders, such as diabetes mellitus, hypertension and cardiovascular diseases (Huang et al., 2010).

- Peroxisome proliferator-activated receptor, which controls lipid homeostasis with isoform-specific lipid regulation, insulin action and cell proliferation and is linked to obesity, dyslipidemia and atherosclerosis risk (Berger and Moller, 2001; Schug et al., 2011).

- Pregnane X receptor (PXR), which regulates the detoxification and clearance of some xenobiotic substances, exerting a protective function (Ekins et al., 2009; Francis et al., 2003). PXR has been associated to cancer, and to inflammatory and metabolic diseases (Banerjee et al., 2015).

- Retinoid X receptor (RXR), which regulates metabolic homeostasis and forms heterodimers with numerous other nuclear receptors. Drugs that target RXR heterodimers are used to treat cancer, dermatologic diseases, endocrine disorders, and the metabolic syndrome (Penvose et al., 2019; Shulman and Mangelsdorf, 2005).

- Farnesoid X receptor (FXR), or bile-acid activated transcription factor, which contributes to the liver physiology and can be targeted to treat metabolic and hepatic disorders (Francis et al., 2003).

2.1.2. Data collection

In this study we considered four different sources for data collection, namely (Table 1):

- ChEMBL25 (Gaulton et al., 2017), which is a large-scale, open database containing drug-like bioactive molecules with *in vitro* bioactivity annotations. For the chosen NRs, we filtered bioactivity data referred to single proteins (Table 1) according to the BioAssay Ontology (BAO) signature (Visser et al., 2011) BAO_0000190, BAO_0000188, BAO_0000192, BAO_0000034, BAO_0000186, BAO_0000199, BAO_0002583 and BAO_0002809. As an additional filter, we used ChEMBL25 confidence score – which is based on the assessed record quality and ranges from 0 (non-curated data entries), to 9 (high-quality direct single-protein) – to retain compounds with confidence score greater than 8. Records annotated as "potential transcription error" were removed (seven

records). Records with exhaustive assay type information were retained (see supporting material for the list of considered assays).

- BindingDB (Gilson et al., 2016), which is a public database of measured binding affinities focusing on small, drug-like ligands; bioactivity data referred to nuclear receptors.

- NR-DBIND (Nuclear Receptors DataBase Including Negative Data) (Réau et al., 2018), which is a repository dedicated to drug-like nuclear receptor ligands. All the data referred to the selected NRs were collected.

- Tox21 (NIH). The Tox21 (Toxicology in the 21st Century) program (Huang, 2016.; Huang et al., 2015; Kleinstreuer et al., 2017; NIH) involves several U.S. national institutes and adopts high-throughput screening (HTS) *in vitro* techniques to test large numbers of chemicals that could be toxic *in vivo*. For this purpose, Tox21 established a library of 10K chemicals - composed of environmental chemicals and approved drugs - which has been screened against different cell-based assays. Some of these assays (Table 1) focused on nuclear receptor modulation were considered in our study. In particular, we collected the NR-related data of Tox21 from PubChem BioAssay Repository. (Kim et al., 2019). Molecules labelled as antagonists in agonism assays (or as agonists in antagonism assays) were removed. Records with inconclusive readouts were removed.

For ER and PPAR, which had more than 1000 isoform-specific annotations, isoform-related bioactivity data were collected separately (*i.e*, alpha and beta isoforms for ER, and alpha, delta and gamma for PPAR), obtaining a total of 11 macromolecular targets (AR, ERα, ERβ, PR, GR, PPARα, PPARδ, PPARγ, PXR, RXR, FXR).

For the selected targets, we collected *in vitro* data referred to binding, agonistic and antagonistic effects (hereafter referred to as "endpoints"), obtaining a total of 33 endpoints. Database entries corresponding to the following two types of experimental readouts were retained: (i) half maximal concentration on the dose-response curve for inhibition or effect (IC_{50} and EC_{50}, respectively) and (ii) the dissociation and inhibition constants (K_d and K_i), which

describe the affinity between a ligand and a protein (with K_d measuring the equilibrium between the ligand-protein complex and the dissociated components, while K_i being specific for inhibitors). For Tox21, the activity concentration at half-maximal response (AC_{50}) as determined by a panel of *in vitro* assays (Tice et al. 2013) was considered.

Table 1 Summary of the considered data sources. Receptor acronym, number of *in vitro* records, PubChem Assay ID and ChEMBL ID are reported. For targets having more than 1000 isoform-specific records (i.e., ER and PPAR), the experimental data referred to each isoform was collected separately.

Target	No. bioactivity records				PubChem Assay ID	ChEMBL ID
	Tox21	ChEMBL	BindingDB	NR-DBIND		
AR	10486	8095	4591	1,513	743053, 743063, 743054	CHEMBL1871
ERα	10486	11148	1308	2,054	743053, 743078, 743091	CHEMBL206
ERβ	10486	7749	9151	1,826	1259394, 1259396	CHEMBL242
FXR	9305	3769	2552	136	743239, 743240	CHEMBL2047
GR	10486	11934	217	1,935	720719, 720725	CHEMBL2034
PPARα	0	7108	3929	1,018	n.a.	CHEMBL239
PPARδ	10486	4941	2118	525	743227, 743226	CHEMBL3979
PPARγ	10486	11362	2118	1,454	743140, 743199	CHEMBL235
PXR	9667	1964	659	1	1347033	CHEMBL3401
PR	9667	5239	3324	1,403	1347036, 1347031	CHEMBL208
RXR	9667	3564	5406	340	1159531	CHEMBL2061, CHEMBL1870, CHEMBL2004

2.1.3. Data aggregation and curation

Data from different sources were collected and arranged in a record with the following format : (i) ligand molecular structure (expressed as simplified Molecular Input Line Entry System [SMILES] strings (Weininger, 1988)), (ii) experimental readout (including the unit of measure and the experimental response value), (iii) effect type, if available (agonism, antagonism, binding), (iv) target organism and (v) target nuclear receptor (among the 11 selected). On each of these records, the data curation procedure was carried out with the following sequential steps:

1. Only records referred to *Homo sapiens* were retained;

2. Records with the experimental readout expressed as EC_{50}, IC_{50}, AC_{50}, K_i or K_d were retained.

3. Each readout was converted into nanomolar concentration units (nM).

4. All records referring to disconnected structures, salts, mixtures, inorganic compounds and compounds containing elements different from H, C, N, O, F, Br, I, Cl, P or S were removed. All the structures were converted into canonical SMILES strings (O'Boyle, 2012).

5. Each record was assigned a discrete bioactivity label, according to its experimental readout, as follows: (i) "active", for experimental bioactivities equal to or lower than 10,000 nM; (ii) "weakly active", for activity values between 10,000 and 100,000 nM; (iii) "inactive", for entries with activity values exceeding 100,000 nM. Records containing a range of potency (specified as '<' or '>') were retained only if the specified range was either lower than 10,000 nM or higher than 100,000 nM (and subsequently assigned to the "active" or "inactive" classes, respectively);

6. For each target, records referred to the same molecule (as identified by the canonical SMILES string) were merged. The information obtained from such multiple records was used to assess the reliability of the assigned label(s) for a given molecule on a given target. If all the records for a molecule showed the same bioactivity label on a target, the molecule-target pair was retained in the dataset. Molecules having conflicting labels in the corresponding records for a given target and a given endpoint (*e.g.*, presence of both "active" and "inactive" labels) were

assigned the label "inconclusive", to highlight the lack of a final bioactivity assessment. Whenever a molecule was retained for at least one of the macromolecular targets, the lack of collected bioactivity information for other targets was identified with the label "missing".

2.2. Data analysis

2.2.1. Chemical similarity analysis

Molecular similarity analysis was carried out to investigate the degree of diversity between the molecular structures contained in the four different data sources. Pairwise molecular similarities were quantified using Jaccard-Tanimoto similarity coefficient computed on extended connectivity fingerprints (Rogers and Hahn, 2010), which capture the presence of atom-centered fragments of a predefined radius. The data were projected in a reduced space using a multidimensional scaling (MDS), which reproduces similarities in a low-dimensional plot (Seber, 2009).

2.2.2. Ligand overlap analysis

We considered the number of active molecules shared between pairs of endpoints as a measure of overlap. For any given pair of endpoints (i and j), the overlap in their activity annotations (S_{ij}) was calculated using the following index:

$$S_{ij} = \frac{a}{a+b} \tag{1}$$

where a is the number of molecules active for both endpoints i and j; b is the number of molecules with different activity labels for i and j. Therefore, S_{ij} gives the fraction of molecules annotated as actives in both endpoints, without considering the presence of shared inactive molecules. Note that weakly active molecules were not considered in this analysis.

2.2.3. Pocket-centric analysis

The selected protein targets were evaluated for the overlap of their binding pockets, using the PocketMatch algorithm (Yeturu and Chandra, 2008). PocketMatch compares in a frame-invariant

manner the binding site, by calculating 90 lists of sorted distances capturing the shape and the

chemical nature of the site. The algorithms provide a score (PMscore) ranging from 0 to 100 for

any considered pair of binding sites; the greater the score, the higher the overlap. For this analysis

we used the crystallographic structures of ligand-nuclear receptor complexes from the PDBbind

database ("PDBbind 2018") summarized in Table 2.

After removing the structures including an allosteric ligand, we aligned all the remaining

structures and, in each of them, we selected only residues within 5 Å from any of the

crystallographic ligands. This procedure returns the overlapping portion of each crystallographic

receptor in correspondence of the binding site, compared to all the receptors, that was used for

the calculation of the PMscores.

Table 2 Summary of PDBbind crystallographic structures.

Target	No. ligands	PDB structures
AR	22	1E3G, 1Z95, 2AM9, 2AMA, 2AX6, 2AX9, 2HVC, 2IHQ, 2NW4, 2OZ7, 3B5R, 3B65, 3B66, 3B67, 3B68, 3G0W, 3V49, 4QL8, 5CJ6, 5T8E, 5T8J, 5V8Q
ERα	13	1X7E, 1X7R, 2I0J, 3ERD, 3ERT, 5FQP, 5FQT, 5FQV
ERβ	36	1NDE, 1QKN, 1U3Q, 1U3R, 1U3S, 1U9E, 1X76, 1X78, 1X7B, 1YY4, 1YYE, 1ZAF, 2GIU, 2I0G, 2J7X, 2JJ3, 2NV7, 2QTU, 2Z4B
FXR	68	3DCT, 3OKH, 3OKI, 3OLF, 3OMM, 3OOF, 3OOK, 4OIV, 5Q0I, 5Q0J, 5Q0L, 5Q0M, 5Q0N, 5Q0O, 5Q0P, 5Q0Q, 5Q0R, 5Q0S, 5Q0T, 5Q0U, 5Q0V, 5Q0W, 5Q0X, 5Q0Y, 5Q10, 5Q11, 5Q12, 5Q13, 5Q14, 5Q15, 5Q16, 5Q17, 5Q18, 5Q19, 5Q1A, 5Q1B, 5Q1C, 5Q1D, 5Q1F, 5Q1G, 5Q1I
GR	18	1NHZ, 1P93, 3K22, 3K23, 4CSJ, 4P6W, 4P6X
PPARα	11	1I7G, 1KKQ, 3FEI, 3G8I, 3KDT, 3KDU
PPARδ	8	3DY6, 3GWX, 3GZ9, 3PEQ, 3TKM
PPARγ	59	1FM9, 1I7I, 1NYX, 1ZEO, 2ATH, 2F4B, 2G0G, 2G0H, 2GTK, 2HFP, 2I4J, 2I4Z, 2P4Y, 2Q8S, 2YFE, 3B1M, 3FEJ, 3FUR, 3G9E, 3H0A, 3IA6, 3LMP, 3OSI, 3OSW, 3R5N, 3R8I, 3SZ1, 3T03, 3TY0, 3U9Q, 4A4V4A4W, 4JAZ, 4PRG, 4R06, 4XTA, 4XUH, 4XUM, 4Y29, 5F9B, 5LSG, 5TWO, 5U5L
PR	16	1A28, 1SQN, 1SR7, 1ZUC, 2W8Y, 3G8O, 3HQ5, 3KBA, 4OAR
PXR	4	1ILH, 1M13, 2O9I
RXR	20	1RDT, 3FAL, 3NSQ, 3OZJ, 3PCU, 3R2A, 3R5M, 4K4J, 4K6I, 4M8E, 4M8H, 4POH, 4POJ, 4PP3, 4PP5, 4ZSH, 5MKJ

2.3. Software and code

Data curation and integration was performed in KNIME 4.0.1 (Berthold et al., 2007). SMILES were canonicalized using in KNIME 4.0.1 ('RDKit Canon SMILES' node). Pocket overlap scores were computed using PocketMatch (Yeturu and Chandra, 2008) in Python v3.6. Extended connectivity fingerprints (ECFPs)(Rogers and Hahn, 2010) were calculated with Dragon 7 (KodeSrl, 2017) with the following settings: "Bits per pattern" = 2; "Count fragments": True; "Atom Options": [Atom type, Aromaticity, Connectivity total, Charge, Bond order]. Atomic scaffolds (Bemis and Murcko, 1996), molecular weight, number of aromatic rings, rotatable bonds and octanol-water partition coefficients were computed with RDKit 2019.09.01 ('GetScaffoldForMol' function with default settings). Multidimensional scaling was computed using MATLAB v2018b (The Mathworks Inc) 'mdscale' function in (Criterion = 'metricstress'; Start = 'random'. Stress error = 0.356) with two dimensions. Ligand-based analysis and agglomerative hierarchical clustering (Köhn and Hubert 2014) with unweighted average Euclidean distance were performed using in-house MATLAB 2018b code (The Mathworks Inc). Structural alignment between crystallographic receptors and residue selection was performed using Pymol ("The PyMOL").

3. Results

In what follows, we analyze the contribution of the individual data sources to the final dataset, in terms of novel and shared molecules and molecular scaffold diversity. NURA dataset is then analyzed for the distribution of bioactivity labels for each selected target. Finally, a ligand- and structure-based analysis allows to obtain some additional data-driven insights into the captured structure-activity landscapes.

3.1. Contribution of the individual sources of data

Each database source provided a different contribution to the final dataset. The final dataset contained (Figure 1A):

- 6504 molecules from Tox21, with 150571 activity labels in total (1.73% active, 3.76% weakly active and 94.51% inactive), no activity labels for RXR antagonism were retained;

- 3951 molecules from ChEMBL, with 12159 activity labels in total (82.29% active, 6.28% weakly active and 11.43% inactive);

- 5491 molecules from NR-DBIND, with 13711 activity labels (90.74% active, 3.80% weakly active and 5.46% inactive), no activity labels for PPARα were retained;

- 1125 molecules from BindingDB, with 1570 activity labels (81.21% active, 6.18% weakly active and 12.61% inactive), no activity labels for RXR and PXR antagonism and for PPARα were retained

Tox21 data contains a larger number of inactive compounds (94.51%), mostly due to its focus on toxicological evaluation of man-made chemicals. On the contrary, medicinal chemistry databases focus mostly on bioactive compounds (82.29%, 90.74% and 82.29% for ChEMBL, NR-DBIND and BindingDB, respectively) (Réau et al., 2018).
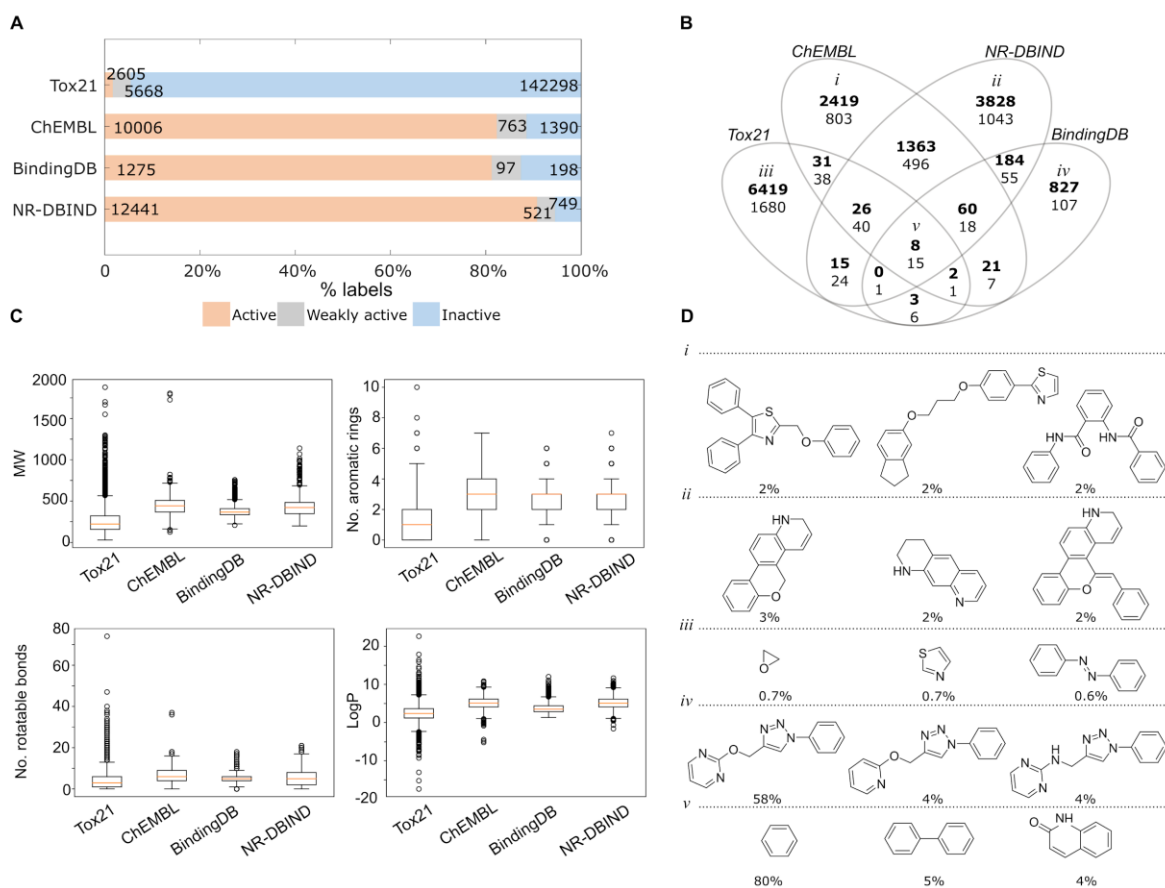
Figure 1. Analysis of the individual sources used to develop NURA dataset. (A) Percentage of records labeled as active (activity lower than 10,000 nM), weakly active (activity between 10,000 nM and 100,000 nM) and inactive (activity higher than 100,000 nM) grouped by data source. (B) Venn diagram of the data collected from Tox21, ChEMBL, NR-DBIND and Binding-DB. The numbers of shared and not shared molecules (in bold) and scaffolds are reported; (C) distribution of molecular weights (MW), number of aromatic rings, rotatable bonds and octanol-water partition coefficients (LogP) per data source. Tox21 molecules have statistically significant ($p < 0.05$, t-test) values in the computed properties compared to the other data sources. (D) Three most frequently occurring scaffolds present in only one source and in all sources (the frequency reported as percentage). Roman numerals correspond to the set the scaffolds belong to, as specified in (B).

We extracted the most frequent atomic molecular scaffolds (Bemis and Murcko, 1996) for each source to investigate the structural similarity between the molecules annotated in the considered data sources. 1,713 molecules out of 15,206 (11%), corresponding to 701 unique scaffolds out of 4,334 (16%), are shared among two or more sources (Figure 1B). Most of the shared scaffold (576, corresponding to 13% of the total) are shared between the sources aiming at medicinal chemistry applications, *i.e.*, ChEMBL, BindingDB and NR-DBIND (Fig. 1A). This reflects a certain similarity of the chemical space covered by these sources. At the same time, each source contributes with unique atomic scaffolds *i.e.*, 1,680 novel scaffolds contained in Tox21 (39%), 803 in ChEMBL (19%), 1,043 in NR-DBIND (24%) and 107 in BindingDB (2%). These aspects underscore the benefit of merging different sources to expand the atomic scaffolds covered in the curated dataset. Additionally, Tox21 covers a significantly different property space (*i.e.*, molecular weight, lipophilicity, number of aromatic rings and rotatable bonds; $p < 0.05$, t-test) than the other databases.

In order to further investigate overlap of the considered chemical sources, we represented the chemical space of the cured dataset by means of a multidimensional scaling (MDS), which compresses the information on molecular similarity in a two-dimensional plot (Fig 2A). In this representation, regions mainly characterized by molecules labelled as active can be identified (Fig 2A). These regions correspond in particular to the overlap between ChEMBL, BindingDB and NR-DBIND molecules (Fig. 2B). The main region of overlap (Fig 2B, i) contains drug-like compounds with heteroaromatic rings and alicyclic compounds with alkyne bonds and hydroxyl functional group, while a smaller region of overlap contains alicyclic compound with hormone-like scaffolds (Fig2A ii). On the contrary, Tox21 molecules occupy different regions, mostly characterized by inactive molecules, which also contain inactive linear aliphatic compounds (Fig 2B, iii). Finally, BindingDB contributes a unique set of molecules binding to RXR (Fig. 2B, iv), containing triazole and pyridine heterocycles with fluorine substituents.
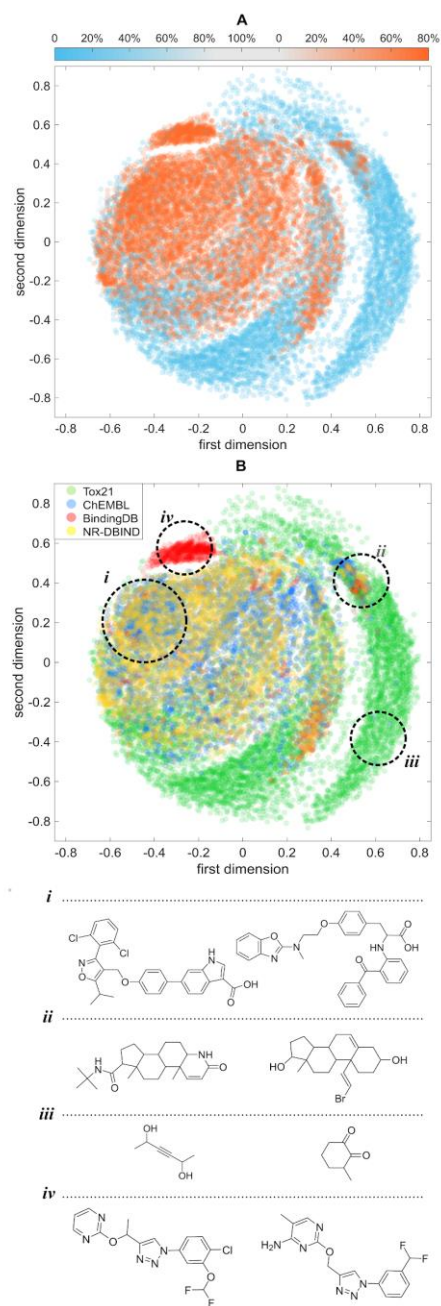
Figure 2. Multidimensional scaling of the molecules in the curated NURA dataset, as obtained on ECFPs (stress error = 0.356); (A) molecules are colored based on their percentage of "active" labels over their total number of annotated endpoints; (B) molecules are colored based on the original source, with some representative structures highlighted.

3.2. NURA dataset

The aggregation and curing of data from the selected sources led to a dataset containing 15,247 molecules with activity annotation for 33 endpoints, *i.e.,* 11 NRs with the respective labels for three activity modulations ("binding", "agonism" or "antagonism"). Each endpoint contains on average 4.5k molecules with annotated activity (Fig. 3). The endpoints with the highest number of annotations are the PPARγ binding (7,362 molecules), GR binding (7,128 molecules) and ERβ binding (6,779 molecules). The endpoints relative to antagonism on RXR (119 molecules), PPARα (19 molecules) and PXR (10 molecules) contain the lowest number of annotations. The dataset contains a different balance between active and inactive chemicals depending on the endpoint considered. For instance, antagonism on RXR, binding and agonism on PPARα show the largest percentage of molecules labelled as active (96.7%, 89.2%, 90.9%, respectively), while the endpoints relative to PPARδ antagonism, PPARγ antagonism, and FXR antagonism mainly comprise inactive molecules (99.1%, 95.6% and 94.8%, respectively). 87% of the molecules have an activity label for at least two endpoints, with an average of 11 annotations (over the 33 endpoints) per molecule.
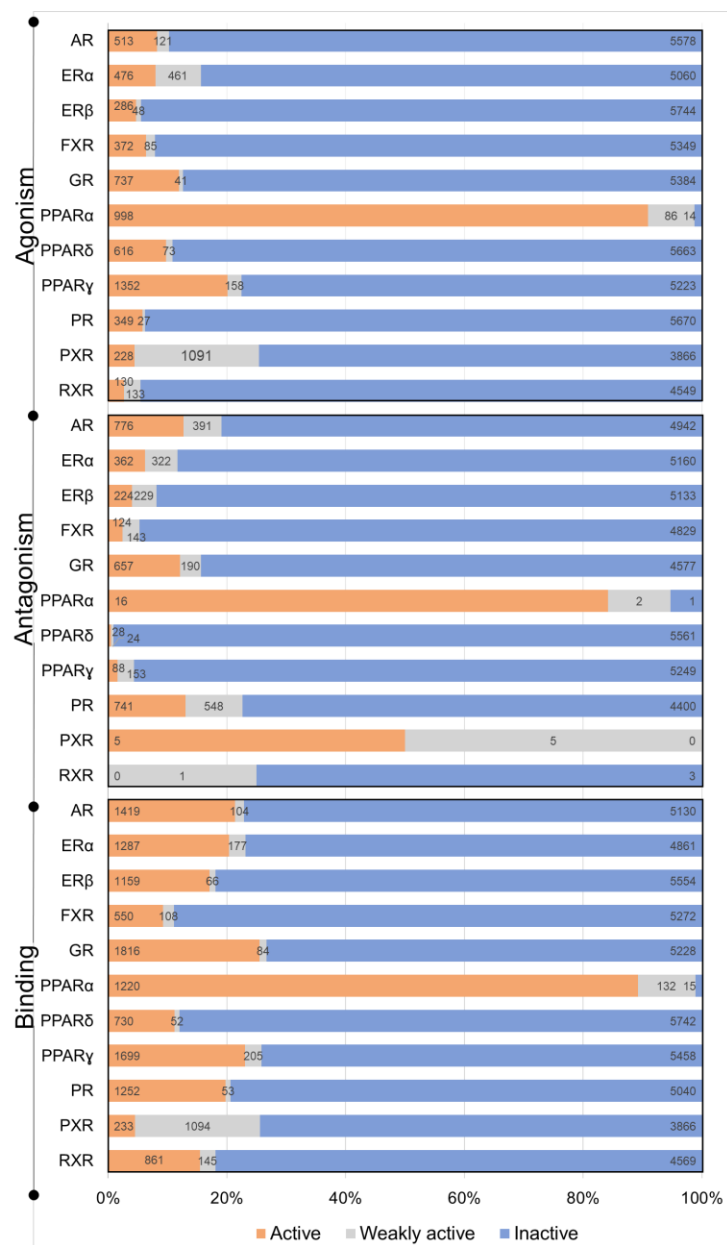
Figure 3. Distribution of molecules per considered endpoint in the curated NURA dataset, divided into active (activity lower than 10,000 nM), weakly active (activity ranging from 10,000 nM to 100,000 nM) and inactive (activity larger than 100,000 nM). Percentages over the total and absolute numbers are reported.

3.3. Data-driven insights

To enrich the study with data-driven insights, we performed two types of *post-hoc* analysis: (i) a "ligand-centric" analysis, aimed to identify active ligands shared among different endpoints, (ii) a "pocket-centric" analysis, aimed to identify correlation patterns of the binding pockets.

The degree of overlap in active molecules between the considered endpoints was analyzed by computing the fraction of shared active molecules among pairs of endpoints (see Eq. 1). As expected, binding-agonism and binding-antagonism pairs referred to the same nuclear receptor are characterized by high overlap (Fig. 4A; fraction of common active molecules higher than 0.66 and 0.85, respectively), while little to no overlap is present for agonism-antagonism pairs (lower than 24% of shared actives for all targets). The only exception is RXR, where only one molecule is shared (5-Fluorinated trienoic acid), which behaves as both agonist and antagonist (Gernert et al., 2003). AR, GR and PR, as well as PPAR and ER isoforms show an high fraction of common active molecules, *i.e.* 0.85, 0.91, and 0.94 between AR-GR, AR-PR and GR-PR for binding, respectively; 0.95 between ERα-ERβ for binding; 0.99, 0.99 and 0.88 between PPARα-PPARδ, PPARα-PPARγ and PPARδ-PPARδ, respectively.

A

B

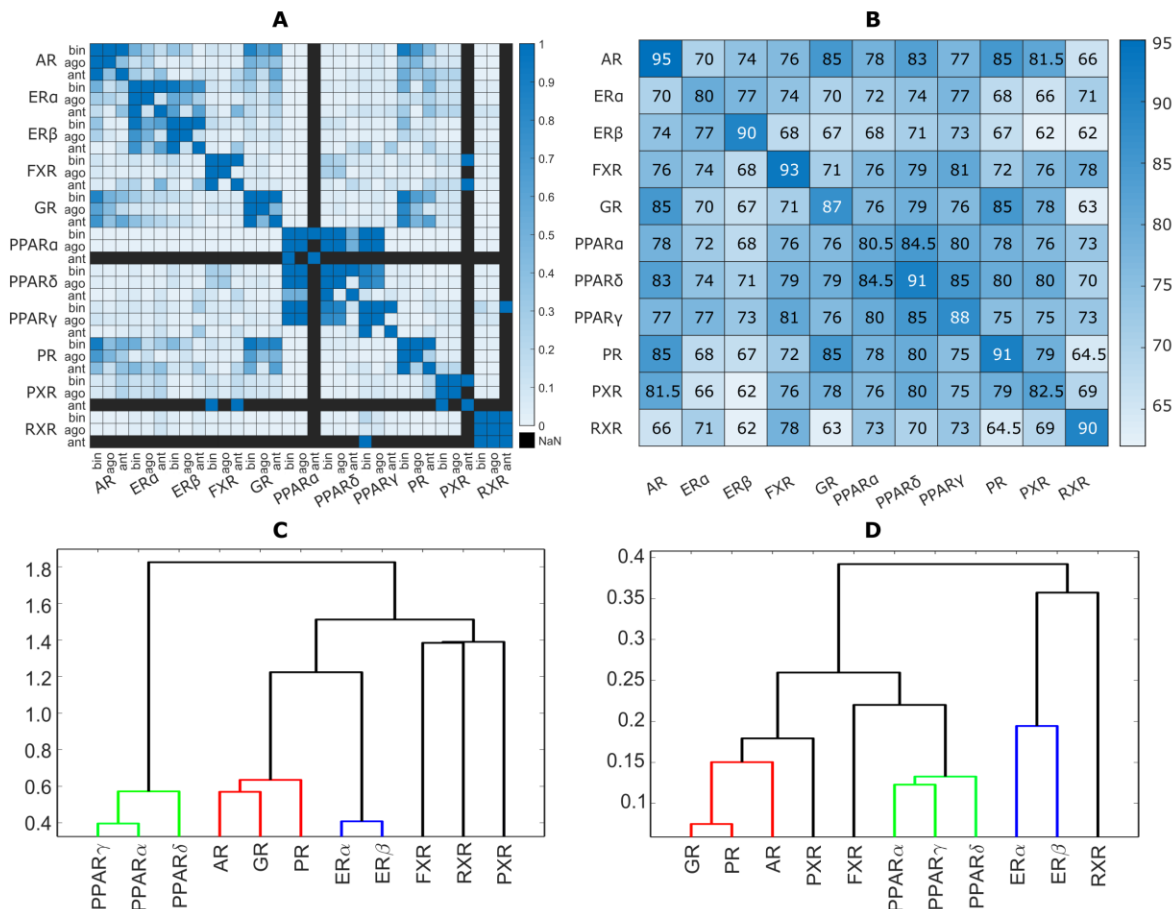|	AR	ERα	ERβ	FXR	GR	PPARα	PPARδ	PPARγ	PR	PXR	RXR
AR	95	70	74	76	85	78	83	77	85	81.5	66
ERα	70	80	77	74	70	72	74	77	68	66	71
ERβ	74	77	90	68	67	68	71	73	67	62	62
FXR	76	74	68	93	71	76	79	81	72	76	78
GR	85	70	67	71	87	76	79	76	85	78	63
PPARα	78	72	68	76	76	80.5	84.5	80	78	76	73
PPARδ	83	74	71	79	79	84.5	91	85	80	80	70
PPARγ	77	77	73	81	76	80	85	88	75	75	73
PR	85	68	67	72	85	78	80	75	91	79	64.5
PXR	81.5	66	62	76	78	76	80	75	79	82.5	69
RXR	66	71	62	78	63	73	70	73	64.5	69	90

C

D

Figure 4. Summary of the data-driven analysis. (A) Heatmap of the degree of shared active molecules calculated on pair of endpoints considering only active and inactive labels. The colors indicate the degree of shared active molecules from blue (high) to white (low) scores. Black color highlights endpoints that do not have any ligand in common ("NaN"). (B) Heatmap of the median of the PMscores for each pair of targets, the darker, the higher the PMscore. (C) Dendrogram derived from the degree of shared active molecules calculated on pair of endpoints and targets considering only active and inactive labels. (D) Dendrogram derived from the median of the PMscores for each pair of targets, the darker the blue the higher the PMscore.

To analyze the physico-chemical, volumetric and geometrical diversity of the binding pockets of the chosen receptors, we calculated the median of the PMscores for each pair of targets (Fig. 4B, standard deviations are reported in Supporting Figure S1). The diagonal values are computed

using different crystallographic structures of the same receptor, and, thus, they represent both the experimental uncertainty in the crystallographic structure and the pocket flexibility. The lowest diagonal scores are those of ERα and PPARα.

Despite the studied receptors belong to the same superfamily, some diversity in the pocket features can be observed, with the lowest PMscore being equal to 62. This highlights a good coverage of the dataset in terms of included receptors, which might possess relatively different binding pockets. This binding pocket analysis might be an additional support to complement structure-activity investigations in the field of polypharmacology and/or selectivity optimization for nuclear receptors.

To further compare the ligand-centric and the pocket-centric analysis, we applied hierarchical clustering to both ligand-based overlap scores (Eq.1 and Fig. 4C) and structure-based scores (PMscores, Fig. 4D). Despite molecules annotated as binders might not necessarily bind in the orthosteric site, a good overlap between the ligand-based and structure-based hierarchical clustering can be observed (Fig. 4). The ligand- and structure-based dendrograms reproduce some of the known evolutionary relationships, *i.e.*, among ERα and ERβ, PPAR subtypes, or among the steroid hormone receptors GR, PR, and AR (Mangelsdorf et al. 1995; Edman et al. 2015; Holzer et al. 2017). The good correspondence between the ligand- and structure-based information indicates a good coverage of the obtained dataset, in terms of structure-activity relationships represented. The observed correspondence is, in fact, not always obtained by considering each source separately (Supporting Figure S2). The overlap between the analyzed endpoints (both in terms of ligands and pockets) can be of interest for subsequent future application in multi-task learning. In particular, the target correlation play a fundamental role when dealing with neural networks multi-task learning (Caruana, 1997; Ramsundar et al., 2015; Sadawi et al., 2019).

4. Conclusions and outlook

Aiming to provide a comprehensive dataset on nuclear receptor bioactivity, in this work we integrated and curated information on binding, agonism and antagonism for 11 selected nuclear receptors, using four well-known chemical databases. The resulting dataset, NURA, includes 15,247 molecules with binding, agonism and/or antagonism annotations for 11 NRs, with 11 endpoints annotated on average per molecule.

The data curation and aggregation pipeline successful allowed to bridge the gap between toxicology-related databases (containing information mostly on inactive molecules) and medicinal-chemistry-related databases (mostly focusing on the chemical space of bioactive compounds). Our results show that NURA dataset is enriched in terms of number of molecules, structural diversity and covered atomic scaffolds compared to the single sources. To the best of our knowledge, NURA dataset is the most exhaustive collection of small molecules annotated for their modulation of the chosen nuclear receptors.

The dataset developed in this work can serve as a basis to develop machine learning methods for toxicological and/or medicinal chemistry applications, *e.g.,* to predict the modulation of a panel of receptors or the selectivity among the selected NRs. In fact, the increased coverage of the chemical and bioactivity space and of atomic scaffolds offers the opportunity to develop models with an increased applicability domain and improved robustness compared to those developed on the single sources of data. Moreover, for most of the receptors, the data aggregation improved the balance between active and inactive molecules.

To increase the usefulness of the developed dataset to the scientific community, NURA dataset can be downloaded for free at the following URL: https://michem.unimib.it/download/data/nura/.

Author contributions

F.G., D.B. and C.V. conceptualized the study. C.V. collected and curated the dataset molecules and performed the ligand-based analysis. C.V. and S.M. performed the structure-based analysis, with the support of L.B. C.V. and F.G. drafted the manuscript; all authors contributed to manuscript revision and editing.

Acknowledgements

References

Banerjee, M., Robbins, D., Chen, T., 2015. Targeting xenobiotic receptors PXR and CAR in human diseases. Drug
Discov. Today 20, 618–628.

Bemis, G.W., Murcko, M.A., 1996. The properties of known drugs. 1. Molecular frameworks. J. Med. Chem. 39,
2887–2893.

Berger, J., Moller, D.E., 2001. The mechanisms of action of PPARs. Annu. Rev. Med. 53, 409–435.

Berthold, M.R., Cebron, N., Dill, F., Gabriel, T.R., Kötter, T., Meinl, T., Ohl, P., Sieb, C., Thiel, K., Wiswedel, B., 2007.
KNIME: The Konstanz Information Miner, in: Studies in Classification, Data Analysis, and Knowledge
Organization (GfKL 2007). Springer.

Caruana, R., 1997. Multitask Learning. Mach. Learn. 28, 41–75.

Cronin, M.T.D., Schultz, T.W., 2003. Pitfalls in QSAR. Journal of Molecular Structure: The Ochem 622, 39–51.

Davey, R.A., Grossmann, M., 2016. Androgen Receptor Structure, Function and Biology: From Bench to Bedside.
Clin. Biochem. Rev. 37, 3.

Ekins, S., Kortagere, S., Iyer, M., Reschly, E.J., Lill, M.A., Redinbo, M.R., Krasowski, M.D., 2009. Challenges
Predicting Ligand-Receptor Interactions of Promiscuous Proteins: The Nuclear Receptor PXR. PLoS Comput.
Biol. 5, e1000594.

Fourches, D., Muratov, E., Tropsha, A., 2010. Trust, but verify: on the importance of chemical structure curation in
cheminformatics and QSAR modeling research. J. Chem. Inf. Model. 50, 1189–1204.

Francis, G.A., Fayard, E., Picard, F., Auwerx, J., 2003. Nuclear Receptors and the Control of Metabolism. Annu. Rev.
Physiol. 65, 261–311.

Gaulton, A., Hersey, A., Nowotka, M.L., Patricia Bento, A., Chambers, J., Mendez, D., Mutowo, P., Atkinson, F.,
Bellis, L.J., Cibrian-Uhalte, E., Davies, M., Dedman, N., Karlsson, A., Magarinos, M.P., Overington, J.P.,
Papadatos, G., Smit, I., Leach, A.R., 2017. The ChEMBL database in 2017. Nucleic Acids Res. 45, D945–D954.

Gernert, D.L., Ajamie, R., Ardecky, R.A., Bell, M.G., Leibowitz, M.D., Mais, D.A., Mapes, C.M., Michellys, P.Y.,
Rungta, D., Reifel-Miller, A., Tyhonas, J.S., Yumibe, N., Grese, T.A., 2003. Design and synthesis of fluorinated
RXR modulators. Bioorg. Med. Chem. Lett. 13, 3191–3195.

Gilson, M.K., Liu, T., Baitaluk, M., Nicola, G., Hwang, L., Chong, J., 2016. BindingDB in 2015: A public database for
medicinal chemistry, computational chemistry and systems pharmacology. Nucleic Acids Res. 44, D1045–D1053.

Griffen, E.J., Dossetter, A.G., Leach, A.G., Montague, S., 2018. Can we accelerate medicinal chemistry by
augmenting the chemist with Big Data and artificial intelligence? Drug Discov. Today 23, 1373–1384.

Grisoni, F., Merk, D., Byrne, R., Schneider, G., 2018. Scaffold-Hopping from Synthetic Drugs by Holistic Molecular

Representation. Sci. Rep. 8, 16469.

Halevy, A., Norvig, P., Pereira, F., 2009. The Unreasonable Effectiveness of Data. IEEE Intelligent Systems. https://doi.org/10.1109/mis.2009.36

Heitel, P., Gellrich, L., Kalinowsky, L., Heering, J., Kaiser, A., Ohrndorf, J., Proschak, E., Merk, D., 2019. Computer-Assisted Discovery and Structural Optimization of a Novel Retinoid X Receptor Agonist Chemotype. ACS Med. Chem. Lett. 10, 203–208.

Huang, P., Chandra, V., Rastinejad, F., 2010. Structural overview of the nuclear receptor superfamily: insights into physiology and therapeutics. Annu. Rev. Physiol. 72, 247–272.

Huang, R., 2016 Chapter 12 A Quantitative High-Throughput Screening Data Analysis Pipeline for Activity Profi ling. Methods Mol. Biol. 1473. https://doi.org/10.1007/978-1-4939-6346-1_12

Huang, R., Sakamuru, S., Martin, M.T., Reif, D.M., Judson, R.S., Houck, K.A., Casey, W., Hsieh, J.-H., Shockley, K.R., Ceger, P., Fostel, J., Witt, K.L., Tong, W., Rotroff, D.M., Zhao, T., Shinn, P., Simeonov, A., Dix, D.J., Austin, C.P., Kavlock, R.J., Tice, R.R., Xia, M., 2015. Profiling of the Tox21 10K compound library for agonists and antagonists of the estrogen receptor alpha signaling pathway. Sci. Rep. 4, 5664.

Khandelwal, A., Krasowski, M.D., Reschly, E.J., Sinz, M.W., Swaan, P.W., Ekins, S., 2008. Machine Learning Methods and Docking for Predicting Human Pregnane X Receptor Activation. Chemical Research in Toxicology. https://doi.org/10.1021/tx800102e

Kim, S., Chen, J., Cheng, T., Gindulyte, A., He, J., He, S., Li, Q., Shoemaker, B.A., Thiessen, P.A., Yu, B., Zaslavsky, L., Zhang, J., Bolton, E.E., 2019. PubChem 2019 update: improved access to chemical data. Nucleic Acids Res. 47, D1102–D1109.

Kleinstreuer, N.C., Ceger, P., Watt, E.D., Martin, M., Houck, K., Browne, P., Thomas, R.S., Casey, W.M., Dix, D.J., Allen, D., Sakamuru, S., Xia, M., Huang, R., Judson, R., 2017. Development and Validation of a Computational Model for Androgen Receptor Activity. Chem. Res. Toxicol. 30, 946–964.

KodeSrl, 2017. Dragon (software for molecular descriptor calculation).

Mansouri, K., Abdelaziz, A., Rybacka, A., Roncaglioni, A., Tropsha, A., Varnek, A., Zakharov, A., Worth, A., Richard, A.M., Grulke, C.M., Trisciuzzi, D., Fourches, D., Horvath, D., Benfenati, E., Muratov, E., Wedebye, E.B., Grisoni, F., Mangiatordi, G.F., Incisivo, G.M., Hong, H., Ng, H.W., Tetko, I.V., Balabin, I., Kancherla, J., Shen, J., Burton, J., Nicklaus, M., Cassotti, M., Nikolov, N.G., Nicolotti, O., Andersson, P.L., Zang, Q., Politi, R., Beger, R.D., Todeschini, R., Huang, R., Farag, S., Rosenberg, S.A., Slavov, S., Hu, X., Judson, R.S., 2016. CERAPP: Collaborative estrogen receptor activity prediction project. Environ. Health Perspect. 124, 1023–1033.

Mansouri, K., Kleinstreuer, N., Abdelaziz, A.M., Alberga, D., Alves, V.M., Andersson, P.L., Andrade, C.H., Bai, F.,

Balabin, I., Ballabio, D., Benfenati, E., Bhhatarai, B., Boyer, S., Chen, J., Consonni, V., Farag, S., Fourches, D., García-Sosa, A.T., Gramatica, P., Grisoni, F., Grulke, C.M., Hong, H., Horvath, D., Hu, X., Huang, R., Jeliazkova, N., Li, J., Li, X., Liu, H., Manganelli, S., Mangiatordi, G.F., Maran, U., Marcou, G., Martin, T., Muratov, E., Nguyen, D.-T., Nicolotti, O., Nikolov, N.G., Norinder, U., Papa, E., Petitjean, M., Piir, G., Pogodin, P., Poroikov, V., Qiao, X., Richard, A.M., Roncaglioni, A., Ruiz, P., Rupakheti, C., Sakkiah, S., Sangion, A., Schramm, K.-W., Selvaraj, C., Shah, I., Sild, S., Sun, L., Taboureau, O., Tang, Y., Tetko, I.V., Todeschini, R., Tong, W., Trisciuzzi, D., Tropsha, A., Van Den Driessche, G., Varnek, A., Wang, Z., Wedebye, E.B., Williams, A.J., Xie, H., Zakharov, A.V., Zheng, Z., Judson, R.S., 2020. CoMPARA: Collaborative Modeling Project for Androgen Receptor Activity. Environ. Health Perspect. 128, 027002.

MATLAB R2018b. The MathWorks, Inc., Natick, Massachusetts, United States., 2018. URL www.mathworks.com

Merk, D., Grisoni, F., Friedrich, L., Gelzinyte, E., Schneider, G., 2018. Computer-Assisted Discovery of Retinoid X Receptor Modulating Natural Products and Isofunctional Mimetics. J. Med. Chem. 61, 5442–5447.

Motta, S., Callea, L., Giani Tagliabue, S., Bonati, L., 2018. Exploring the PXR ligand binding mechanism with advanced Molecular Dynamics methods. Sci. Rep. 8, 16207.

Mueller, S.O., Korach, K.S., 2001. Estrogen receptors and endocrine diseases: lessons from estrogen receptor knockout mice. Curr. Opin. Pharmacol. 1, 613–619.

NIH, Tox21 Public data [WWW Document]. National Institutes of Health, National Center for Advancing Translational Sciences. URL https://tripod.nih.gov/tox21/assays/

Niu, A.-Q., Xie, L.-J., Wang, H., Zhu, B., Wang, S.-Q., 2016. Prediction of selective estrogen receptor beta agonist using open data and machine learning approach. Drug Des. Devel. Ther. 10, 2323–2331.

O'Boyle, N.M., 2012. Towards a Universal SMILES representation - A standard method to generate canonical SMILES based on the InChI. J. Cheminform. 4, 22.

Olah, M., Rad, R., Ostopovici, L., Bora, A., Hadaruga, N., Hadaruga, D., Moldovan, R., Fulias, A., Mractc, M., Oprea, T.I., 2007. WOMBAT and WOMBAT-PK: Bioactivity Databases for Lead and Drug Discovery. Chemical Biology. https://doi.org/10.1002/9783527619375.ch13b

Park, S.-J., Kufareva, I., Abagyan, R., 2010. Improved docking, screening and selectivity prediction for small molecule nuclear receptor modulators using conformational ensembles. J. Comput. Aided Mol. Des. 24, 459–471.

PDBbind 2018 URL http://www.pdbbind-cn.org/ (accessed 11.10.19).

Penvose, A., Keenan, J.L., Bray, D., Ramlall, V., Siggers, T., 2019. Comprehensive study of nuclear receptor DNA binding provides a revised framework for understanding receptor specificity. Nat. Commun. 10, 2514.

Ramsundar, B., Kearnes, S., Riley, P., Webster, D., Konerding, D., Pande, V., Edu, P., 2015. Massively Multitask

Networks for Drug Discovery.

Réau, M., Lagarde, N., Zagury, J.-F., Montes, M., 2018. Nuclear Receptors DataBase Including Negative Data (NR-DBIND): A database dedicated to nuclear receptors binding data including negative data and pharmacological profile. J. Med. Chem. acs.jmedchem.8b01105.

Rogers, D., Hahn, M., 2010. Extended-Connectivity Fingerprints. J. Chem. Inf. Model. 50, 742–754.

Rupp, M., Schroeter, T., Steri, R., Zettl, H., Proschak, E., Hansen, K., Rau, O., Schwarz, O., Müller-Kuhrt, L., Schubert-Zsilavecz, M., Müller, K.-R., Schneider, G., 2010. From Machine Learning to Natural Product Derivatives that Selectively Activate Transcription Factor PPARγ. ChemMedChem. https://doi.org/10.1002/cmdc.200900469

Sadawi, N., Olier, I., Vanschoren, J., van Rijn, J.N., Besnard, J., Bickerton, R., Grosan, C., Soldatova, L., King, R.D., 2019. Multi-task learning with a natural metric for quantitative structure activity relationship learning. J. Cheminform. 11, 68.

Schug, T.T., Janesick, A., Blumberg, B., Heindel, J.J., 2011. Endocrine disrupting chemicals and disease susceptibility. J. Steroid Biochem. Mol. Biol. 127, 204–215.

Seber, G.A.F., 2009. Multivariate observations. Wiley-Interscience.

Shulman, A.I., Mangelsdorf, D.J., 2005. Retinoid x receptor heterodimers in the metabolic syndrome. N. Engl. J. Med. 353, 604–615.

The PyMOL Molecular Graphics System, Version 2.2, Schrödinger, LLC.

Tice, R.R., Austin, C.P., Kavlock, R.J., Bucher, J.R., 2013. Improving the Human Hazard Characterization of Chemicals: A Tox21 Update. Environ. Health Perspect. 121, 756–765.

Tropsha, A., 2010. Best Practices for QSAR Model Development, Validation, and Exploitation. Mol. Inform. 29, 476–488.

Vangala, S., Pinjari, J., Patole, P., Ravindran, S., Gangal, R., Wangikar, P., Basu, S., Ahmed, T., Rastogi, H., 2012. Translational Drug Discovery Research: Integration of Medicinal Chemistry, Computational Modeling, Pharmacology, ADME, and Toxicology. Encyclopedia of Drug Metabolism and Interactions. https://doi.org/10.1002/9780470921920.edm038

Visser, U., Abeyruwan, S., Vempati, U., Smith, R.P., Lemmon, V., Schürer, S.C., 2011. BioAssay Ontology (BAO): a semantic description of bioassays and high-throughput screening results. BMC Bioinformatics 12, 257.

Wassermann, A.M., Bajorath, J., 2011. BindingDB and ChEMBL: online compound databases for drug discovery. Expert Opin. Drug Discov. 6, 683–687.

Weininger, D., 1988. SMILES, a chemical language and information system. 1. Introduction to methodology and encoding rules. J. Chem. Inf. Model. 28, 31–36.

Yeturu, K., Chandra, N., 2008. PocketMatch: A new algorithm to compare binding sites in protein structures. BMC
Bioinformatics 9, 1–17.

Young, D., Martin, T., Venkatapathy, R., Harten, P., 2008. Are the Chemical Structures in Your QSAR Correct?
QSAR & Combinatorial Science. https://doi.org/10.1002/qsar.200810084

Supporting Information

Table S1. List of selected ChEMBL assays.

Antagonist activity at human AR expressed in HEK293 cells measured after 24 hrs by luciferase reporter gene assay
Antagonist activity at wild type AR expressed in human SC cells assessed as inhibition of 0.3 to 10 nM DHT-induced cell proliferation after 3 days by WST-8 assay
Antagonist activity at AR in human LNCAP cells receptor assessed as inhibition of R1881-induced transcriptional activation at 10 uM by ARE-luciferase reporter gene assay
Antagonist activity at human AR expressed in HEK293 cells at 30 uM after 24 hrs by luciferase reporter gene assay
Antagonist activity at AR in human MDA-kb2 cells co-transfected with MMTV-luc assessed as decrease in DHT-induced luciferase activity at 1 mM by reporter gene assay
Antagonist activity at AR F876L mutant (unknown origin) expressed in human PC3 cells assessed as inhibition of DHT-induced receptor transactivation after 24 hrs by PSA-luciferase reporter gene assay
Antagonist activity at wild type AR expressed in human SC cells assessed as inhibition of 1 nM DHT-induced cell proliferation after 3 days by WST-8 assay
Antagonist activity at AR T877A mutant (unknown origin) transfected in human PC3 cells assessed as inhibition of DHT-induced receptor transcriptional activation after 24 hrs by PSA-luciferase reporter gene assay
Antagonist activity at wild type AR in human PC3 cells assessed as suppression of DHT-induced receptor transcriptional activation after 24 hrs by PSA-luciferase reporter gene assay
Antagonist activity at AR receptor in human LNCAP cells assessed as inhibition of R1881-induced transcriptional activation at 10 nM to 10 uM by ARE-uciferase reporter gene assay
Antagonist activity at AR F876L mutant (unknown origin) transfected in human PC3 cells assessed as suppression of DHT-induced receptor transcriptional activity at 500 nM after 24 hrs by PSA-luciferase reporter gene assay
Antagonist activity at AR W741C/T877A double mutant (unknown origin) transfected in human PC3 cells assessed as inhibition of DHT-induced receptor transcriptional activation after 24 hrs by PSA-luciferase reporter gene assay
Antagonist activity at human GAL4-DBD fused AR ligand binding domain transfected in human Huh7 cells co-expressing GAL4-RE-Luc assessed as reduction in dihydrotestosterone-induced luciferase activity after 16 hrs by luciferase reporter gene assay
Antagonist activity at AR in human LNCAP cells assessed as suppression of DHT-induced receptor transcriptional activity at 500 nM after 24 hrs by dual luciferase reporter gene assay
Antagonist activity at AR T877A mutant expressed in human LNCaP cells assessed as inhibition of 10 nM DHT-stimulated cell proliferation after 6 days by WST-8 assay
Antagonist activity at AR in human MDA-kb2 cells co-transfected with MMTV-luc assessed as decrease in DHT-induced luciferase activity by reporter gene assay
Antagonist activity at AR in human MDA-kb2 cells assessed as inhibition of DHT-stimulated AR activity co-treated with DHT by luciferase reporter gene assay
Antagonist activity against pSG5-tagged human androgen receptor expressed in COS1 cells assessed as receptor-mediated testosterone-induced transcriptional activity at 10 uM by AR-regulated rat probasin promoter fragment driven firefly luciferase reporter assay (Rvb = 100 +/- 5.7%)
Antagonist activity at AR (unknown origin) expressed in African green monkey COS7 cells at 7.5 uM after 24 hrs by dual luciferase reporter gene assay
Antagonist activity at human AR overexpressed in human LNCAP cells by luciferase reporter gene assay
Antagonist activity at human AR expressed in COS7 cells receptor assessed as inhibition of androgen-induced transcriptional activation at 10 nM to 10 uM by ARE-luciferase reporter gene assay

Antagonist activity at human AR expressed in COS7 cells receptor assessed as inhibition of R1881-induced transcriptional activation at 10 uM by ARE-luciferase reporter gene assay
Antagonist activity at human wild type AR expressed in human MDA-MB-435 cells by transactivation assay
Antagonist activity at GAL4-fused human AR LBD (667 to 919 residues) expressed in CHO-K1 cells assessed as inhibition of dihydrotestosterone-induced transactivation activity after 5 to 6 hrs by luciferase reporter gene assay
Antagonist activity at wild type human AR expressed in human LNCAP cells by transactivation assay
Antagonist activity at AR T877A mutant in human LNCAP cells assessed as inhibition of DHT-induced proliferation after 48 hrs by MTT assay
Antagonist activity against pSG5-tagged human androgen receptor expressed in COS1 cells assessed as reduction in receptor-mediated transcriptional activity by AR-regulated rat probasin promoter fragment driven firefly luciferase reporter assay
Antagonist activity at human AR in MDA-MB453-MMTV-luci cells by functional assay
Antagonist activity at human AR expressed in human HeLa cells co-transfected with MMTV-Luc-Hyg after 48 hrs by transient-luciferase reporter gene assay
Antagonist activity at human AR ligand binding domain expressed in african green monkey COS7 cells in presence of 5-alpha-dihydrotestosterone by Gal4 hybrid assay
Antagonist activity at AR in human LNCAP cells assessed as suppression of DHT-induced receptor transcriptional activity at 5 uM after 24 hrs by dual luciferase reporter gene assay
Antagonist activity at human AR overexpressed in human LNCAP cells at 1 uM by luciferase reporter gene assay in the presence of agonist R1881
Antagonist activity at human ERalpha expressed in african green monkey CV1 cells co-transfected with ERE-MMTV-Luc by luciferase reporter gene assay relative to control
Antagonist activity at human ERbeta expressed in african green monkey CV1 cells co-transfected with ERE-MMTV-Luc by luciferase reporter gene assay relative to control
Antagonist activity at human ERbeta expressed in african green monkey CV1 cells co-transfected with ERE-MMTV-Luc by luciferase reporter gene assay
Antagonist activity at human ERalpha expressed in african green monkey CV1 cells co-transfected with ERE-MMTV-Luc by luciferase reporter gene assay
Antagonist activity at human wild type ERalpha expressed in HEK293T cells co-expressing ERE assessed as inhibition of estradiol-induced transactivation by luciferase reporter gene assay
Antagonist activity at human wild type ERbeta expressed in HEK293T cells co-expressing ERE assessed as inhibition of estradiol-induced transactivation by luciferase reporter gene assay
Antagonist activity at ERalpha (unknown origin) expressed in human HuH7 cells assessed as inhibition of E2-induced ERE-TATA activation up to 100 uM after 30 hrs by luciferase reporter gene assay
Antagonist activity at human Gal4-fused ER-beta expressed in HEK293 cells assessed as inhibition of 17beta-estradiol-induced effect at 1 uM by luciferase reporter gene assay
Antagonist activity at human recombinant ERalpha expressed in MCF7 cells assessed as ERE-driven transactivation at 2.5 uM by luciferase reporter assay relative to estradiol
Antagonist activity at human estrogen receptor expressed in mouse C2C12 cells at 5 uM pretreated for 1 day measured 36 hrs post transfection by luciferase reporter gene assay in presence of ER agonist estradiol
Antagonist activity at ER-beta (unknown origin) transfected in HEK293T cells assessed as inhibition of transcriptional activity after 24 hrs by luciferase reporter gene assay
Antagonist activity at ER-alpha (unknown origin) transfected in HEK293T cells assessed as inhibition of transcriptional activity after 24 hrs by luciferase reporter gene assay relative to 17-beta estradiol

Antagonist activity at full length ERbeta (unknown origin) expressed in human HeLa cells assessed as reduction in 17-beta estradiol-induced response at 10'-5M incubated for 24 hrs by ERE-driven luciferase reporter gene assay relative to untreated control
Antagonist activity at ERalpha (unknown origin) expressed in human HepG2 cells assessed as inhibition of transcriptional activation after 24 hrs by ERE-luciferase reporter gene assay relative to 17beta-estradiol
Antagonist activity at ER-beta (unknown origin) transfected in HEK293T cells assessed as inhibition of transcriptional activity after 24 hrs by luciferase reporter gene assay relative to 17-beta estradiol
Antagonist activity at human Gal4-fused ER-beta expressed in HEK293 cells assessed as inhibition of 17beta-estradiol-induced effect by luciferase reporter gene assay
Antagonist activity at full length ERalpha (unknown origin) expressed in human HeLa cells up to 10 uM incubated for 24 hrs by ERE-driven luciferase reporter gene assay
Antagonist activity at full length ERalpha (unknown origin) expressed in human HeLa cells incubated for 24 hrs by ERE-driven luciferase reporter gene assay
Antagonist activity at human wild type ERalpha expressed in human HeLa cells co-expressing ERE assessed as inhibition of transactivation activity by luciferase reporter gene assay
Antagonist activity at ERbeta (unknown origin) expressed in human HepG2 cells assessed as inhibition of 17beta-estradiol-induced transcriptional activation after 24 hrs by ERE-luciferase reporter gene assay relative to 17beta-estradiol
Antagonist activity at human Gal4-fused ER-beta expressed in HEK293 cells assessed as inhibition of 17beta-estradiol-induced effect at 3 uM by luciferase reporter gene assay
Antagonist activity at full length ERbeta (unknown origin) expressed in human HeLa cells incubated for 24 hrs by ERE-driven luciferase reporter gene assay
Antagonist activity at ERbeta (unknown origin) expressed in human HepG2 cells assessed as inhibition of 17beta-estradiol-induced transcriptional activation after 24 hrs by ERE-luciferase reporter gene assay
Antagonist activity at human Gal4-fused ER-alpha expressed in HEK293 cells assessed as inhibition of 17beta-estradiol-induced effect by luciferase reporter gene assay
Antagonist activity at human ER ligand binding domain expressed in african green monkey COS7 cells in presence of 17-beta-estradiol by Gal4 hybrid assay
Antagonist activity at human wild type ERbeta expressed in human HeLa cells co-expressing ERE assessed as inhibition of transactivation activity by luciferase reporter gene assay
Antagonist activity at ER-alpha (unknown origin) transfected in HEK293T cells assessed as inhibition of transcriptional activity after 24 hrs by luciferase reporter gene assay
Antagonist activity at human ERalpha expressed in human HeLa cells coexpressing ERE-E1b-Luc assessed as inhibition of estradiol-induced transcriptional activation at 1 uM after 48 hrs by luciferase reporter gene assay
Antagonist activity at ERalpha in human MCF7:WS8 cells assessed as E2-induced ERE activation after 18 hrs by luciferase reporter gene assay
Antagonist activity at human Gal4-fused ER-alpha expressed in HEK293 cells assessed as inhibition of 17beta-estradiol-induced effect at 3 uM by luciferase reporter gene assay
Antagonist activity at human LXR-alpha expressed in African green monkey CV1 cells measured after 18 to 20 hrs in presence of LXR pan agonist 1-(2,4-difluorobenzyl)-2-oxo-6-(4-phenoxyphenyl)-4-(trifluoromethyl)-1,2-dihydropyridine-3-carbonitrile by luciferase reporter gene assay
Antagonist activity at human LXR-beta expressed in HEK293 cells after 16 hrs by luciferase reporter gene assay
Antagonist activity at human LXR-alpha expressed in HEK293 cells after 16 hrs by luciferase reporter gene assay
Antagonist activity at human LXR-alpha expressed in African green monkey CV1 cells measured after 18 to 20 hrs in presence of LXR pan agonist 1-(2,4-difluorobenzyl)-2-oxo-6-(4-phenoxyphenyl)-4-(trifluoromethyl)-1,2-dihydropyridine-3-carbonitrile by luciferase reporter gene assay relative to control

Antagonist activity at human LXR-beta expressed in African green monkey CV1 cells up to 10000 nM measured after 18 to 20 hrs in presence of LXR pan agonist 1-(2,4-difluorobenzyl)-2-oxo-6-(4-phenoxyphenyl)-4-(trifluoromethyl)-1,2-dihydropyridine-3-carbonitrile by luciferase reporter gene assay
Antagonist activity at human LXR-beta transfected in HEK293 cells at 30 uM after 16 hrs by luciferase reporter gene assay in presence of 0.1 uM N-(4-(1,1,1,3,3,3-hexafluoro-2-hydroxypropan-2-yl)phenyl)-N-(2,2,2-trifluoroethyl)benzenesulfonamide
Antagonist activity at human LXR-beta expressed in HEK293 cells assessed as inhibition of T0901317-induced effect after 16 hrs by luciferase reporter gene assay
Antagonist activity at human LXR-alpha expressed in HEK293 cells assessed as inhibition of T0901317-induced effect after 16 hrs by luciferase reporter gene assay
Antagonist activity at human LXR-alpha transfected in HEK293 cells after 16 hrs by luciferase reporter gene assay in presence of 0.3 uM N-(4-(1,1,1,3,3,3-hexafluoro-2-hydroxypropan-2-yl)phenyl)-N-(2,2,2-trifluoroethyl)benzenesulfonamide
Antagonist activity at human LXR-alpha transfected in HEK293 cells at 30 uM after 16 hrs by luciferase reporter gene assay in presence of 0.3 uM N-(4-(1,1,1,3,3,3-hexafluoro-2-hydroxypropan-2-yl)phenyl)-N-(2,2,2-trifluoroethyl)benzenesulfonamide
Antagonist activity at human LXR-beta transfected in HEK293 cells after 16 hrs by luciferase reporter gene assay in presence of 0.1 uM N-(4-(1,1,1,3,3,3-hexafluoro-2-hydroxypropan-2-yl)phenyl)-N-(2,2,2-trifluoroethyl)benzenesulfonamide
Antagonist activity against human FXR expressed in human HeLa cells incubated for 24 hrs by luciferase reporter gene assay
Antagonist activity at human FXR expressed in COS1 cells assessed as inhibition of CDCA-induced receptor activation after 2 days by luciferase reporter gene assay
Antagonist activity at FXR expressed in human HepG2 cells assessed as inhibition of CDCA-mediated transactivation at 10 uM after 48 hrs by luciferase reporter gene assay
Antagonist activity at human FXR expressed in human HepG2 cells assessed as upregulation of CYP7A1 gene transactivation at 10 uM by measuring relative luciferase activity by transient transfection reporter assay relative to control
Antagonist activity at human FXR expressed in human HepG2 cells assessed as upregulation of CYP7A1 gene transactivation at 100 uM by measuring relative luciferase activity by transient transfection reporter assay relative to control
Antagonist activity at human FXR expressed in african green monkey CV1 cells co-expressing RXRE with RXR co-factor by luciferase reporter gene assay
Antagonist activity at human FXR expressed in HEK293 cells assessed as inhibition of GW4064-induced transactivation after 24 hrs by luciferase reporter gene assay
Antagonist activity at FXR (unknown origin) expressed in human HepG2 cells assessed as inhibition of 6-ECDCA-induced FXR/Src-1-mediated transcription activation complex formation at 15 uM after 18 hrs by chromatin immunoprecipitation assay
Antagonist activity at FXR expressed in human HepG2 cells assessed as inhibition of CDCA-mediated transactivation at 50 uM after 48 hrs by luciferase reporter gene assay
Antagonist activity at FXR expressed in human HepG2 cells assessed as inhibition of 6-ECDCA-mediated transactivation at 50 uM after 48 hrs by luciferase reporter gene assay
Antagonist activity at human full length FXR expressed in HeLa cells cotransfected with pSG5-human RXR at 30 uM after 24 hrs by Dual-Glo luciferase reporter gene assay
Antagonist activity at human FXR expressed in human HepG2 cells assessed as inhibition of CDCA-induced transactivation of SHP gene by measuring relative luciferase activity by transient transfection reporter assay relative to control
Antagonist activity at human FXR expressed in human HepG2 cells assessed as inhibition of CDCA-induced transactivation of SHP gene at 10 uM by measuring relative luciferase activity by transient transfection reporter assay relative to control

Antagonist activity at GAL4-DBD fused human FXR LBD expressed in HEK293T cells assessed as inhibition of GW4064-induced receptor activation at 10 uM after 24 hrs by luciferase reporter gene assay relative to control
Antagonist activity at FXR expressed in human HepG2 cells assessed as inhibition of 6-ECDCA-mediated transactivation at 10 uM after 48 hrs by luciferase reporter gene assay
Antagonist activity at human FXR expressed in human HepG2 cells assessed as inhibition of CDCA-induced transactivation of SHP gene at 100 uM by measuring relative luciferase activity by transient transfection reporter assay relative to control
Antagonist activity at Gal4 DNA binding domain-tagged human FXR ligand binding domain expressed in HEK293 cells assessed as inhibition of receptor-mediated transcriptional activity by luciferase reporter gene assay
Antagonist activity at human FXR expressed in human HeLa cells co-expressing BSEP up to 10 uM after 24 hrs by dual-glo luciferase reporter gene assay
Antagonist activity at GAL4-fused human FXR expressed in HEK293T cells assessed as inhibition of T0901317-induced basal transcriptional activity up to 10 uM after 20 hrs by dual-glo luciferase reporter gene assay
Antagonist activity at human FXR expressed in human HepG2 cells assessed as inhibition of CDCA-induced transactivation of SHP gene at 50 uM by measuring relative luciferase activity by transient transfection reporter assay relative to control
Antagonist activity at FXR (unknown origin) expressed in human HepG2 cells assessed as inhibition of 6-ECDCA-induced NCoR binding to chromatin at 15 uM after 18 hrs by chromatin immunoprecipitation assay
Antagonist activity at human FXR expressed in human HeLa cells assessed as inhibition of receptor activation by BSEP promoter-driven firefly luciferase reporter gene assay relative to untreated control
Antagonist activity at human full length FXR expressed in HeLa cells cotransfected with pSG5-human RXR after 24 hrs by Dual-Glo luciferase reporter gene assay
Antagonist activity at human full length FXR expressed in HeLa cells cotransfected with pSG5-human RXR at 10 uM after 24 hrs by Dual-Glo luciferase reporter gene assay
Antagonist activity at human FXR expressed in human HeLa cells assessed as inhibition of receptor activation by BSEP promoter-driven firefly luciferase reporter gene assay
Antagonist activity at human FXR expressed in CV-1 cells assessed as inhibition of CDCA-induced receptor transactivation after 24 hrs by luciferase reporter gene assay
Antagonist activity at human FXR expressed in monkey CV1 cells after 24 hrs by ecdysone receptor response element-driven luciferase reporter assay
Antagonist activity at human FXR expressed in CV-1 cells assessed as inhibition of CDCA-induced receptor transactivation upto 100 uM after 24 hrs by luciferase reporter gene assay
Antagonist activity at GAL4-DBD fused human FXR LBD expressed in HEK293T cells assessed as inhibition of CDCA-induced receptor activation after 24 hrs by luciferase reporter gene assay
Antagonist activity at FXR (unknown origin) expressed in human HepG2 cells co-expressing RXR assessed as inhibition of CDCA-induced transactivation at 50 uM after 18 hrs by luciferase reporter gene assay
Antagonist activity at GAL4-fused human FXR expressed in HEK293 cells assessed as inhibition of T0901317-stimulated transcriptional activity after 20 hrs by dual-glo luciferase reporter gene assay
Antagonist activity at human FXR expressed in CV-1 cells assessed as inhibition of CDCA-induced transactivation after 24 hrs by luciferase reporter gene assay
Antagonist activity at FXR (unknown origin) expressed in human HepG2 cells co-expressing RXR assessed as inhibition of CDCA-induced transactivation after 18 hrs by luciferase reporter gene assay
Antagonist activity at GAL4-DBD fused human FXR LBD expressed in HEK293T cells assessed as inhibition of CDCA-induced receptor activation at 10 uM after 24 hrs by luciferase reporter gene assay relative to control

Antagonist activity at human FXR transfected in human HuH7 cells co-transfected with human BSEP promoter reporter plasmid at 10 uM after 30 hrs by dual-luciferase reporter assay relative to chenodeoxycholate
Antagonist activity at human FXR expressed in HepG2 cells assessed as inhibition of CDCA-induced transactivation at 10 uM after 18 hrs by luciferase reporter gene assay
Antagonist activity at human FXR transfected in human HepG2 cells assessed as supression of CDCA-induced transcriptional activity at 50 uM by beta-galactosidase reporter gene assay
Antagonist activity at human FXR expressed in HEK293 cells assessed as inhibition of GW-4064-induced response at 100 uM by GAL4 activation assay
Antagonist activity against FXR (unknown origin) expressed in human HepG2 cells assessed as inhibition of CDCA-induced stimulation of FXR response element IR1-mediated receptor transactivation at 50 uM by luciferase reporter gene assay
Antagonist activity at human GR expressed in H4IIEC3 cells by tyrosine amino transferase GRE activation assay
Antagonist activity at GR in human HepG2 cells assessed as inhibition of protein mediated-transcriptional activity at 10 uM by MMTV-promoter driven luciferase reporter gene assay
Antagonist activity at recombinant GR LBD expressed in HEK293T cells co-expressing GAL4 DBD assessed as inhibition of dexamethasone-induced transactivation at 20 uM by luciferase reporter gene assay
Antagonist efficacy at human GR expressed in CV1 cells by GRE activation assay relative to Dexamethasone
Antagonist activity at human GR ligand binding domain expressed in african green monkey COS7 cells in presence of Dexamethasone by Gal4 hybrid assay
Antagonist activity at GR in human HepG2 cells assessed as inhibition of protein mediated-transcriptional activity by MMTV-promoter driven luciferase reporter gene assay
Antagonist activity at human GR expressed in CV1 cells by GRE activation assay
Antagonist activity at glucocorticoid receptor (unknown origin) expressed in mouse C2C12 cells at 5 uM pretreated for 1 day measured 36 hrs post transfection by luciferase reporter gene assay in presence of GR agonist dextromethorphan
Antagonist activity at human GR receptor expressed in human HeLa cells assessed as inhibition of DHT-induced response after 40 hrs by luciferase/beta-galactosidase-based reporter gene assay
Antagonist activity at GAL4-fused human GR LBD (443 to 777 residues) expressed in CHO-K1 cells assessed as inhibition of dexamethasone-induced transactivation activity after 5 to 6 hrs by luciferase reporter gene assay
Antagonist activity against pSG5-Gal4-tagged human PPAR-alpha ligand binding domain expressed in COS1 cells assessed as inhibition of bezafibrate-induced receptor activation at 1 nM to 100000 nM incubated for 19 hrs by pGL3-5XUAS-SV40 luciferase reporter gene assay
Antagonist activity against pSG5-Gal4-tagged human PPAR-beta/delta ligand binding domain expressed in COS1 cells assessed as inhibition of GW501516-induced receptor activation incubated for 19 hrs by pGL3-5XUAS-SV40 luciferase reporter gene assay
Antagonist activity against pSG5-Gal4-tagged human PPAR-gamma ligand binding domain expressed in COS1 cells assessed as inhibition of rosiglitazone-induced receptor activation at 20 nM to 20000 nM incubated for 19 hrs by pGL3-5XUAS-SV40 luciferase reporter gene assay
Antagonist activity at human PPAR-alpha assessed as inhibition of GW7647-induced effect after overnight incubation by cell-based luciferase reporter gene assay
Antagonist activity against pSG5-Gal4-tagged human PPAR-alpha ligand binding domain expressed in COS1 cells assessed as inhibition of bezafibrate-induced receptor activation at 1 nM to 100000 nM incubated for 19 hrs by pGL3-5XUAS-SV40 luciferase reporter gene assay
Antagonist activity against pSG5-Gal4-tagged human PPAR-beta/delta ligand binding domain expressed in COS1 cells assessed as inhibition of GW501516-induced receptor activation incubated for 19 hrs by pGL3-5XUAS-SV40 luciferase reporter gene assay

Antagonist activity against pSG5-Gal4-tagged human PPAR-gamma ligand binding domain expressed in COS1 cells assessed as inhibition of rosiglitazone-induced receptor activation at 20 nM to 20000 nM incubated for 19 hrs by pGL3-5XUAS-SV40 luciferase reporter gene assay
Antagonist activity at human PPAR-alpha assessed as inhibition of GW7647-induced effect after overnight incubation by cell-based luciferase reporter gene assay
Antagonist activity at human PR B-form expressed in human PC3 cells assessed as inhibition of R5020-induced transactivation at 1 uM after 24 hrs by luciferase reporter gene assay
Antagonist activity at human PR in T47D cells assessed as MMTV-driven transactivation at 5 uM by luciferase reporter assay relative to progesterone
Antagonist activity at human PR B-form expressed in human PC3 cells assessed as inhibition of R5020-induced transactivation at 0.1 uM after 24 hrs by luciferase reporter gene assay
Antagonistic activity against Progesterone receptor (PR) in transcriptional activation assay in human T47D breast carcinoma cell line
Antagonist activity at recombinant PR LBD expressed in HEK293T cells co-expressing GAL4 DBD assessed as inhibition of progesterone-induced transactivation at 20 uM by luciferase reporter gene assay
Antagonist activity at PR in human T47D cells assessed as inhibition of progesterone-induced response after 24 hrs by alkaline phosphatase assay
Antagonist activity at GAL4-fused human PR LBD (680 to 933 residues) expressed in CHO-K1 cells assessed as inhibition of progesterone-induced transactivation activity after 5 to 6 hrs by luciferase reporter gene assay
Antagonist activity at PR in human T47D cells assessed as inhibition of progesterone-induced alkaline phosphatase expression after 24 hrs by alkaline phopshatase assay
Antagonist activity at human full-length PXR transfected in human HepG2 cells co-transfected with pSG5-RXR assessed as reversal of rifaximin-induced transactivation at 10 to 25 uM after 18 hrs by luciferase reporter gene assay
Antagonist activity at human PXR expressed in human HepG2 cells coexpressing CYP3A4 assessed as inhibition of rifampicin-induced receptor activation up to 100 uM after 24 hrs by dual luciferase reporter gene assay
Antagonist activity at GAL4-tagged human PXR isoform 1 ligand binding domain (138 to 434 residues) expressed in HEK293T cells at 1 uM after 12 to 14 hrs by dual-glo luciferase reporter gene assay
Antagonist activity at human full-length PXR transfected in human HepG2 cells co-transfected with pSG5-RXR assessed as reversal of rifaximin-induced transactivation at 50 uM after 18 hrs by luciferase reporter gene assay
Antagonist activity at full length human PXR transfected in human HepG2 cells assessed as reduction in rifaximin-induced receptor transactivation after 18 hrs by luciferase reporter assay
Antagonist activity at Gal4 DNA binding domain-tagged human PXR ligand binding domain expressed in HEK293 cells assessed as inhibition of receptor-mediated transcriptional activity by luciferase reporter gene assay
Antagonist activity at human PXR transfected in African green monkey CV1 cells assessed as inhibition of SR12813-induced transactivation after 24 hrs by luciferase reporter gene assay
Antagonist activity at human PXR expressed in human HepG2 cells coexpressing CYP3A4 assessed as inhibition of rifampicin-induced receptor activation at 30 uM after 24 hrs by dual luciferase reporter gene assay
Antagonist activity at GAL4-fused human PXR expressed in HEK293 cells assessed as inhibition of T0901317-stimulated transcriptional activity after 20 hrs by dual-glo luciferase reporter gene assay
Antagonist activity at human PXR transfected in human HepG2 cells co-transfected with pSG5-RXR/pCMV-beta-galactosidase/p(CYP3A4)-TK-Luc assessed as inhibition of rifaximin-induced transactivation after 18 hrs by luciferase reporter gene assay

Antagonist activity at human PXR transfected in human HepG2 cells co-transfected with pSG5-RXR/pCMV-beta-galactosidase/p(CYP3A4)-TK-Luc assessed as inhibition of rifaximin-induced transactivation at 50 uM after 18 hrs by luciferase reporter gene assay
Antagonist activity at GAL4-fused human PXR expressed in HEK293T cells assessed as inhibition of T0901317-induced basal transcriptional activity up to 10 uM after 20 hrs by dual-glo luciferase reporter gene assay
Antagonist activity at full length human PXR transfected in human HepG2 cells assessed as reduction in rifaximin-induced receptor transactivation at 50 uM after 18 hrs by luciferase reporter assay
Antagonist activity at AR T877A mutant in human LNCAP cells assessed as inhibition of DHT-induced TMPRSS2 mRNA level at 5 uM after 24 hrs by SYBR Green dye based qPCR method
Antagonist activity at AR T877A mutant in human LNCAP cells assessed as inhibition of DHT-induced c-Myc mRNA level at 1 uM after 24 hrs by SYBR Green dye based qPCR method
Antagonist activity at AR T877A mutant in human LNCAP cells assessed as inhibition of DHT-induced TMPRSS2 mRNA level at 1 uM after 24 hrs by SYBR Green dye based qPCR method
Antagonist activity at AR T877A mutant in human LNCAP cells assessed as inhibition of DHT-induced PSA mRNA level at 1 uM after 24 hrs by SYBR Green dye based qPCR method
Antagonist activity at AR T877A mutant in human LNCAP cells assessed as inhibition of DHT-induced PSA mRNA level at 5 uM after 24 hrs by SYBR Green dye based qPCR method
Antagonist activity at AR T877A mutant in human LNCAP cells assessed as inhibition of DHT-induced c-Myc mRNA level at 5 uM after 24 hrs by SYBR Green dye based qPCR method
Antagonist activity at AR T877A mutant in human LNCAP cells assessed as inhibition of DHT-induced Cyclin D1 mRNA level at 5 uM after 24 hrs by SYBR Green dye based qPCR method
Antagonist activity at AR T877A mutant expressed in human LNCaP cells assessed as inhibition of 10 nM testosterone-induced PSA production after 48 hrs by ELISA method
Antagonist activity at AR T877A mutant in human LNCAP cells assessed as inhibition of DHT-induced Cyclin D1 mRNA level at 1 uM after 24 hrs by SYBR Green dye based qPCR method
Antagonist activity at FXR in human Hep3B cells assessed as inhibition of CDCA-induced SHP expression level at 0.2 to 5 uM after 24 hrs by RT-PCR method
Antagonist activity at FXR in human Hep3B cells assessed as inhibition of CDCA-induced decrease in CYP7A1 expression level at 0.2 to 5 uM after 24 hrs by RT-PCR method
Antagonist activity at AR in human LNCAP cells assessed as downregulation of AR protein expression after 24 hrs by Western blot analysis
Antagonist activity at human beta2-AR expressed in CHOK1 cells assessed as inhibition of cimaterol-induced CRE-SPAP production at 2 uM after 5 hrs
Antagonist activity at AR in human LNCAP cells assessed as downregulation of PSA mRNA levels at 500 nM after 24 hrs in presence of DHT by RT-PCR analysis
Antagonist activity at AR in human LNCAP cells assessed as downregulation of PSA mRNA levels at 5 uM after 24 hrs in presence of DHT by RT-PCR analysis
Antagonist activity at human beta1-AR expressed in CHOK1 cells assessed as inhibition of cimaterol-induced CRE-SPAP production at 2 uM after 5 hrs
Antagonist activity at AR in human MCF7 cells assessed as reduction in AR level at 30 uM after 24 hrs by Western blot analysis relative to control
Antagonist activity at human beta2-AR expressed in CHOK1 cells assessed as inhibition of cimaterol-induced CRE-SPAP production at 20 uM after 5 hrs
Antagonist activity at AR in human LNCAP cells assessed as suppression of DHT-induced AR protein level measured after 24 hrs relative to control
Antagonist activity at human beta1-AR expressed in CHOK1 cells assessed as inhibition of cimaterol-induced CRE-SPAP production at 20 uM after 5 hrs
Antagonist activity at AR in human LNCAP cells assessed as effect on cell proliferation after 6 days
Antagonist activity at human alpha2a-AR expressed in CHO cells assessed as inhibition of (-)-noradrenaline-induced acidification rate after 240 mins by cytosensor microphysiometric analysis

Antagonist activity at AR in human LNCAP cells assessed as suppression of DHT-induced AR protein level at 10 uM measured after 24 hrs relative to control
Antagonist activity at AR in human bicalutamide-resistant LNCAP cells assessed as inhibition of cell proliferation after 6 days
Antagonist activity at AR in bicalutamide-resistant human LNCAP cells assessed as effect on cell proliferation after 6 days
Antagonist activity at human beta1-AR expressed in CHOK1 cells assessed as inhibition of cimaterol-induced CRE-SPAP production at 100 uM after 5 hrs
Antagonist activity at human beta2-AR expressed in CHOK1 cells assessed as inhibition of cimaterol-induced CRE-SPAP production at 100 uM after 5 hrs
Antagonist activity at estrogen receptor in human Ishikawa cells assessed as inhibition of ERE-dependent alkaline phosphatase levels at 1 uM
Antagonist activity at ERbeta in HEK293 cells assessed as inhibition of ERE-dependent luciferase expression at 1 uM
Antagonist activity at ERalpha in human MCF7:D5L cells assessed as inhibition of ERE-dependent luciferase expression at 1 uM
Antagonist activity at ER in human MCF7:WS8 cells assessed as inhibition of estradiol-induced cell growth by measuring DNA level at 10'-6 M after 7 days by fluorescence analysis
Antagonist activity at ER in human MCF7:WS8 cells assessed as inhibition of estradiol-induced cell growth by measuring DNA level after 7 days treated at highesy drug concentration by fluorescence analysis
Antagonist activity at human ERalpha receptor expressed in human MCF7:D5L cells co-expressing ERE assessed as inhibition of estradiol-induced of luciferase gene expression at 1 uM after 18 hrs relative to ICI182780
Antagonist activity at human ERbeta receptor expressed in human HEK293 cells co-expressing ERE assessed as inhibition of estradiol-induced of luciferase gene expression at 1 uM after 18 hrs relative to ICI182780
Antagonist activity at ER in human MCF7:WS8 cells assessed as inhibition of estradiol-induced cell growth by measuring DNA level after 7 days by fluorescence analysis
Antagonist activity at estrogen receptor in human Ishikawa cells assessed as inhibition of ERE-dependent alkaline phosphatase levels at 1 uM relative to ICI-182780
Antagonist activity at ERbeta in HEK293 cells assessed as inhibition of ERE-dependent luciferase expression at 1 uM relative to ICI-182780
Antagonist activity at ER alpha in human MCF7 cells assessed as inhibition of estradiol-induced PR expression treated for 24 hrs after incubation with estradiol for 30 mins by laser scanning imaging cytometer analysis
Antagonist activity at ERalpha in human MCF7:D5L cells assessed as inhibition of ERE-dependent luciferase expression at 1 uM relative to ICI-182780
Antagonist activity at human FXR in human HepG2 cells assessed as inhibition of CDCA induced SHP gene expression at 5 to 40 uM after 24 hrs by RT-PCR analysis
Antagonist activity at FXR in human HepG2 cells assessed as inhibition of CDCA-induced Cyp7A1 gene expression at 50 uM by real time PCR
Antagonist activity at human FXR in human HepG2 cells assessed as reduction in triglyceride level after 24 hrs
Antagonist activity at FXR in human HepG2 cells assessed as inhibition of CDCA-induced OSTbata gene expression at 50 uM by real time PCR
Antagonist activity at human FXR in human HepG2 cells assessed as reduction in triglyceride level at 10 uM after 24 hrs
Antagonist activity at human FXR in human HepG2 cells assessed as inhibition of CDCA induced BSEP gene expression at 5 to 40 uM after 24 hrs by RT-PCR analysis
Antagonist activity at FXR (unknown origin) expressed in human HepG2 cells co-expressing RXR assessed as inhibition of CyP7alpha1 gene expression at 50 uM after 18 hrs by RT-PCR analysis

Antagonist activity at human FXR in human HepG2 cells assessed as reduction in cholesterol level after 24 hrs
Antagonist activity at human FXR in human HepG2 cells assessed as reduction in triglyceride level at 40 uM after 24 hrs
Antagonist activity at human FXR in human HepG2 cells assessed as reduction in cholesterol level at 10 uM after 24 hrs
Antagonist activity at human FXR in human HepG2 cells assessed as inhibition of CDCA induced SREBP1c gene expression at 5 to 40 uM after 24 hrs by RT-PCR analysis
Antagonist activity at FXR in human HepG2 cells assessed as inhibition of CDCA-induced BSEP gene expression at 50 uM by real time PCR
Antagonist activity at human FXR in human HepG2 cells assessed as inhibition of CDCA induced decrease of Cyp7A1 gene expression at 5 to 40 uM after 24 hrs by RT-PCR analysis
Antagonist activity at FXR (unknown origin) expressed in human HepG2 cells co-expressing RXR assessed as inhibition of CDCA-induced SHP gene expression at 50 uM after 18 hrs by RT-PCR analysis
Antagonist activity at FXR (unknown origin) expressed in human HepG2 cells co-expressing RXR assessed as inhibition of CDCA-induced OSTalpha gene expression at 50 uM after 18 hrs by RT-PCR analysis
Antagonist activity at human FXR in human HepG2 cells assessed as reduction in cholesterol level at 40 uM after 24 hrs
Antagonist activity at FXR in human HepG2 cells assessed as inhibition of CDCA-induced OSTalpha gene expression at 50 uM by real time PCR
Antagonist activity at human GR DNA binding domain transfected in CHO cells co-transfected with MMTV-luciferase gene assessed as inhibition of cortisol-induced luciferase activity
Antagonist activity at GR in human A549 cells transfected with luciferase gene linked to MMTV promoter assessed as inhibition of dexamethasone-induced luciferase transactivation activity after 24 hrs
Antagonist activity at GR in human A549 cells transfected with luciferase gene linked to MMTV promoter assessed as inhibition of dexamethasone-induced luciferase transactivation activity after 24 hrs relative to RU486
Antagonist activity at ERalpha in human MCF7 cells assessed as reduction in E2-induced PR expression at 20 uM incubated for 2 hrs prior to E2-induction measured after 14 hrs by qPCR analysis
Antagonist activity at human PR expressed in human T47D cells assessed as inhibition of progesterone-induced alkaline phosphatase relative to R5020
Antagonist activity at PR in human T47D cells assessed as inhibition of progesterone-inducted alkaline phosphatase expression after 24 hrs by plate reader analysis
Antagonist activity at ER alpha in human MCF7 cells assessed as inhibition of estradiol-induced PR expression treated for 24 hrs after incubation with estradiol for 30 mins by laser scanning imaging cytometer analysis
Antagonist activity at human PR expressed in human T47D cells assessed as inhibition of progesterone induced alkaline phosphatase
Antagonist activity at PXR (unknown origin) transfected in human HepG2 cells assessed as inhibition of rifampicin-induced reporter gene transcription
Antagonist activity against PXR in human HepG2 cells assessed as inhibition of rifaximin-induced CYP3A4 gene expression at 25 uM after 18 hrs by quantitative real-time PCR analysis
Antagonist activity at PXR expressed in human HepG2 cells assessed as inhibition of rifaximin-induced CYP3A4 mRNA expression at 50 uM by RT-PCR analysis
Antagonist activity at PXR in human HepG2 cells assessed as inhibition of rifaximin-induced CYP3A4 mRNA expression at 50 uM after 18 hrs by real time-PCR analysis
Agonist activity at human gal-AR expressed in african green monkey CV1 cells co-expressing MH100 with pGRIP1 co-factor by luciferase reporter gene assay

Agonist activity at human AR expressed in African green monkey CV1 cells assessed as supression of beta-catenin at 1000 nM after 17 hrs by Wnt 12xTcf-luciferase reporter gene assay relative to control
Agonist activity at AR F876L mutant (unknown origin) transfected in human PC3 cells assessed as receptor transcriptional activation at 500 nM after 24 hrs in absence of DHT by PSA-luciferase reporter gene assay
Agonist activity at AR T877A mutant (unknown origin) transfected in human PC3 cells assessed as receptor transcriptional activation at 50 to 5000 nM after 24 hrs in absence of DHT by PSA-luciferase reporter gene assay
Agonist activity at AR F876L mutant (unknown origin) expressed in human PC3 cells assessed as receptor transcriptional activation at 50 to 5000 nM after 24 hrs in absence of DHT by PSA-luciferase reporter gene assay
Agonist activity at AR T877A mutant (unknown origin) expressed in human PC3 cells assessed as receptor transactivation at 5 uM after 24 hrs by PSA-luciferase reporter gene assay
Agonist activity at AR in human MDA-kb2 cells co-transfected with MMTV-luc assessed as luciferase activity by reporter gene assay
Agonist activity at AR W741C/T877A double mutant (unknown origin) transfected in human PC3 cells assessed as receptor transcriptional activation at 50 to 5000 nM after 24 hrs in absence of DHT by PSA-luciferase reporter gene assay
Agonist activity at wild type AR in human PC3 cells assessed as receptor transcriptional activation at 50 to 5000 nM after 24 hrs in absence of DHT by PSA-luciferase reporter gene assay
Agonist activity at AR W741C/T877A double mutant (unknown origin) expressed in human PC3 cells assessed as receptor transactivation at 5 uM after 24 hrs by PSA-luciferase reporter gene assay
Agonist activity at human gal-AR expressed in african green monkey CV1 cells co-expressing MH100 with pGRIP1 co-factor up to 10 uM by luciferase reporter gene assay relative to control
Agonist activity at human AR expressed in African green monkey CV1 cells assessed as N/C interaction after 17 hrs by luciferase reporter gene assay
Agonist activity at human AR expressed in African green monkey CV1 cells after 17 hrs by ARE-driven luciferase reporter gene assay
Agonist activity at human AR expressed in human HeLa cells co-transfected with MMTV-Luc-Hyg after 48 hrs by transient-luciferase reporter gene assay
Agonist activity at human AR expressed in African green monkey CV1 cells assessed as supression of beta-catenin at >= 1 nM after 17 hrs by Wnt 12xTcf-luciferase reporter gene assay relative to control
Agonist activity at wild type AR expressed in human SC cells assessed as effect on cell proliferation by WST-8 assay
Agonist activity at human AR overexpressed in human LNCAP cells assessed as fold increase at 1 uM by luciferase reporter gene assay relative to R1881
Agonist activity at human AR expressed in African green monkey COS7 cells after 24 hrs by luciferase reporter gene assay
Agonist activity at human A2A-AR expressed in FlpIn-CHO cells assessed as inhibition of forskolin-stimulated cAMP accumulation by measuring agonist transduction coefficient preincubated for 40 mins followed by forskolin addition measured after 30 mins by Alphascreen assay
Agonist activity at human AR ligand binding domain expressed in african green monkey COS7 cells by Gal4 hybrid assay
Agonist activity at human A2A-AR expressed in FlpIn-CHO cells assessed as inhibition of forskolin-stimulated cAMP accumulation preincubated for 40 mins followed by forskolin addition measured after 30 mins by Alphascreen assay relative to control
Agonist activity at human A2A-AR expressed in FlpIn-CHO cells assessed as inhibition of forskolin-stimulated cAMP accumulation preincubated for 40 mins followed by forskolin addition measured after 30 mins by Alphascreen assay

Agonist activity at AR receptor in human LNCAP cells at 10 nM to 10 uM by ARE-luciferase reporter gene assay
Agonist activity at human AR expressed in CV1 cells after 17 hrs by luciferase reporter gene assay
Agonist activity at pSG5-tagged human androgen receptor W741L mutant expressed in COS1 cells assessed as receptor-mediated transcriptional activity by AR-regulated rat probasin promoter fragment driven firefly luciferase reporter assay relative to control
Agonist activity at AR in human MDA-kb2 cells co-transfected with MMTV-luc assessed as increase in DHT-induced luciferase activity at 1 mM by reporter gene assay
Agonist activity at pSG5-tagged human androgen receptor T877A mutant expressed in COS1 cells assessed as receptor-mediated transcriptional activity by AR-regulated rat probasin promoter fragment driven firefly luciferase reporter assay relative to control
Agonist activity at human AR expressed in African green monkey CV1 cells assessed as androgen receptor beta-catenin interaction after 17 hrs by luciferase reporter gene assay
Agonist activity at human wild type ERbeta expressed in human HeLa cells co-expressing ERE assessed as transactivation activity by luciferase reporter gene assay
Agonist activity at human ERalpha expressed in human HeLa cells coexpressing ERE-E1b-Luc assessed as transcriptional activation after 48 hrs by luciferase reporter gene assay relative to estradiol
Agonist activity at human ERbeta expressed in african green monkey CV1 cells co-transfected with ERE-MMTV-Luc after 24 hrs by luciferase reporter gene assay relative to control
Agonist activity at human wild type ERalpha expressed in human HeLa cells co-expressing ERE assessed as transactivation activity by luciferase reporter gene assay
Agonist activity at human ER-alpha transfected in HEK293 cells after 48 hrs by luciferase reporter gene assay relative to estrone
Agonist activity at human ER-alpha transfected in HEK293 cells after 48 hrs by luciferase reporter gene assay
Agonist activity at GPR30 in human MCF7 cells endogenously expressing both GPR30 and ER assessed as PI3K activation at 10 nM by PIP3 nuclear accumulation assay
Agonist activity at human ER-beta transfected in HEK293 cells after 48 hrs by luciferase reporter gene assay relative to estrone
Agonist activity at estrogen receptor-alpha in human MCF7 cells by ERE-luciferase reporter gene assay
Agonist activity at human ERalpha expressed in african green monkey CV1 cells co-transfected with ERE-MMTV-Luc after 24 hrs by luciferase reporter gene assay
Agonist activity at human ERalpha expressed in african green monkey CV1 cells co-transfected with ERE-MMTV-Luc after 24 hrs by luciferase reporter gene assay relative to control
Agonist activity at ERbeta (unknown origin) expressed in human HepG2 cells assessed as transcriptional activation after 24 hrs by ERE-luciferase reporter gene assay
Agonist activity at ER-alpha (unknown origin) transfected in HEK293T cells assessed as stimulation of transcriptional activity after 24 hrs by luciferase reporter gene assay
Agonist activity at human ER-beta transfected in human 293 cells assessed as ALP reporter protein expression after 72 hrs by chemiluminescence assay
Agonist activity at human ERbeta expressed in african green monkey CV1 cells co-transfected with ERE-MMTV-Luc after 24 hrs by luciferase reporter gene assay
Agonist activity at human full-length ERbeta receptor expressed in human HEC1 cells co-expressing (ERE)2-pS2-luc gene assessed as transcriptional activation after 24 hrs by luciferase reporter gene assay
Agonist activity at human ER-beta transfected in HEK293 cells after 48 hrs by luciferase reporter gene assay
Agonist activity at ER-alpha (unknown origin) transfected in HEK293T cells after 24 hrs by Steady-Glo luciferase reporter gene assay relative to estradiol

Agonist activity at human full-length ERalpha receptor expressed in human HEC1 cells co-expressing (ERE)2-pS2-luc gene assessed as transcriptional activation after 24 hrs by luciferase reporter gene assay relative to estradiol
Agonist activity at ERalpha (unknown origin) expressed in human HepG2 cells assessed as transcriptional activation after 24 hrs by ERE-luciferase reporter gene assay
Agonist activity at human ER-alpha transfected in human 293 cells assessed as ALP reporter protein expression after 72 hrs by chemiluminescence assay
Agonist activity at human full-length ERbeta receptor expressed in human HEC1 cells co-expressing (ERE)2-pS2-luc gene assessed as transcriptional activation after 24 hrs by luciferase reporter gene assay relative to estradiol
Agonist activity at human Gal4-fused ER-alpha expressed in HEK293 cells at 10 uM by luciferase reporter gene assay relative to 17beta-estradiol
Agonist activity at ER-beta (unknown origin) transfected in HEK293T cells assessed as stimulation of transcriptional activity after 24 hrs by luciferase reporter gene assay
Agonist activity at human ERbeta expressed in human HEC1 cells assessed as transcriptional activation after 24 hrs by ERE-luciferase reporter gene transfection assay relative to estradiol
Agonist activity at human ERalpha expressed in human HEC1 cells assessed as transcriptional activation after 24 hrs by ERE-luciferase reporter gene transfection assay
Agonist activity at ERbeta (unknown origin) expressed in human HepG2 cells assessed as transcriptional activation after 24 hrs by ERE-luciferase reporter gene assay relative to 17beta-estradiol
Agonist activity at human ERalpha expressed in human HEC1 cells assessed as transcriptional activation after 24 hrs by ERE-luciferase reporter gene transfection assay relative to estradiol
Agonist activity at ER-beta (unknown origin) transfected in HEK293T cells after 24 hrs by Steady-Glo luciferase reporter gene assay
Agonist activity at full length ERalpha (unknown origin) expressed in human HeLa cells incubated for 24 hrs by ERE-driven luciferase reporter gene assay
Agonist activity at ER-beta (unknown origin) transfected in HEK293T cells assessed as stimulation of transcriptional activity after 24 hrs by luciferase reporter gene assay relative to 17-beta estradiol
Agonist activity at human recombinant ERalpha expressed in MCF7 cells assessed as ERE-driven transactivation at 2.5 uM by luciferase reporter assay relative to DMSO
Agonist activity at ER in human T47D-Kbluc cells at 10'-14 to 10'-7 M after 24 hrs by luciferase reporter gene assay
Agonist activity at ERalpha (unknown origin) expressed in human HepG2 cells assessed as transcriptional activation after 24 hrs by ERE-luciferase reporter gene assay relative to 17beta-estradiol
Agonist activity at human ERbeta expressed in human HEC1 cells assessed as transcriptional activation after 24 hrs by ERE-luciferase reporter gene transfection assay
Agonist activity at ER-alpha (unknown origin) transfected in HEK293T cells after 24 hrs by Steady-Glo luciferase reporter gene assay
Agonist activity at human full-length ERalpha receptor expressed in human HEC1 cells co-expressing (ERE)2-pS2-luc gene assessed as transcriptional activation after 24 hrs by luciferase reporter gene assay
Agonist activity at ER-alpha (unknown origin) transfected in HEK293T cells assessed as stimulation of transcriptional activity after 24 hrs by luciferase reporter gene assay relative to 17-beta estradiol
Agonist activity at ER-beta (unknown origin) transfected in HEK293T cells after 24 hrs by Steady-Glo luciferase reporter gene assay relative to estradiol
Agonist activity at full length ERbeta (unknown origin) expressed in human HeLa cells incubated for 24 hrs by ERE-driven luciferase reporter gene assay
Agonist activity at human Gal4-fused ER-beta expressed in HEK293 cells at 10 uM by luciferase reporter gene assay relative to 17beta-estradiol

Agonist activity at human Gal4-fused ER-alpha expressed in HEK293 cells by luciferase reporter gene assay
Agonist activity at estrogen receptor in human MCF7 cells assessed as ERE-mediated transcriptional activity after 24 hrs by luciferase assay
Agonist activity at human ER ligand binding domain expressed in african green monkey COS7 cells by Gal4 hybrid assay
Agonist activity at human Gal4-fused ER-beta expressed in HEK293 cells by luciferase reporter gene assay
Agonist activity at human LXR-beta expressed in HEK293 cells after 16 hrs by luciferase reporter gene assay
Agonist activity at recombinant human GAL4-DBD-fused LXRalpha-LBD expressed in HEK293T cells at 1 uM in presence of LXR-agonist 22(R)-hydroxycholesterol measured after 12 to 14 hrs by dual-glo luciferase reporter gene assay
Agonist activity at human LXR alpha expressed in Huh7 cells by GAL4 transactivation assay relative to TO901317
Agonist activity at recombinant human GAL4-DBD-fused LXRalpha-LBD expressed in HEK293T cells at 10 uM in presence of LXR-agonist 22(R)-hydroxycholesterol measured after 12 to 14 hrs by dual-glo luciferase reporter gene assay
Agonist activity at human LXR-beta transfected in HEK293 cells after 16 hrs by luciferase reporter gene assay
Agonist activity at human LXR beta expressed in Huh7 cells by GAL4 transactivation assay relative to TO901317
Agonist activity at human LXR alpha expressed in Huh7 cells by GAL4 transactivation assay
Agonist activity at human LXR beta expressed in Huh7 cells by GAL4 transactivation assay
Agonist activity at human LXRbeta expressed in African green monkey kidney CV1 cells co-expressing pTAL-LXRE including LXR response element incubated for 20 hrs by luciferase reporter gene assay
Agonist activity at human LXR-beta expressed in African green monkey CV1 cells measured after 18 to 20 hrs by luciferase reporter gene assay
Agonist activity at GAL4-fused LXR alpha (unknown origin) expressed in HEK293T cells after 20 hrs by luciferase reporter gene assay
Agonist activity at human LXR-alpha transfected in HEK293 cells after 16 hrs by luciferase reporter gene assay
Agonist activity at human LXR-alpha expressed in African green monkey CV1 cells measured after 18 to 20 hrs by luciferase reporter gene assay
Agonist activity at human LXR-beta transfected in HEK293 cells at 30 uM after 16 hrs by luciferase reporter gene assay
Agonist activity at human LXR beta receptor expressed in CHO cells by reporter assay relative to TO901317
Agonist activity at human LXR-beta expressed in African green monkey CV1 cells measured after 18 to 20 hrs by luciferase reporter gene assay relative to pan agonist 1-(2,4-difluorobenzyl)-2-oxo-6-(4-phenoxyphenyl)-4-(trifluoromethyl)-1,2-dihydropyridine-3-carbonitrile
Agonist activity at human LXR beta receptor expressed in CHO cells by reporter assay
Agonist activity at LXR-alpha (unknown origin) expressed in HEK293 cells assessed as transcriptional activation at 1 to 25 uM after 40 hrs by luciferase reporter gene assay
Agonist activity at LXR (unknown origin) in human HepG2 cells assessed as receptor transactivation at 10 uM incubated for 18 hrs by Gal4 luciferase reporter gene assay
Agonist activity at human LXRalpha expressed in African green monkey kidney CV1 cells co-expressing pTAL-LXRE including LXR response element incubated for 20 hrs by luciferase reporter gene assay

Agonist activity at human LXR-alpha transfected in HEK293 cells at 30 uM after 16 hrs by luciferase reporter gene assay
Agonist activity at human LXRalpha expressed in African green monkey kidney CV1 cells co-expressing pTAL-LXRE including LXR response element incubated for 20 hrs by luciferase reporter gene assay relative to T0901317
Agonist activity at human LXRbeta expressed in African green monkey kidney CV1 cells co-expressing pTAL-LXRE including LXR response element incubated for 20 hrs by luciferase reporter gene assay relative to T0901317
Agonist activity at human LXR-alpha expressed in African green monkey CV1 cells measured after 18 to 20 hrs by luciferase reporter gene assay relative to pan agonist 1-(2,4-difluorobenzyl)-2-oxo-6-(4-phenoxyphenyl)-4-(trifluoromethyl)-1,2-dihydropyridine-3-carbonitrile
Agonist activity at LXR-beta in human HeLa cells assessed as induction of ABCA1 by beta-galactosidase/luciferase reporter gene assay
Agonist activity at LXR-beta in human HeLa cells assessed as induction of ABCA1 by beta-galactosidase/luciferase reporter gene assay relative to control
Agonist activity at human LXR-alpha expressed in HEK293 cells after 16 hrs by luciferase reporter gene assay
Agonist activity at FXR (unknown origin) expressed in HEK293T cells after 24 hrs by GAL4-luciferase reporter gene assay
Agonist activity at FXR expressed in human HepG2 cells at 50 uM after 48 hrs by luciferase reporter gene based transactivation assay
Agonist activity at human FXR expressed in HepG2 cells assessed as renilla luciferase activity at 20 uM by luciferase based transactivation assay
Agonist activity at FXR LBD expressed in human HepG2 cells co-expressing GAL4 DBD and pG5-luc assessed as luciferase activity at 1 uM after 48 hrs by transient transfection reporter assay relative to control
Agonist activity at human FXR expressed in human HepG2 cells assessed as down-regulation of CYP7A1 gene transactivation at 10 uM by measuring relative luciferase activity by transient transfection reporter assay relative to control
Agonist activity at human full length FXR expressed in HeLa cells cotransfected with pSG5-human RXR at 10 uM after 24 hrs by Dual-Glo luciferase reporter gene assay
Agonist activity at Homo sapiens (human) FXR ligand binding domain expressed in HepG2 cells assessed as transactivation of SHP gene expression at 10 uM after 48 hr by luciferase reporter gene assay relative to control
Agonist activity at FXR LBD expressed in human HepG2 cells co-expressing GAL4 DBD and pG5-luc assessed as PLTP promoter-driven luciferase activity at 100 nM after 48 hrs by transient transfection reporter assay relative to control
Agonist activity at human FXR expressed in HEK293 cells by luciferase reporter gene assay
Agonist activity at human full length FXR expressed in HeLa cells cotransfected with pSG5-human RXR at 50 uM after 24 hrs by Dual-Glo luciferase reporter gene assay
Agonist activity at FXR LBD expressed in human HepG2 cells co-expressing GAL4 DBD and pG5-luc assessed as SHP promoter-driven luciferase activity at 100 nM after 48 hrs by transient transfection reporter assay relative to control
Agonist activity at human FXR expressed in COS1 cells at 50 uM by luciferase assay relative to 6-enantiomeric chenodeoxy cholic acid
Agonist activity at human full length FXR expressed in HeLa cells cotransfected with pSG5-human RXR at 30 uM after 24 hrs by Dual-Glo luciferase reporter gene assay
Agonist activity at FXR (unknown origin) expressed in human HepG2 cells assessed as stimulation of FXR response element IR1-mediated receptor transactivation at 1 uM by luciferase reporter gene assay
Agonist activity at human FXR expressed in african green monkey CV1 cells assessed as induction of transactivation activity after 45 hrs by luciferase/beta-galactosidase reporter gene assay

Agonist activity at human FXR expressed in cells assessed as transactivation by luciferase transcriptional reporter gene assay
Agonist activity at FXR (unknown origin) expressed in human HepG2 cells assessed as stimulation of FXR response element IR1-mediated receptor transactivation at 50 uM in presence of CDCA by luciferase reporter gene assay
Agonist activity at human FXR expressed in human HepG2 cells assessed as transactivation of SHP gene at 400 uM by measuring relative luciferase activity by transient transfection reporter assay
Agonist activity at GAL4-fused human FXR expressed in HEK293T cells assessed as activation of basal transcriptional activity after 20 hrs by dual-glo luciferase reporter gene assay
Agonist activity at human FXR transfected in african green monkey CV1 cells by luciferase reporter gene transient transfection assay relative to GW-4064
Agonist activity against human FXR expressed in COS1 cells by luciferase assay relative to 6-enantiomeric chenodeoxy cholic acid
Agonist activity at human FXR expressed in COS1 cells at 100 uM by luciferase assay relative to 6-enantiomeric chenodeoxy cholic acid
Agonist activity at human FXR expressed in COS1 cells at 100 uM after 5 hrs by CRE-driven luciferase reporter gene assay relative to 6ECDCA
Agonist activity at human FXR expressed in COS1 cells at 31.6 uM by luciferase assay relative to 6-enantiomeric chenodeoxycholic acid
Agonist activity at human FXR transfected in HEK293 cells assessed as transcriptional activity by luciferase reporter gene assay relative to GW4064
Agonist activity at FXR LBD expressed in human HepG2 cells co-expressing GAL4 DBD and pG5-luc assessed as SHP promoter-driven luciferase activity at 1 uM after 48 hrs by transient transfection reporter assay relative to control
Agonist activity at human FXR expressed in HepG2 cells assessed as renilla luciferase activity at 1 uM by luciferase based transactivation assay
Agonist activity at human FXR expressed in cells assessed as transactivation by luciferase transcriptional reporter gene assay relative to GW4064
Agonist activity at human FXR expressed in human HepG2 cells assessed as transactivation of SHP gene by measuring relative luciferase activity by transient transfection reporter assay relative to control
Agonist activity at Homo sapiens (human) FXR ligand binding domain expressed in HepG2 cells assessed as transactivation of GAL4 gene expression at 1 uM after 48 hr by luciferase reporter gene assay relative to control
Agonist activity at human FXR expressed in COS1 cells by luciferase reporter gene assay
Agonist activity at human full length FXR transfected in HEK293 cells coexpressing pTRexDest/pGL2promotor assessed as luciferase activity by direct reporter cellular assay relative to GW-4064
Agonist activity at GAL4-fused human FXR expressed in HEK293T cells assessed as activation of basal transcriptional activity after 20 hrs by dual-glo luciferase reporter gene assay
Agonist activity at FXR LBD expressed in human HepG2 cells co-expressing GAL4 DBD and pG5-luc assessed as luciferase activity at 100 nM after 48 hrs by transient transfection reporter assay relative to control
Agonist activity at FXR LBD expressed in human HepG2 cells co-expressing GAL4 DBD and pG5-luc assessed as transrepression of rat CYP7A1 promoter-driven luciferase activity after 48 hrs by transient transfection reporter assay relative to control
Agonist activity at FXR LBD expressed in human HepG2 cells co-expressing GAL4 DBD and pG5-luc assessed as PLTP promoter-driven luciferase activity after 48 hrs by transient transfection reporter assay relative to control
Agonist activity at FXR (unknown origin) expressed in HEK293 cells assessed as transcriptional activity by GAL4 NR reporter cell-based assay

Agonist activity at human FXR-LBD expressed in HEL293 cells by Gal4-luciferase assay relative to GW-4064
Agonist activity at Homo sapiens (human) FXR ligand binding domain expressed in HepG2 cells assessed as transactivation of GAL4 gene expression at 100 nM after 48 hr by luciferase reporter gene assay relative to control
Agonist activity at FXR LBD expressed in human HepG2 cells co-expressing GAL4 DBD and pG5-luc assessed as transrepression of rat CYP7A1 promoter-driven luciferase activity at 100 nM after 48 hrs by transient transfection reporter assay relative to control
Agonist activity at FXR in human HepG2 cells at 10 uM after 48 hrs by luciferase reporter gene based transactivation assay
Agonist activity at Gal4 DNA binding domain-tagged human FXR ligand binding domain expressed in HEK293 cells assessed as activation of receptor-mediated transcriptional activity by luciferase reporter gene assay
Agonist activity at C-terminal Gal4-tagged human FXR (187 to 472 residues) expressed in HEK-293 cells co-expressing pFRluc by mammalian one hybrid assay relative to GW4064
Agonist activity at human FXR expressed in human HeLa cells assessed as receptor activation at 30 uM by BSEP promoter-driven firefly luciferase reporter gene assay relative to 3 uM GW4064
Agonist activity at human FXR transfected in HEK293 cells after 24 hrs by luciferase reporter gene assay
Agonist activity at human FXR LBD transfected in african green monkey CV1 cells after overnight incubation by luciferase reporter gene assay
Agonist activity at gal4-tagged human FXR-ligand binding domain expressed in human HEK293 cells by luciferase reporter gene assay
Agonist activity at GAL4-DBD fused human FXR LBD expressed in HEK293T cells at 10 uM after 24 hrs by luciferase reporter gene assay relative to CDCA
Agonist activity at human FXR transfected in african green monkey CV1 cells by luciferase reporter gene transient transfection assay
Agonist activity at FXR LBD expressed in human HepG2 cells co-expressing GAL4 DBD and pG5-luc assessed as SHP promoter-driven luciferase activity at 10 uM after 48 hrs by transient transfection reporter assay relative to control
Agonist activity at FXR (unknown origin) expressed in human HepG2 cells assessed as receptor transactivation at 100 nM to 50 uM incubated for 16 hrs by FXR response element driven HSP27-TK-luciferase reporter gene assay
Agonist activity at human FXR expressed in human HeLa cells assessed as transactivation after 24 hrs by luciferase reporter gene assay relative to GW4064
Agonist activity at FXR LBD expressed in human HepG2 cells co-expressing GAL4 DBD and pG5-luc assessed as luciferase activity at 10 uM after 48 hrs by transient transfection reporter assay relative to control
Agonist activity at Homo sapiens (human) FXR ligand binding domain expressed in HepG2 cells assessed as transactivation of SHP gene expression at 100 nM after 48 hr by luciferase reporter gene assay relative to control
Agonist activity at human GST-fused FXR LBD expressed in HEK293 cells coexpressing GAL4-DNA bindig domain and pFRluc by mammalian one-hybrid assay
Agonist activity at FXR (unknown origin) transfected into african green monkey CV1 cells assessed as ligand-mediated transcription by luciferase reporter/ transient transfection assay relative to GW4064
Agonist activity at FXR (unknown origin) expressed in HEK293T cells after 16 hrs by beta-lactamase reporter gene assay relative to control
Agonist activity at FXR LBD expressed in human HepG2 cells co-expressing GAL4 DBD and pG5-luc assessed as transrepression of rat CYP7A1 promoter-driven luciferase activity at 10 uM after 48 hrs by transient transfection reporter assay relative to control

Agonist activity at human FXR expressed in human HeLa cells assessed as transactivation at 30 uM after 24 hrs by luciferase reporter gene assay relative to GW4064
Agonist activity at human full length FXR expressed in HeLa cells cotransfected with pSG5-human RXR after 24 hrs by Dual-Glo luciferase reporter gene assay relative to 3 uM GW4064
Agonist activity at human FXR expressed in COS1 cells after 5 hrs by CRE-driven luciferase reporter gene assay relative to 6ECDCA
Agonist activity at human FXR expressed in COS1 cells after 5 hrs by CRE-driven luciferase reporter gene assay
Agonist activity at human GST-fused FXR LBD expressed in HEK293 cells coexpressing GAL4-DNA bindig domain and pFRluc by mammalian one-hybrid assay relative to GW-4064
Agonist activity at Homo sapiens (human) FXR ligand binding domain expressed in HepG2 cells assessed as transactivation of GAL4 gene expression at 10 uM after 48 hr by luciferase reporter gene assay relative to control
Agonist activity at gal4-tagged human FXR-ligand binding domain expressed in human HEK293 cells by luciferase reporter gene assay relative to GW-4064
Agonist activity at GAL4-fused human FXR expressed in HEK293 cells assessed as activation of basal transcriptional activity up to 10 uM after 20 hrs by dual-glo luciferase reporter gene assay
Agonist activity at human FXR expressed in african green monkey CV1 cells co-expressing ECRE with RXR co-factor up to 10 uM by luciferase reporter gene assay relative to CDCA
Agonist activity at human recombinant FXR expressed in HEK293 cells coexpressing CMX-GAL4N by luciferase reporter gene assay
Agonist activity at recombinant human GST-tagged FXR ligand binding domain (193 to 472 residues) expressed in baculovirus infected insect cells assessed as induction of interaction with biotin labelled SRC-1 after 1 hr by HTRF assay relative to GW4064
Agonist activity at GAL4-fused human FXR expressed in HEK293T cells assessed as activation of basal transcriptional activity after 20 hrs by dual-glo luciferase reporter gene assay
Agonist activity at Homo sapiens (human) FXR ligand binding domain expressed in HepG2 cells assessed as transactivation of SHP gene expression at 1 uM after 48 hr by luciferase reporter gene assay relative to control
Agonist activity at FXR LBD expressed in human HepG2 cells co-expressing GAL4 DBD and pG5-luc assessed as PLTP promoter-driven luciferase activity at 10 uM after 48 hrs by transient transfection reporter assay relative to control
Agonist activity at human FXR expressed in COS1 cells by luciferase assay
Agonist activity at FXR (unknown origin) expressed in human HepG2 cells assessed as stimulation of FXR response element IR1-mediated receptor transactivation at 10 uM by luciferase reporter gene assay
Agonist activity at human FXR expressed in human HeLa cells assessed as transactivation after 24 hrs by luciferase reporter gene assay
Agonist activity at human FXR expressed in human HeLa cells assessed as transactivation at 3 uM after 24 hrs by luciferase reporter gene assay relative to GW4064
Agonist activity at human FXR expressed in human HeLa cells assessed as receptor activation by BSEP promoter-driven firefly luciferase reporter gene assay
Agonist activity at human FXR expressed in human HeLa cells assessed as receptor activation by BSEP promoter-driven firefly luciferase reporter gene assay relative to 3 uM GW4064
Agonist activity at C-terminal Gal4-tagged human FXR (187 to 472 residues) expressed in HEK-293 cells co-expressing pFRluc by mammalian one hybrid assay
Agonist activity at human recombinant FXR expressed in HEK293 cells coexpressing CMX-GAL4N by luciferase reporter gene assay relative to GW4064
Agonist activity at GAL4 DNA binding domain tagged FXR ligand binding domain (unknown origin) expressed in human HepG2 cells assessed as receptor transactivation measured by relative luciferase activity at 1 uM by luciferase reporter gene based mammalian one-hybrid assay relative to untreated control

Agonist activity at human full length FXR transfected in HEK293 cells coexpressing pTRexDest/pGL2promotor assessed as luciferase activity by direct reporter cellular assay
Agonist activity at GAL4-fused human FXR LBD expressed in human HepG2 cells up to 2 uM after 20 hrs by luciferase reporter gene assay
Agonist activity at FXR (unknown origin) transfected into african green monkey CV1 cells assessed as ligand-mediated transcription by luciferase reporter/ transient transfection assay
Agonist activity at human recombinant FXR expressed in HEK293 cells coexpressing CMX-GAL4N at 10 uM by luciferase reporter gene assay
Agonist activity at GAL4-fused human FXR expressed in HEK293T cells assessed as activation of basal transcriptional activity after 20 hrs by dual-glo luciferase reporter gene assay relative to apo-receptor
Agonist activity at human full length FXR expressed in HeLa cells cotransfected with pSG5-human RXR after 24 hrs by Dual-Glo luciferase reporter gene assay
Agonist activity at GAL4 DNA binding domain tagged FXR ligand binding domain (unknown origin) expressed in human HepG2 cells assessed as receptor transactivation measured by relative luciferase activity at 100 nM by luciferase reporter gene based mammalian one-hybrid assay relative to untreated control
Agonist activity at human FXR expressed in HEK293T cells assessed as BSEP promoter driven cellular transcriptional activity after 24 hrs by luciferase reporter gene assay
Agonist activity at GAL4-fused human FXR expressed in HEK293T cells assessed as activation of basal transcriptional activity after 20 hrs by dual-glo luciferase reporter gene assay
Agonist activity at human FXR expressed in african green monkey CV1 cells co-expressing ECRE with RXR co-factor by luciferase reporter gene assay
Agonist activity at human FXR transfected in human HuH7 cells co-transfected with human BSEP promoter reporter plasmid at 10 uM after 30 hrs by dual-luciferase reporter assay relative to control
Agonist activity at recombinant human GST-tagged FXR ligand binding domain (193 to 472 residues) expressed in baculovirus infected insect cells assessed as induction of interaction with biotin labelled SRC-1 after 1 hr by HTRF assay
Agonist activity at human FXR LBD transfected in african green monkey CV1 cells assessed as maximum efficacy after overnight incubation by luciferase reporter gene assay relative to GW4064
Agonist activity at human FXR transfected in HEK293 cells assessed as transcriptional activity by luciferase reporter gene assay
Agonist activity at human FXR-LBD expressed in HEL293 cells by Gal4-luciferase assay
Agonist activity at FXR (unknown origin) expressed in human HepG2 cells assessed as receptor transactivation at 10 uM incubated for 16 hrs by FXR response element driven HSP27-TK-luciferase reporter gene assay
Agonist activity at human FXR expressed in HEK293T cells assessed as BSEP promoter driven cellular transcriptional activity after 24 hrs by luciferase reporter gene assay relative to GW4064
Agonist activity at GAL4 DNA binding domain tagged FXR ligand binding domain (unknown origin) expressed in human HepG2 cells assessed as receptor transactivation measured by relative luciferase activity at 10 uM by luciferase reporter gene based mammalian one-hybrid assay relative to untreated control
Agonistic activity against VP-16 GR transcriptional activation assay in human Huh-7 cells
Agonist activity at human GR expressed in CV1 cells by GRE activation assay
Agonistic activity against VP-16 GR transcriptional activation assay in human Huh-7 cells; No effect up to 10-100 uM
Agonist activity at GR in human HepG2 cells assessed as protein mediated-transcriptional activity by MMTV-promoter driven luciferase reporter gene assay
Agonist activity at human GR ligand binding domain expressed in african green monkey COS7 cells by Gal4 hybrid assay
Agonist activity at GR in human A549 cells by NF-kappaB transrepression assay

Agonist activity at human GR in A549 cells by NFkappaB transrepression assay relative to Dexamethasone
Agonist activity at GR in human HeLa cells transfected with MMTV promoter at 2 uM by luciferase transactivation assay relative to dexamethasone
Agonist efficacy at human GR expressed in CV1 cells by GRE activation assay relative to Dexamethasone
Agonist activity at human PPAR-gamma expressed in HEK293 cells at 5 uM after 18 hrs by luciferase reporter gene assay in presence of T0070907
Agonist activity at PPAR-gamma (unknown origin) expressed in HEK293 cells by luciferase reporter gene assay
Agonist activity at pSG5-Gal4-tagged human PPAR-beta/delta ligand binding domain expressed in COS1 cells assessed as receptor activation incubated for 19 hrs by pGL3-5XUAS-SV40 luciferase reporter gene assay
Agonist activity at PPAR-beta (unknown origin) expressed in HEK293 cells by luciferase reporter gene assay
Agonist activity at PPAR-delta (unknown origin) expressed in HEK293t cells co-transfected with tk-PPRE-luciferase vector at 10 uM after 24 hrs by by transactivation assay relative to GW0742
Agonist activity at PPAR-alpha (unknown origin) expressed in CV-1 cells co-transfected with tk-PPRE-luciferase vector after 24 hrs by by transactivation assay
Agonist activity at human PPAR-gamma expressed in HEK293 cells at 30 ug/ml after 18 hrs by luciferase reporter gene assay in presence of T0070907
Agonist activity at full length human PPAR-alpha transfected in human HepG2 cells by luciferase reporter gene assay
Agonist activity at PPAR-alpha (unknown origin) expressed in HEK293 cells by TR-FRET assay
Agonist activity at human PPAR alpha expressed in CV1 cells by GAL4 transactivation assay
Agonist activity at human PPAR-gamma1 LBD (176 to 477) transfected in african green monkey CV1 cells after 40 hrs by beta galactosidase-based luciferase reporter gene assay relative to rosiglitazone
Agonist activity at full length human PPAR-gamma transfected in human HepG2 cells by luciferase reporter gene assay
Agonist activity at PPAR gamma in human HEK cells by transactivation assay
Agonist activity at human PPAR gamma in a HepG2 cells by PPAR-GAL4 transactivation assay relative to darglitazone
Agonist activity at human PPAR gamma in HepG2 cells by PPAR-GAL4 transactivation assay
Agonist activity at human PPAR gamma in human HepG2 cells after 20 hrs by luciferase reporter assay
Agonist activity at human PPAR-delta expressed in african green monkey CV-1 cells after 24 hrs by luciferase reporter gene assay
Agonist activity at human PPAR alpha in a HepG2 cells by PPAR-GAL4 transactivation assay
Agonist activity at Gal4-tagged human PPAR-alpha expressed in HEK cells by transactivation assay
Agonist activity at human PPAR delta expressed in CV1 cells by GAL4 transactivation assay
Agonist activity at human PPAR alpha in a HepG2 cells by PPAR-GAL4 transactivation assay relative to GW-2331
Agonist activity at PPAR alpha (unknown origin) transfected in HEK293 cells at 1 uM after 24 hrs by dual-luciferase reporter gene assay
Agonist activity at human PPAR gamma in HepG2 cells by PPAR-GAL4 transactivation assay relative to darglitazone
Agonist activity at PPAR delta (unknown origin) transfected in HEK293 cells at 0.001 to 1000 uM after 24 hrs by DR-4 luciferase reporter gene assay

Agonist activity at PPAR delta (unknown origin) transfected in HEK293 cells at 0.001 to 1000 uM after 24 hrs by pGL3-Luciferase reporter gene assay
Agonist activity at human PPAR gamma transfected in NIH3T3 cells by luciferase activity assay at 10 uM
Agonist activity at human PPARgamma in HepG2 cells by PPAR-GAL4 transactivation assay
Agonist activity at PPAR gamma (unknown origin) transfected in HEK293 cells at 1 uM after 24 hrs by dual-luciferase reporter gene assay
Agonist activity at human PPAR-gamma expressed in african green monkey CV-1 cells after 24 hrs by luciferase reporter gene assay
Agonist activity at PPAR gamma (unknown origin) transfected in HEK293 cells at 0.1 to 100 uM after 24 hrs by DR-1 luciferase reporter gene assay
Agonist activity at PPAR alpha in human HEK cells by transactivation assay
Agonist activity at human PPAR alpha in HepG2 cells by PPAR-GAL4 transactivation assay relative to GW-2331
Agonist activity at human PPAR-gamma expressed in HEK293 cells at 30 ug/ml after 18 hrs by luciferase reporter gene assay relative to control
Agonist activity at human PPAR alpha in HepG2 cells by PPAR-GAL4 transactivation assay
Agonist activity at human PPAR gamma in a HepG2 cells by PPAR-GAL4 transactivation assay
Agonist activity at human PPAR delta by cell based cotransfection assay
Agonist activity at PPAR-alpha (unknown origin) expressed in HEK293 cells by luciferase reporter gene assay
Agonist activity at PPAR-gamma (unknown origin) expressed in CV-1 cells co-transfected with tk-PPRE-luciferase vector at 10 uM after 24 hrs by by transactivation assay relative to rosiglitazone
Agonist activity at human PPARalpha in HepG2 cells by PPAR-GAL4 transactivation assay
Agonist activity at PPAR-gamma (unknown origin) expressed in CV-1 cells co-transfected with tk-PPRE-luciferase vector after 24 hrs by by transactivation assay
Agonist activity at Gal4-tagged human PPAR-gamma expressed in HEK cells by transactivation assay
Agonist activity at human PPAR delta by cell based reporter assay
Agonist activity at PPAR delta (unknown origin) transfected in HEK293 cells at 1 uM after 24 hrs by dual-luciferase reporter gene assay
Agonist activity at PPAR delta (unknown origin) transfected in HEK293 cells after 24 hrs by dual-luciferase reporter gene assay
Agonist activity at human PPAR-alpha expressed in african green monkey CV-1 cells after 24 hrs by luciferase reporter gene assay
Agonist activity at human PPAR-gamma1 LBD (176 to 477) transfected in african green monkey CV1 cells after 40 hrs by beta galactosidase-based luciferase reporter gene assay
Agonist activity at PPAR-delta (unknown origin) expressed in HEK293t cells co-transfected with tk-PPRE-luciferase vector after 24 hrs by by transactivation assay
Agonist activity at human PPAR alpha in human HepG2 cells after 20 hrs by luciferase reporter assay
Agonist activity at PPAR-alpha (unknown origin) expressed in CV-1 cells co-transfected with tk-PPRE-luciferase vector at 10 uM after 24 hrs by by transactivation assay relative to GW7647
Agonist activity at human PPAR-gamma expressed in HEK293 cells at 5 uM after 18 hrs by luciferase reporter gene assay in presence of T0070907
Agonist activity at PPAR-gamma (unknown origin) expressed in HEK293 cells by luciferase reporter gene assay
Agonist activity at pSG5-Gal4-tagged human PPAR-beta/delta ligand binding domain expressed in COS1 cells assessed as receptor activation incubated for 19 hrs by pGL3-5XUAS-SV40 luciferase reporter gene assay

Agonist activity at PPAR-beta (unknown origin) expressed in HEK293 cells by luciferase reporter gene assay
Agonist activity at PPAR-delta (unknown origin) expressed in HEK293t cells co-transfected with tk-PPRE-luciferase vector at 10 uM after 24 hrs by by transactivation assay relative to GW0742
Agonist activity at PPAR-alpha (unknown origin) expressed in CV-1 cells co-transfected with tk-PPRE-luciferase vector after 24 hrs by by transactivation assay
Agonist activity at human PPAR-gamma expressed in HEK293 cells at 30 ug/ml after 18 hrs by luciferase reporter gene assay in presence of T0070907
Agonist activity at full length human PPAR-alpha transfected in human HepG2 cells by luciferase reporter gene assay
Agonist activity at PPAR-alpha (unknown origin) expressed in HEK293 cells by TR-FRET assay
Agonist activity at human PPAR alpha expressed in CV1 cells by GAL4 transactivation assay
Agonist activity at human PPAR-gamma1 LBD (176 to 477) transfected in african green monkey CV1 cells after 40 hrs by beta galactosidase-based luciferase reporter gene assay relative to rosiglitazone
Agonist activity at full length human PPAR-gamma transfected in human HepG2 cells by luciferase reporter gene assay
Agonist activity at PPAR gamma in human HEK cells by transactivation assay
Agonist activity at human PPAR gamma in a HepG2 cells by PPAR-GAL4 transactivation assay relative to darglitazone
Agonist activity at human PPAR gamma in HepG2 cells by PPAR-GAL4 transactivation assay
Agonist activity at human PPAR gamma in human HepG2 cells after 20 hrs by luciferase reporter assay
Agonist activity at human PPAR-delta expressed in african green monkey CV-1 cells after 24 hrs by luciferase reporter gene assay
Agonist activity at human PPAR alpha in a HepG2 cells by PPAR-GAL4 transactivation assay
Agonist activity at Gal4-tagged human PPAR-alpha expressed in HEK cells by transactivation assay
Agonist activity at human PPAR delta expressed in CV1 cells by GAL4 transactivation assay
Agonist activity at human PPAR alpha in a HepG2 cells by PPAR-GAL4 transactivation assay relative to GW-2331
Agonist activity at PPAR alpha (unknown origin) transfected in HEK293 cells at 1 uM after 24 hrs by dual-luciferase reporter gene assay
Agonist activity at human PPAR gamma in HepG2 cells by PPAR-GAL4 transactivation assay relative to darglitazone
Agonist activity at PPAR delta (unknown origin) transfected in HEK293 cells at 0.001 to 1000 uM after 24 hrs by DR-4 luciferase reporter gene assay
Agonist activity at PPAR delta (unknown origin) transfected in HEK293 cells at 0.001 to 1000 uM after 24 hrs by pGL3-Luciferase reporter gene assay
Agonist activity at human PPAR gamma transfected in NIH3T3 cells by luciferase activity assay at 10 uM
Agonist activity at human PPARgamma in HepG2 cells by PPAR-GAL4 transactivation assay
Agonist activity at PPAR gamma (unknown origin) transfected in HEK293 cells at 1 uM after 24 hrs by dual-luciferase reporter gene assay
Agonist activity at human PPAR-gamma expressed in african green monkey CV-1 cells after 24 hrs by luciferase reporter gene assay
Agonist activity at PPAR gamma (unknown origin) transfected in HEK293 cells at 0.1 to 100 uM after 24 hrs by DR-1 luciferase reporter gene assay
Agonist activity at PPAR alpha in human HEK cells by transactivation assay

Agonist activity at human PPAR alpha in HepG2 cells by PPAR-GAL4 transactivation assay relative to GW-2331
Agonist activity at human PPAR-gamma expressed in HEK293 cells at 30 ug/ml after 18 hrs by luciferase reporter gene assay relative to control
Agonist activity at human PPAR alpha in HepG2 cells by PPAR-GAL4 transactivation assay
Agonist activity at human PPAR gamma in a HepG2 cells by PPAR-GAL4 transactivation assay
Agonist activity at human PPAR delta by cell based cotransfection assay
Agonist activity at PPAR-alpha (unknown origin) expressed in HEK293 cells by luciferase reporter gene assay
Agonist activity at PPAR-gamma (unknown origin) expressed in CV-1 cells co-transfected with tk-PPRE-luciferase vector at 10 uM after 24 hrs by by transactivation assay relative to rosiglitazone
Agonist activity at human PPARalpha in HepG2 cells by PPAR-GAL4 transactivation assay
Agonist activity at PPAR-gamma (unknown origin) expressed in CV-1 cells co-transfected with tk-PPRE-luciferase vector after 24 hrs by by transactivation assay
Agonist activity at Gal4-tagged human PPAR-gamma expressed in HEK cells by transactivation assay
Agonist activity at human PPAR delta by cell based reporter assay
Agonist activity at PPAR delta (unknown origin) transfected in HEK293 cells at 1 uM after 24 hrs by dual-luciferase reporter gene assay
Agonist activity at PPAR delta (unknown origin) transfected in HEK293 cells after 24 hrs by dual-luciferase reporter gene assay
Agonist activity at human PPAR-alpha expressed in african green monkey CV-1 cells after 24 hrs by luciferase reporter gene assay
Agonist activity at human PPAR-gamma1 LBD (176 to 477) transfected in african green monkey CV1 cells after 40 hrs by beta galactosidase-based luciferase reporter gene assay
Agonist activity at PPAR-delta (unknown origin) expressed in HEK293t cells co-transfected with tk-PPRE-luciferase vector after 24 hrs by by transactivation assay
Agonist activity at human PPAR alpha in human HepG2 cells after 20 hrs by luciferase reporter assay
Agonist activity at PPAR-alpha (unknown origin) expressed in CV-1 cells co-transfected with tk-PPRE-luciferase vector at 10 uM after 24 hrs by by transactivation assay relative to GW7647
Agonist activity at recombinant PR-LBD expressed in HEK293T cells co-expressing GAL4 DBD at 20 uM by transactivation assay
Agonist activity at human PR B-form expressed in human PC3 cells assessed as receptor transactivation at 1 uM after 24 hrs by luciferase reporter gene assay
Agonist activity at human PR expressed in human HepG2 cells assessed as MMTV gene promoter transactivation at 100 uM by measuring relative luciferase activity by transient transfection reporter assay relative to control
Agonist activity against Progesterone receptor (PR) in transcriptional activation assay in human T47D breast carcinoma cell line
Agonist activity at human PR B-form expressed in human PC3 cells assessed as receptor transactivation at 0.1 uM after 24 hrs by luciferase reporter gene assay
Agonist activity at human PR expressed in human HepG2 cells assessed as MMTV gene promoter transactivation at 10 uM by measuring relative luciferase activity by transient transfection reporter assay relative to control
Agonist activity at PR in human T47D cells assessed as induction of alkaline phosphatase expression after 24 hrs by alkaline phosphatase assay
Agonist activity at GAL4-fused human PXR expressed in HEK293T cells assessed as activation of basal transcriptional activity after 20 hrs by dual-glo luciferase reporter gene assay

Agonist activity at PXR (unknown origin) expressed in human HepG2 cells assessed as induction of CYP3A4 transactivation at 1.25 uM after 16 hrs by luciferase reporter gene assay
Agonist activity at Gal4 DNA binding domain-tagged human PXR ligand binding domain expressed in HEK293 cells assessed as activation of receptor-mediated transcriptional activity by luciferase reporter gene assay
Agonist activity at human PXR transfected in HEK293 cells after 24 hrs by luciferase reporter gene assay relative to T0901317
Agonist activity at PXR (unknown origin) expressed in human HepG2 cells assessed as induction of CYP3A4 transactivation at 2.5 uM after 16 hrs by luciferase reporter gene assay
Agonist activity at PXR expressed in human HepG2 cells after 24 hrs by p3A4-luciferase reporter gene assay
Agonist activity at PXR (unknown origin) expressed in human HepG2 cells assessed as induction of CYP3A4 transactivation at 10 uM after 16 hrs by luciferase reporter gene assay
Agonist activity at GAL4-fused human PXR expressed in HEK293 cells assessed as activation of basal transcriptional activity up to 10 uM after 20 hrs by dual-glo luciferase reporter gene assay
Agonist activity at GAL4-fused human PXR expressed in HEK293T cells assessed as activation of basal transcriptional activity after 20 hrs by dual-glo luciferase reporter gene assay
Agonist activity at PXR (unknown origin) expressed in human HepG2 cells assessed as induction of CYP3A4 transactivation after 16 hrs by luciferase reporter gene assay
Agonist activity at human full-length PXR transfected in human HepG2 cells co-transfected with pSG5-RXR assessed as induction of transactivation by dual-luciferase reporter gene assay
Agonist activity at GAL4-fused human PXR expressed in HEK293T cells assessed as activation of basal transcriptional activity after 20 hrs by dual-glo luciferase reporter gene assay
Agonist activity at PXR expressed in human HepG2 cells assessed as transactivation at 10 uM after 48 hrs by luciferase reporter gene assay
Agonist activity at human PXR transfected in human HepG2 cells co-transfected with pSG5-RXR/pCMV-beta-galactosidase/p(CYP3A4)-TK-Luc at 10 uM after 18 hrs by luciferase reporter gene assay
Agonist activity at PXR (unknown origin) in human HepG2 cells co-transfcted with RXR assessed as receptor transactivation at 10 uM incubated for 18 hrs by Gal4 luciferase reporter gene assay
Agonist activity at human PXR expressed in human HepG2 cells assessed as induction of CYP3A4 measured after 24 hrs by AlamarBlue dye-based luciferase reporter gene assay
Agonist activity at GAL4-fused human PXR expressed in HEK293T cells assessed as activation of basal transcriptional activity after 20 hrs by dual-glo luciferase reporter gene assay relative to apo-receptor
Agonist activity at PXR (unknown origin) expressed in human HepG2 cells assessed as induction of CYP3A4 transactivation at 40 uM after 16 hrs by luciferase reporter gene assay
Agonist activity at human PXR expressed in human HepG2 cells assessed as induction of CYP3A4 measured after 24 hrs by AlamarBlue dye-based luciferase reporter gene assay relative to control
Agonist activity at human PXR expressed in human HepG2 cells assessed as induction of transactivation at 10 uM after 18 hrs by luciferase reporter gene assay
Agonist activity at human PXR transfected in HEK293 cells after 24 hrs by luciferase reporter gene assay
Agonist activity at PXR LBD (unknown origin) transfected in human HepG2 cells co-expressing GAL4-DBD assessed as CYP3A4 expression at 10 uM after 18 hrs by luciferase reporter gene assay
Agonist activity at GAL4-fused human PXR expressed in HEK293T cells assessed as activation of basal transcriptional activity after 20 hrs by dual-glo luciferase reporter gene assay
Agonist activity at PXR (unknown origin) expressed in HEK293 cells assessed as transcriptional activity by GAL4 NR reporter cell-based assay
Agonist activity at PXR (unknown origin) expressed in human HepG2 cells assessed as induction of CYP3A4 transactivation at 20 uM after 16 hrs by luciferase reporter gene assay

Agonist activity at full length human ROR gamma expressed in human Jurkat cells assessed as IL17 promoter activation by luciferase reporter gene assay
Agonist activity at human His6-tagged ROR gamma ligand binding domain (residues 262 to 507) expressed in Escherichia coli BL21 (DE3) cells assessed as increase in recruitment of coactivator peptide by AlphaScreen biochemical assay
Agonist activity at FXR in human HepG2 cells assessed as induction of CYP7A1 mrNA expression at 10 uM by quantitative PCR method
Agonist activity at FXR in human HepG2 cells assessed as induction of OSTalpha mrNA expression at 50 uM by quantitative PCR method
Agonist activity at FXR in human HepG2 cells assessed as induction of OSTalpha mrNA expression at 0.3 uM by quantitative PCR method
Agonist activity at FXR in human HepG2 cells assessed as induction of BSEP mrNA expression at 0.3 uM by quantitative PCR method
Agonist activity at FXR in human HepG2 cells assessed as induction of IBABP mrNA expression at 50 uM by quantitative PCR method
Agonist activity at FXR in human HepG2 cells assessed as induction of IBABP mrNA expression at 10 uM by quantitative PCR method
Agonist activity at FXR in human HepG2 cells assessed as induction of SHP mrNA expression at 0.1 uM by quantitative PCR method
Agonist activity at FXR in human HepG2 cells assessed as induction of IBABP mrNA expression at 3 uM by quantitative PCR method
Agonist activity at FXR in human HepG2 cells assessed as induction of SHP mrNA expression at 3 uM by quantitative PCR method
Agonist activity at FXR in human HepG2 cells assessed as induction of SHP mrNA expression at 10 uM by quantitative PCR method
Agonist activity at FXR in human HepG2 cells assessed as induction of IBABP mrNA expression at 1 uM by quantitative PCR method
Agonist activity at FXR in human HepG2 cells assessed as induction of IBABP mrNA expression at 0.3 uM by quantitative PCR method
Agonist activity at FXR in human HepG2 cells assessed as induction of OSTalpha mrNA expression at 3 uM by quantitative PCR method
Agonist activity at FXR in human HepG2 cells assessed as induction of BSEP mrNA expression at 1 uM by quantitative PCR method
Agonist activity at FXR in human HepG2 cells assessed as induction of CYP7A1 mrNA expression at 3 uM by quantitative PCR method
Agonist activity at FXR in human HepG2 cells assessed as induction of SHP mrNA expression at 50 uM by quantitative PCR method
Agonist activity at FXR in human HepG2 cells assessed as induction of OSTalpha mrNA expression at 0.1 uM by quantitative PCR method
Agonist activity at FXR in human HepG2 cells assessed as induction of CYP7A1 mrNA expression at 0.1 uM by quantitative PCR method
Agonist activity at FXR in human HepG2 cells assessed as induction of OSTalpha mrNA expression at 10 uM by quantitative PCR method
Agonist activity at FXR in human HepG2 cells assessed as induction of BSEP mrNA expression at 3 uM by quantitative PCR method
Agonist activity at FXR in human HepG2 cells assessed as increase in BSEP mRNA expression at 10 uM by RT-PCR method
Agonist activity at FXR in human HepG2 cells assessed as induction of CYP7A1 mrNA expression at 50 uM by quantitative PCR method
Agonist activity at FXR in human HepG2 cells assessed as induction of BSEP mrNA expression at 50 uM by quantitative PCR method

Agonist activity at FXR in human HepG2 cells assessed as induction of CYP7A1 mrNA expression at 0.3 uM by quantitative PCR method
Agonist activity at FXR in human HepG2 cells assessed as induction of SHP mrNA expression at 1 uM by quantitative PCR method
Agonist activity at FXR in human HepG2 cells assessed as induction of OSTalpha mrNA expression at 1 uM by quantitative PCR method
Agonist activity at FXR in human HepG2 cells assessed as induction of CYP7A1 mrNA expression at 1 uM by quantitative PCR method
Agonist activity at FXR in human HepG2 cells assessed as induction of BSEP mrNA expression at 10 uM by quantitative PCR method
Agonist activity at FXR in human HepG2 cells assessed as induction of BSEP mrNA expression at 0.1 uM by quantitative PCR method
Agonist activity at FXR in human HepG2 cells assessed as induction of IBABP mrNA expression at 0.1 uM by quantitative PCR method
Agonist activity at FXR in human HepG2 cells assessed as induction of SHP mrNA expression at 0.3 uM by quantitative PCR method
Agonist activity at FXR in human HepG2 cells assessed as increase in SHP mRNA expression at 10 uM by RT-PCR method
Agonist activity at FXR in human HepG2 cells assessed as increase in OSTalpha mRNA expression at 10 uM by RT-PCR method
Agonist activity at PPAR-alpha in human HepG2 cells assessed as reduction in SCD1 gene expression at 100 uM by quantitative PCR method
Agonist activity at PPAR-alpha in human HepG2 cells harboring PPAR-alpha siRNA assessed as reduction in intracellular TG level at 100 uM after 24 hrs by enzymatic method
Agonist activity at PPAR-alpha in human HepG2 cells assessed as reduction in FAS gene expression at 100 uM by quantitative PCR method
Agonist activity at PPAR-alpha in human HepG2 cells assessed as increase in acyl-coA synthetase mRNA expression at 100 uM by quantitative PCR method
Agonist activity at PPAR-alpha in human HepG2 cells assessed as increase in CPT1 mRNA expression at 10 uM by quantitative PCR method
Agonist activity at PPAR-alpha in human HepG2 cells assessed as increase in CPT1 mRNA expression at 100 uM by quantitative PCR method
Agonist activity at PPAR-alpha in human HepG2 cells assessed as increase in FATP4 mRNA expression at 10 uM by quantitative PCR method
Agonist activity at PPAR-alpha in human HepG2 cells assessed as increase in FATP4 mRNA expression at 100 uM by quantitative PCR method
Agonist activity at PPAR-alpha in human HepG2 cells assessed as increase in acyl-coA oxidase mRNA expression at 100 uM by quantitative PCR method
Agonist activity at PPAR-alpha in human HepG2 cells assessed as reduction in cholesterol level at 1 to 100 uM after 24 hrs by enzymatic method
Agonist activity at PPAR-alpha in human HepG2 cells assessed as reduction in SREBP-1c gene expression at 100 uM by quantitative PCR method
Agonist activity at PPAR-alpha in human HepG2 cells assessed as reduction in intracellular TG level at 100 uM after 24 hrs by enzymatic method
Agonist activity at PPAR-alpha in human HepG2 cells assessed as effect on LPL gene expression at 100 uM by quantitative PCR method
Agonist activity at PPAR-alpha in human HepG2 cells assessed as increase in acyl-coA synthetase mRNA expression at 10 uM by quantitative PCR method
Agonist activity at PPAR-alpha in human HepG2 cells assessed as reduction in SCD1 gene expression at 100 uM by quantitative PCR method
Agonist activity at PPAR-alpha in human HepG2 cells harboring PPAR-alpha siRNA assessed as reduction in intracellular TG level at 100 uM after 24 hrs by enzymatic method

Agonist activity at PPAR-alpha in human HepG2 cells assessed as reduction in FAS gene expression at 100 uM by quantitative PCR method
Agonist activity at PPAR-alpha in human HepG2 cells assessed as increase in acyl-coA synthetase mRNA expression at 100 uM by quantitative PCR method
Agonist activity at PPAR-alpha in human HepG2 cells assessed as increase in CPT1 mRNA expression at 10 uM by quantitative PCR method
Agonist activity at PPAR-alpha in human HepG2 cells assessed as increase in CPT1 mRNA expression at 100 uM by quantitative PCR method
Agonist activity at PPAR-alpha in human HepG2 cells assessed as increase in FATP4 mRNA expression at 10 uM by quantitative PCR method
Agonist activity at PPAR-alpha in human HepG2 cells assessed as increase in FATP4 mRNA expression at 100 uM by quantitative PCR method
Agonist activity at PPAR-alpha in human HepG2 cells assessed as increase in acyl-coA oxidase mRNA expression at 100 uM by quantitative PCR method
Agonist activity at PPAR-alpha in human HepG2 cells assessed as reduction in cholesterol level at 1 to 100 uM after 24 hrs by enzymatic method
Agonist activity at PPAR-alpha in human HepG2 cells assessed as reduction in SREBP-1c gene expression at 100 uM by quantitative PCR method
Agonist activity at PPAR-alpha in human HepG2 cells assessed as reduction in intracellular TG level at 100 uM after 24 hrs by enzymatic method
Agonist activity at PPAR-alpha in human HepG2 cells assessed as effect on LPL gene expression at 100 uM by quantitative PCR method
Agonist activity at PPAR-alpha in human HepG2 cells assessed as increase in acyl-coA synthetase mRNA expression at 10 uM by quantitative PCR method
Agonist activity at PXR in human primary hepatocytes assessed as upregulation of UGT1A1 mRNA expression at 10 uM after 24 hrs by qRT-PCR method
Agonist activity at PXR in human primary hepatocytes assessed as upregulation of MDR/ABCB1 mRNA expression at 10 uM after 24 hrs by qRT-PCR method
Agonist activity at PXR in human HepaRG cells assessed as upregulation of CYP1B1 mRNA expression at 10 uM after 24 hrs by qRT-PCR method
Agonist activity at PXR in human primary hepatocytes assessed as upregulation of CYP2C9 mRNA expression at 10 uM after 24 hrs by qRT-PCR method
Agonist activity at PXR in human primary hepatocytes assessed as upregulation of CYP3A4 mRNA expression at 10 uM after 24 hrs by qRT-PCR method
Agonist activity at PXR in human primary hepatocytes assessed as upregulation of CYP3A5 mRNA expression at 10 uM after 24 hrs by qRT-PCR method
Agonist activity at human alpha2a-AR expressed in CHO cells assessed as rate of acidification after 240 mins by cytosensor microphysiometric analysis
Agonist activity at human alpha2a-AR expressed in CHO cells assessed as rate of acidification after 240 mins by cytosensor microphysiometric analysis relative to (-)-noradrenaline
Agonist activity at human alpha2b-AR expressed in CHO cells assessed as rate of acidification after 240 mins by cytosensor microphysiometric analysis relative to (-)-noradrenaline
Agonist activity at AR in human bicalutamide-resistant LNCAP cells assessed as effect on cell proliferation after 6 days
Agonist activity at AR in human LNCAP cells assessed as effect on cell proliferation after 6 days
Agonist activity at human alpha2c-AR expressed in CHO cells assessed as rate of acidification after 240 mins by cytosensor microphysiometric analysis relative to (-)-noradrenaline
Agonist activity at human alpha2b-AR expressed in CHO cells assessed as rate of acidification after 240 mins by cytosensor microphysiometric analysis
Agonist activity at AR in bicalutamide-resistant human LNCAP cells assessed as effect on cell proliferation after 6 days

Agonist activity at human alpha2c-AR expressed in CHO cells assessed as rate of acidification after 240 mins by cytosensor microphysiometric analysis
Agonist activity at estrogen receptor in human Ishikawa cells assessed as induction of ERE-dependent alkaline phosphatase level at 0.1 uM relative to control
Agonist activity at estrogen receptor alpha in human MCF7 cells assessed as ER alpha phosphorylation at 10 uM after 24 hrs by immunoblotting analysis
Agonist activity at ER in human MCF7:WS8 cells assessed as GREB1 gene expression at 10'-6 M after 48 hrs by RT-PCR analysis
Agonist activity at ER in human T47D cells assessed as stimulation of cell proliferation
Agonist activity at ER in human MCF7:WS8 cells assessed as cell growth by measuring DNA level at 0.56 X 10'-9 M after 7 days by fluorescence analysis
Agonist activity at ER in human MCF7:WS8 cells assessed as increase in PgR gene expression at 10'-10 M after 48 hrs by RT-PCR analysis
Agonist activity at ER in human MCF7:WS8 cells assessed as increase in pS2 gene expression at 10'-10 M after 48 hrs by RT-PCR analysis
Agonist activity at ER in human MCF7:WS8 cells assessed as increase in GREB1 gene expression at 10'-10 M after 48 hrs by RT-PCR analysis
Agonist activity at full length human ERbeta receptor expressed in human HEC-1 cells assessed as (ERE)2-pS2-luc reporter gene transcriptional activity relative to estradiol
Agonist activity at ER in human MCF7:WS8 cells assessed as cell growth by measuring DNA level at 10'-12 to 10'-6 M after 7 days by fluorescence analysis
Agonist activity at ERalpha in human MCF7:D5L cells assessed as induction of ERE-dependent luciferase expression at 1 uM relative to control
Agonist activity at full length human ERbeta receptor expressed in human HEC-1 cells assessed as (ERE)2-pS2-luc reporter gene transcriptional activity
Agonist activity at ER in human MCF7:WS8 cells assessed as pS2 gene expression at 10'-6 M after 48 hrs by RT-PCR analysis
Agonist activity at ER in human MCF7:WS8 cells assessed as cell growth by measuring DNA level at 1.17 X 10'-9 M after 7 days by fluorescence analysis
Agonist activity at estrogen receptor in human Ishikawa cells assessed as induction of ERE-dependent alkaline phosphatase level at 1 uM relative to estradiol
Agonist activity at human ERbeta receptor expressed in human HEK293 cells co-expressing ERE assessed as increase of estradiol-induced luciferase gene expression at 1 uM after 18 hrs relative to estradiol
Agonist activity at ERalpha in human MCF7:D5L cells assessed as induction of ERE-dependent luciferase expression at 1 uM relative to estradiol
Agonist activity at ER in human MCF7:WS8 cells assessed as increase in PgR gene expression at 10'-6 M after 48 hrs by RT-PCR analysis
Agonist activity at ER alpha in human MCF7 cells assessed as PR gene expression after 24 hrs by laser scanning imaging cytometer analysis
Agonist activity at ERbeta in HEK293 cells assessed as induction of ERE-dependent luciferase expression at 1 uM relative to estradiol
Agonist activity at ER in human MCF7:WS8 cells assessed as increase in cell growth by measuring DNA level after 7 days by fluorescence analysis
Agonist activity at ER in human MCF7:WS8 cells assessed as increase in PgR gene expression at 10'-6 M after 48 hrs by RT-PCR analysis relative to control
Agonist activity at full length human ERalpha receptor expressed in human HEC-1 cells assessed as (ERE)2-pS2-luc reporter gene transcriptional activity
Agonist activity at ER in human MCF7:WS8 cells assessed as increase in pS2 gene expression at 10'-6 M after 48 hrs by RT-PCR analysis
Agonist activity at ER in human MCF7:WS8 cells assessed as increase in cell growth by measuring DNA level at 10'-6 M after 7 days by fluorescence analysis

Agonist activity at ER in human MCF7:WS8 cells assessed as increase in GREB1 gene expression at 10'-6 M after 48 hrs by RT-PCR analysis
Agonist activity at LXR in human THP1 cells assessed as reduction in cellular triglyceride after 24 hrs
Agonist activity at LXR in human THP1 cells assessed as upregulation of ABCA1 gene expression at 50 nM after 24 hrs by RT-PCR analysis relative to control
Agonist activity at LXR in human THP1 cells assessed as reduction in cellular triglyceride at 10 uM after 24 hrs
Agonist activity at LXR in human THP1 cells assessed as increase in ApoE mRNA level at 100 uM after 48 hrs by qPCR analysis relative to control
Agonist activity at LXR-alpha in human THP1 cells assessed as increase cholesterol efflux to HDL by FACs analysis
Agonist activity at LXR in human THP1 cells assessed as upregulation of ABCA1 gene expression at 500 nM after 24 hrs by RT-PCR analysis relative to control
Agonist activity at LXR-alpha in human THP1 cells assessed as increase cholesterol efflux to HDL at 1 uM by FACs analysis
Agonist activity at LXR in human U937 cells assessed as upregulation of SCD1 mRNA levels at 10 uM after 16 hrs by qPCR analysis
Agonist activity at LXR in human THP1 cells assessed as reduction in cellular cholesterol after 24 hrs
Agonist activity at LXR in human HepG2 cells assessed as upregulation of SREBP1C expression at 100 uM after 24 hrs by RT-qPCR analysis relative to control
Agonist activity at LXR in human U937 cells assessed as upregulation of FASN mRNA levels at 10 uM after 16 hrs by qPCR analysis
Agonist activity at LXR in human HepG2 cells assessed as increase in cellular triglyceride at 10 uM after 24 hrs relative to control
Agonist activity at LXR in human THP1 cells assessed as upregulation of ABCA1 gene expression after 24 hrs by RT-PCR analysis
Agonist activity at LXR in human HepG2 cells assessed as reduction in cellular triglyceride at 100 uM after 24 hrs
Agonist activity at LXR in human Caco2 cells assessed as increase in ABCG5 mRNA level at 100 uM after 48 hrs by qPCR analysis relative to control
Agonist activity at LXR in human THP1 cells assessed as induction of ABCA1 mRNA expression at 100 uM after 48 hrs by qPCR analysis relative to control
Agonist activity at LXR in human HepG2 cells assessed as upregulation of SREBP1C gene expression at 1 uM after 24 hrs by RT-PCR analysis relative to control
Agonist activity at LXR in human THP1 monocytes assessed as increase in ABCG1 mRNA level at 100 uM after 48 hrs by qPCR analysis relative to control
Agonist activity at LXR in human THP1 cells assessed as upregulation of ABCA1 gene expression at 5 nM after 24 hrs by RT-PCR analysis relative to control
Agonist activity at LXR in human HepG2 cells assessed as upregulation of SREBP1C gene expression at 500 nM after 24 hrs by RT-PCR analysis relative to control
Agonist activity at LXR in human Caco2 cells assessed as decrease in NPC1L1 mRNA level at 100 uM after 48 hrs by qPCR analysis relative to control
Agonist activity at LXR in human HepG2 cells assessed as upregulation of SREBP1C gene expression at 2 nM after 24 hrs by RT-PCR analysis relative to control
Agonist activity at LXR-alpha in human Caco2 cells assessed as reduction in cellular cholesterol level
Agonist activity at LXR in human THP1 cells assessed as upregulation of ABCA1 gene expression at 1 nM after 24 hrs by RT-PCR analysis relative to control
Agonist activity at LXR in human THP1 cells assessed as induction of ABCA1 gene expression at 100 uM after 48 hrs by immunoblot analysis relative to control

Agonist activity at LXR-alpha in human HepG2 cells assessed as reduction in cellular cholesterol level
Agonist activity at LXR in human THP1 cells assessed as induction of ABCA1 gene expression after 48 hrs by qPCR analysis
Agonist activity at LXR in human HepG2 cells assessed as upregulation of SCD1 mRNA levels at 10 uM after 6 hrs by qPCR analysis
Agonist activity at LXR in human THP1 cells assessed as upregulation of ABCA1 gene expression at 1 uM after 24 hrs by RT-PCR analysis relative to control
Agonist activity at LXR in human HepG2 cells assessed as upregulation of SREBP1C gene expression at 167 nM after 24 hrs by RT-PCR analysis relative to control
Agonist activity at LXR in human U937 cells assessed as upregulation of SCD1 mRNA levels at 10 uM after 6 hrs by qPCR analysis relative to control
Agonist activity at LXR in human HepG2 cells assessed as upregulation of SREBP1C gene expression at 56 nM after 24 hrs by RT-PCR analysis relative to control
Agonist activity at LXR in human HepG2 cells assessed as upregulation of SREBP1C gene expression after 24 hrs by RT-PCR analysis
Agonist activity at LXR in human Caco2 cells assessed as increase in ABCA1 mRNA level at 100 uM after 48 hrs by qPCR analysis relative to control
Agonist activity at LXR in human HepG2 cells assessed as upregulation of SREBP1C gene expression at 19 nM after 24 hrs by RT-PCR analysis relative to control
Agonist activity at LXR in human HepG2 cells assessed as upregulation of ABCA1 expression at 10 uM after 24 hrs by RT-qPCR analysis relative to control
Agonist activity at LXR in human HepG2 cells assessed as reduction in cellular triglyceride after 24 hrs
Agonist activity at LXR in human Caco2 cells assessed as increase in ABCG8 mRNA level at 100 uM after 48 hrs by qPCR analysis relative to control
Agonist activity at LXR in human HepG2 cells assessed as reduction in cellular cholesterol after 24 hrs
Agonist activity at LXR in human HepG2 cells assessed as upregulation of ABCG5 expression at 100 uM after 24 hrs by RT-qPCR analysis relative to control
Agonist activity at LXR in human THP1 cells assessed as induction of ABCG1 gene expression at 100 uM after 48 hrs by immunoblot analysis relative to control
Agonist activity at LXR in human HepG2 cells assessed as upregulation of ABCA1 expression at 100 uM after 24 hrs by RT-qPCR analysis relative to control
Agonist activity at LXR in human THP1 cells assessed as upregulation of ABCA1 gene expression at 158 nM after 24 hrs by RT-PCR analysis relative to control
Agonist activity at LXR in human THP1 cells assessed as upregulation of ABCA1 gene expression at 2 nM after 24 hrs by RT-PCR analysis relative to control
Agonist activity at LXR in human THP1 cells assessed as reduction in cellular triglyceride at 100 uM after 24 hrs
Agonist activity at LXR in human HepG2 cells assessed as upregulation of SREBP1c mRNA levels at 10 uM after 6 hrs by qPCR analysis
Agonist activity at LXR-alpha in human THP1 cells assessed as reduced cellular cholesterol concentration at 1 uM
Agonist activity at LXR in human HepG2 cells assessed as upregulation of SREBP1C expression at 10 uM after 24 hrs by RT-qPCR analysis relative to control
Agonist activity at LXR in human HepG2 cells assessed as upregulation of SREBP1C gene expression at 6 nM after 24 hrs by RT-PCR analysis relative to control
Agonist activity at LXR in human U937 cells assessed as upregulation of SREBP1c mRNA levels at 10 uM after 6 hrs by qPCR analysis
Agonist activity at LXR in human HepG2 cells assessed as upregulation of SREBP1C gene expression at 1 nM after 24 hrs by RT-PCR analysis relative to control

Agonist activity at LXR in human HepG2 cells assessed as upregulation of ABCG5 expression at 10 uM after 24 hrs by RT-qPCR analysis relative to control
Agonist activity at LXR in human THP1 cells assessed as induction of ABCG1 gene expression after 48 hrs by qPCR analysis
Agonist activity at LXR in human THP1 cells assessed as upregulation of ABCA1 gene expression at 16 nM after 24 hrs by RT-PCR analysis relative to control
Agonist activity at LXR-alpha in human THP1 cells assessed as reduced cellular cholesterol concentration
Agonist activity at LXR in human THP1 cells assessed as increase in ApoE mRNA level at 1 uM after 48 hrs by qPCR analysis relative to control
Agonist activity at LXR in human U937 cells assessed as downregulation of LPS-induced TNFalpha mRNA expression at 10 uM after 6 hrs by qPCR analysis
Agonist activity at LXR in human HepG2 cells assessed as upregulation of FASN mRNA levels at 10 uM after 6 hrs by qPCR analysis
Agonist activity at LXR in human U937 cells assessed as upregulation of ABCA1 mRNA levels at 10 uM after 6 hrs by qPCR analysis
Agonist activity at LXR in human U937 cells assessed as downregulation of LPS-induced CCL2 mRNA expression at 10 uM after 6 hrs by qPCR analysis
Agonist activity at LXR in human U937 cells assessed as upregulation of FASN mRNA levels at 10 uM after 6 hrs by qPCR analysis
Agonist activity FXR (unknown origin) expressed in human HepG2 cells co-expressing RXR assessed as effect on SHP mRNA level at 50 uM after 18 hrs by RT-PCR analysis
Agonist activity at FXR expressed in human HepG2 cells assessed as increase in BSEP mRNA level at 10 uM by RT-PCR analysis
Agonist activity at FXR expressed in human HepG2 cells assessed as increase in CYP7A1 mRNA level at 10 uM by RT-PCR analysis relative to control
Agonist activity at FXR expressed in human HepG2 cells assessed as decrease in CYP7A1 mRNA level at 10 uM by RT-PCR analysis
Agonist activity at GAL4 DNA binding domain tagged FXR ligand binding domain (unknown origin) expressed in human HepG2 cells co-expressing human human SHP gene promoter assessed as transactivation of SHP promoter driven luciferase activity at 1 uM relative to untreated control
Agonist activity at FXR in human HepG2 cells assessed as decrease in CYP7A1 mRNA expression at 50 uM after 6 hrs by quantitative PCR analysis
Agonist activity FXR (unknown origin) expressed in human HepG2 cells co-expressing RXR assessed as effect on CyP7alpha1 mRNA level at 50 uM after 18 hrs by RT-PCR analysis
Agonist activity FXR (unknown origin) expressed in human HepG2 cells co-expressing RXR assessed as effect on CyP7alpha1 mRNA level at 10 uM after 18 hrs by RT-PCR analysis
Agonist activity FXR (unknown origin) expressed in human HepG2 cells co-expressing RXR assessed as effect on OSTalpha mRNA level at 50 uM after 18 hrs by RT-PCR analysis
Agonist activity at FXR expressed in human HepG2 cells assessed as effect on SHP mRNA level at 10 uM by RT-PCR analysis
Agonist activity at FXR in human HepG2 cells assessed as upregulation of OST-alpha mRNA expression at 10 uM after 18 hrs by RT-PCR analysis
Agonist activity at GAL4 DNA binding domain tagged FXR ligand binding domain (unknown origin) expressed in human HepG2 cells co-expressing human human SHP gene promoter assessed as transactivation of SHP promoter driven luciferase activity at 100 nM relative to untreated control
Agonist activity at FXR expressed in human HepG2 cells assessed as increase in OSTalpha mRNA level at 10 uM by RT-PCR analysis
Agonist activity FXR (unknown origin) expressed in human HepG2 cells co-expressing RXR assessed as effect on OSTalpha mRNA level at 10 uM after 18 hrs by RT-PCR analysis
Agonist activity at human FXR LBD iexpressed in monkey CV-1 cells assessed as transactivation of luciferase reporter gene expression relative to GW 4064

Agonist activity at GAL4 DNA binding domain tagged FXR ligand binding domain (unknown origin) expressed in human HepG2 cells co-expressing human PLTP gene promoter assessed as transactivation of PLTP promoter driven luciferase activity at 10 uM relative to untreated control
Agonist activity at FXR in human HepG2 cells assessed as upregulation of BESP mRNA expression at 10 uM after 18 hrs by RT-PCR analysis
Agonist activity at FXR in human HepG2 cells assessed as upregulation of SHP mRNA expression at 10 uM after 18 hrs by RT-PCR analysis
Agonist activity at GAL4 DNA binding domain tagged FXR ligand binding domain (unknown origin) expressed in human HepG2 cells co-expressing rat CYP7A1 gene promoter assessed as transrepression of CYP7A1 promoter driven luciferase activity relative to untreated control
Agonist activity at GAL4 DNA binding domain tagged FXR ligand binding domain (unknown origin) expressed in human HepG2 cells co-expressing rat CYP7A1 gene promoter assessed as transrepression of CYP7A1 promoter driven luciferase activity at 1 uM relative to untreated control
Agonist activity FXR (unknown origin) expressed in human HepG2 cells co-expressing RXR assessed as effect on SHP mRNA level at 10 uM after 18 hrs by RT-PCR analysis
Agonist activity at GAL4 DNA binding domain tagged FXR ligand binding domain (unknown origin) expressed in human HepG2 cells co-expressing human human SHP gene promoter assessed as transactivation of SHP promoter driven luciferase activity at 100 nM to 10 uM relative to untreated control
Agonist activity at GAL4 DNA binding domain tagged FXR ligand binding domain (unknown origin) expressed in human HepG2 cells co-expressing human human SHP gene promoter assessed as transactivation of SHP promoter driven luciferase activity at 10 uM relative to untreated control
Agonist activity at GAL4 DNA binding domain tagged FXR ligand binding domain (unknown origin) expressed in human HepG2 cells co-expressing rat CYP7A1 gene promoter assessed as transrepression of CYP7A1 promoter driven luciferase activity at 10 uM
Agonist activity at human FXR LBD iexpressed in monkey CV-1 cells assessed as transactivation of luciferase reporter gene expression
Agonist activity at GAL4 DNA binding domain tagged FXR ligand binding domain (unknown origin) expressed in human HepG2 cells co-expressing human PLTP gene promoter assessed as transactivation of PLTP promoter driven luciferase activity relative to untreated control
Agonist activity at GAL4 DNA binding domain tagged FXR ligand binding domain (unknown origin) expressed in human HepG2 cells co-expressing human PLTP gene promoter assessed as transactivation of PLTP promoter driven luciferase activity at 100 nM relative to untreated control
Agonist activity at human FXR expressed in human HepG2 cells assessed as induction of OSTalpha mRNA expression at 50 uM by quantitative RT-PCR analysis
Agonist activity at GAL4 DNA binding domain tagged FXR ligand binding domain (unknown origin) expressed in human HepG2 cells co-expressing rat CYP7A1 gene promoter assessed as transrepression of CYP7A1 promoter driven luciferase activity at 10 uM relative to untreated control
Agonist activity at GAL4 DNA binding domain tagged FXR ligand binding domain (unknown origin) expressed in human HepG2 cells co-expressing rat CYP7A1 gene promoter assessed as transrepression of CYP7A1 promoter driven luciferase activity at 100 nM relative to untreated control
Agonist activity at FXR in human HepG2 cells assessed as inhibition of CYP7A1 mRNA expression at 50 uM for 6 hrs by RT-PCR relative to control
Agonist activity at human FXR expressed in HEK293 cells cotransfected with reporter plasmid pEcREx6-TK-Luc/pCMXhRXR assessed as luciferase activity upto 50 uM by luminometry
Agonist activity at GR in HFF cells assessed as suppression of IL-1-induced IL-6 production at 2 uM relative to dexamethasone
Agonist activity at GR assessed as NF-kappaB-mediated transrepression of secreted placental alkaline phosphatase gene in human A549 cells relative to Dexamethasone
Agonist activity at GR in human A549 cells transfected with luciferase gene linked to MMTV promoter assessed as luciferase transactivation activity after 24 hrs relative to Dexamethasone

Agonist activity at GR in HFF cells assessed as suppression of IL-1-induced IL-6 production
Agonist activity at GR in human A549 cells transfected with luciferase gene linked to MMTV promoter assessed as luciferase transactivation activity after 24 hrs
Agonist activity at GR assessed as MMTV-mediated transactivation of renilla luciferase gene in human A549 cells relative to Dexamethasone
Agonist activity at human GR expressed in NHDF cells assessed as inhibition of IL-6 production by ELISA relative to Dexamethasone
Agonist activity at GR in human SW1353 cells transfected with MMTV reporter construct assessed as luciferase transactivation activity after 16 hrs by scintillation counting analysis relative to dexamethasone
Agonist activity at human GR expressed in NHDF cells assessed as inhibition of IL-6 production by ELISA
Agonist activity at GR in human A549 cells transfected with luciferase gene linked to MMTV promoter assessed as luciferase transactivation activity
Agonist activity at GR in human MG-63 cells assessed as inhibition of vitamin D-induced osteocalcin production at 2 uM relative to dexamethasone
Agonist activity at GR assessed as NF-kappaB-mediated transrepression of secreted placental alkaline phosphatase gene in human A549 cells
Agonist activity at GR in human A549 cells transfected with luciferase gene linked to MMTV promoter assessed as luciferase transactivation activity relative to Dexamethasone
Agonist activity at GR in human SW1353 cells transfected with luciferase gene linked to MMTV promoter assessed as luciferase transactivation activity
Agonist activity at PPAR-alpha in human HepG2 cells harboring PPAR-alpha siRNA assessed as [14C]palmitate oxidation at 100 uM by BODIPY-based FACS analysis
Agonist activity at PPAR-alpha in human HepG2 cells harboring PPAR-alpha siRNA assessed as fatty acid uptake at 100 uM by BODIPY-based FACS analysis
Agonist activity at PPAR-alpha in human HepG2 cells assessed as reduction in SREBP-1c protein expression at 100 uM by immunoblotting
Agonist activity at PPAR-alpha in human HepG2 cells assessed as increase in acyl-coa oxidase protein expression at 10 to 100 uM by immunoblotting
Agonist activity at PPAR-alpha in human HepG2 cells assessed as increase in acyl-coa synthetase protein expression at 10 to 100 uM by immunoblotting
Agonist activity at PPAR-alpha in human HepG2 cells assessed as [14C]palmitate oxidation at 100 uM by BODIPY-based FACS analysis
Agonist activity at PPAR-alpha in human HepG2 cells assessed as fatty acid uptake at 100 uM by BODIPY-based FACS analysis
Agonist activity at PPAR-alpha in human HepG2 cells harboring PPAR-alpha siRNA assessed as increase in FATP4 protein expression at 100 uM after 24 hrs by immunoblotting
Agonist activity at PPAR-alpha in human HepG2 cells assessed as increase in FATP4 protein expression at 10 to 100 uM by immunoblotting
Agonist activity at PPAR-alpha in human HepG2 cells assessed as fatty acid uptake by BODIPY-based FACS analysis
Agonist activity at PPAR-alpha in human HepG2 cells harboring PPAR-alpha siRNA assessed as increase in CPT1 protein expression at 100 uM after 24 hrs by immunoblotting
Agonist activity at PPAR-alpha in human HepG2 cells assessed as increase in CPT1 protein expression at 10 to 100 uM by immunoblotting
Agonist activity at PPAR-alpha in human HepG2 cells harboring PPAR-alpha siRNA assessed as [14C]palmitate oxidation at 100 uM by BODIPY-based FACS analysis
Agonist activity at PPAR-alpha in human HepG2 cells harboring PPAR-alpha siRNA assessed as fatty acid uptake at 100 uM by BODIPY-based FACS analysis
Agonist activity at PPAR-alpha in human HepG2 cells assessed as reduction in SREBP-1c protein expression at 100 uM by immunoblotting

Agonist activity at PPAR-alpha in human HepG2 cells assessed as increase in acyl-coA oxidase protein expression at 10 to 100 uM by immunoblotting
Agonist activity at PPAR-alpha in human HepG2 cells assessed as increase in acyl-coA synthetase protein expression at 10 to 100 uM by immunoblotting
Agonist activity at PPAR-alpha in human HepG2 cells assessed as [14C]palmitate oxidation at 100 uM by BODIPY-based FACS analysis
Agonist activity at PPAR-alpha in human HepG2 cells assessed as fatty acid uptake at 100 uM by BODIPY-based FACS analysis
Agonist activity at PPAR-alpha in human HepG2 cells harboring PPAR-alpha siRNA assessed as increase in FATP4 protein expression at 100 uM after 24 hrs by immunoblotting
Agonist activity at PPAR-alpha in human HepG2 cells assessed as increase in FATP4 protein expression at 10 to 100 uM by immunoblotting
Agonist activity at PPAR-alpha in human HepG2 cells assessed as fatty acid uptake by BODIPY-based FACS analysis
Agonist activity at PPAR-alpha in human HepG2 cells harboring PPAR-alpha siRNA assessed as increase in CPT1 protein expression at 100 uM after 24 hrs by immunoblotting
Agonist activity at PPAR-alpha in human HepG2 cells assessed as increase in CPT1 protein expression at 10 to 100 uM by immunoblotting
Agonist activity at human PR expressed in human T47D cells assessed as stimulation of alkaline phosphatase
Agonist activity at ERalpha in human MCF7 cells assessed as increase in PR expression at 20 uM incubated for 2 hrs measured after 14 hrs by qPCR analysis relative to E2
Agonist activity at PR in human T47D cells assessed as induction of alkaline phosphatase expression after 24 hrs by plate reader analysis
Agonist activity at ER alpha in human MCF7 cells assessed as PR gene expression after 24 hrs by laser scanning imaging cytometer analysis
Agonist activity at human PXR expressed in human HepG2 cells assessed as induction of MDR1 mRNA expression at 50 uM by quantitative RT-PCR analysis
Agonist activity at PXR expressed in human HepG2 cells assessed as increase in CYP3A4 mRNA level at 10 uM by RT-PCR analysis
Agonist activity at human PXR expressed in human HepG2 cells assessed as induction of SULT2A1 mRNA expression at 50 uM by quantitative RT-PCR analysis
Agonist activity at PXR in human HepG2 cells assessed as induction of CYP3A4 mRNA expression at 10 uM after 18 hrs by RT-PCR analysis
Agonist activity at PXR in human HepG2 cells assessed as induction of MDR1 mRNA expression at 10 uM after 18 hrs by RT-PCR analysis
Agonist activity at PXR in human HepG2 cells assessed as induction of MPR3 mRNA expression at 10 uM after 18 hrs by RT-PCR analysis
Agonist activity at ROR gamma in human CD4+ T cells assessed as IL-17 production at 3 uM by ELISA
Antagonist activity at human pSG5-AR assessed as inhibition of dihydrotestosterone-induced effect by reporter gene assay
Antagonist activity at FXR (unknown origin) by coactivator assay
Antagonist activity at human GST-tagged FXR at 4.44 uM after 20 mins by TR-FRET assay relative to control
Antagonist activity at His6-tagged FXR-LBD (unknown origin) assessed as inhibition of CDCA-induced biotinylated SRC1-2 co-activator recruitment at 50 uM by AlphaScreen assay
Antagonist activity at human Gal4-fused FXR assessed as inhibition of chenodeoxycholic acid-induced luciferase activity at 0.03 to 10 uM by reporter gene assay
Antagonist activity at human GST-tagged FXR at 54.8 nM after 20 mins by TR-FRET assay relative to control

Antagonist activity at human GST-tagged FXR at 1.5 uM after 20 mins by TR-FRET assay relative to control
Antagonist activity at human GST-tagged FXR at 1.48 uM after 20 mins by TR-FRET assay relative to control
Antagonist activity at human GTS-tagged FXR after 20 mins by TR-FRET assay
Antagonist activity at GST-tagged FXR LBD (unknown origin) assessed as inhibition of CDCA-induced Bio-SRC-1 recruitment after 30 mins by HTRF assay
Antagonist activity at human GST-tagged FXR at 10 uM after 20 mins by TR-FRET assay relative to control
Antagonist activity at human GST-tagged FXR at 13.3 uM after 20 mins by TR-FRET assay relative to control
Antagonist activity at human GST-tagged FXR at 40 uM after 20 mins by TR-FRET assay relative to control
Antagonist activity at human GST-tagged FXR after 20 mins by TR-FRET assay
Antagonist activity at human GST-tagged FXR at 493 nM after 20 mins by TR-FRET assay relative to control
Antagonist activity at human GST-tagged FXR at 4.4 uM after 20 mins by TR-FRET assay relative to control
Antagonist activity at human GST-tagged FXR at 164 nM after 20 mins by TR-FRET assay relative to control
Antagonist activity at human GTS-tagged FXR at 15 uM after 20 mins by TR-FRET assay
Antagonist activity at GR (unknown origin) by Gal4-based cellular assay
Antagonist activity at GST-tagged PPAR-alpha (unknown origin) assessed as inhibition of GW7647-induced effect after 2 hrs by TR-FRET assay
Antagonist activity at human PPAR-gamma assessed as inhibition of interaction with DRIP-2 by fluorescence polarisation assay
Antagonist activity at GST-tagged PPAR-alpha (unknown origin) assessed as inhibition of GW7647-induced effect after 2 hrs by TR-FRET assay
Antagonist activity at human PPAR-gamma assessed as inhibition of interaction with DRIP-2 by fluorescence polarisation assay
Antagonist activity at PR (unknown origin) by Gal4-based cellular assay
Antagonist activity at human PXR by transient transfection assay
Antagonist activity at human FXR assessed as ligand dependent binding of cofactor to the receptor-ligand complex by TRF method
Antagonist activity at human AR assessed as inhibition of DHT-induced response
Antagonist activity at LXR in human myotubes assessed as downregulation of SCD1 expression at 10 uM after 4 days by qPCR analysis
Agonist activity at human LXR-beta assessed as increase in recruitment of Trap 220/D22 coactivator peptide by TR-FRET assay
Agonist activity at human LXR by transactivation assay
Agonist activity at human LXR by transactivation assay
Agonist activity at human LXR by transactivation assay relative to standard compound
Agonist activity at human LXR by transactivation assay relative to fenofibric acid
Agonist activity at human LXR-alpha assessed as increase in recruitment of Trap 220/Drip2 coactivator peptide by TR-FRET assay
Agonist activity at human recombinant LXR-LBD by Gal4beta transactivation assay relative to T0901317
Agonist activity at human recombinant LXR-LBD by Gal4beta transactivation assay

Agonist activity at human FXR assessed as recruitment of SRC1 peptide by TR-FRET assay
Agonist activity at GST-tagged human FXR LBD assessed as recruitment of biotinylated SRC-1 peptide after 30 mins by AlphaScreen assay relative to CDCA
Agonist activity at GST-tagged FXR LBD (187 to 472 residues) (unknown origin) assessed as FXR interaction with b-CPSSHSSLTERHKILHRLLQEGSPS-COOH by FRET assay
Agonist activity at human GST-fused FXR LBD assessed as cofactor peptide interaction with receptor ligand binding domain by FRET assay
Agonist activity at human FXR assessed as SRC1 peptide interaction with receptor ligand binding domain by FRET assay
Agonist activity at human Gal4-fused FXR assessed as luciferase activity at 0.03 to 10 uM by reporter gene assay
Agonist activity at FXR (unknown origin) by reporter gene assay
Agonist activity at human FXR ligand binding domain transfected with fused Gal4-DBD by transactivation assay
Agonist activity at FXR (unknown origin) by reporter gene assay
Agonist activity at FXR (unknown origin) assessed as ligand-mediated interaction of the SRC1 peptide with protein LBD by FRET assay relative to GW4064
Agonist activity at FXR (unknown origin) by coactivator recruitment assay
Agonist activity at human GST-tagged FXR after 20 mins by TR-FRET assay
Agonist activity at human FXR LBD assessed as SRC1 peptide recruitment by FRET assay relative to GW 4064
Agonist activity at GST-tagged FXR LBD (187 to 472 residues) (unknown origin) assessed as FXR interaction with b-CPSSHSSLTERHKILHRLLQEGSPS-COOH by FRET assay relative to GW4064
Agonist activity at human GST-fused FXR LBD assessed as cofactor peptide interaction with receptor ligand binding domain by FRET assay relative to GW-4064
Agonist activity at FXR (unknown origin) assessed as recruitment of SRC1 peptide to FXR by FRET assay
Agonist activity at Gal4-fused human FXR by luciferase reporter gene transactivation assay relative to GW4064
Agonist activity at human GST-tagged FXR ligand binding domain assessed as recruitment of Src-1 peptide after 30 mins by AlphaScreen assay relative to 10 uM of CDCA
Agonist activity at human GST-fused FXR LBD assessed as coactivator interaction with receptor ligand binding domain by Alphascreen assay relative to CDCA
Agonist activity at human amino-terminal polyhistidine-tagged FXR alpha LBD (amino acids 237 to 472) assessed as maximum efficacy measuring cofactor peptide SRC-1 interaction with receptor ligand binding domain after 2 hrs by FRET assay relative to GW4064
Agonist activity at human amino-terminal polyhistidine-tagged FXR alpha LBD (amino acids 237 to 472) assessed as cofactor peptide SRC-1 interaction with receptor ligand binding domain after 2 hrs by FRET assay
Agonist activity at human GST-tagged FXR ligand binding domain assessed as recruitment of Src-1 peptide after 30 mins by AlphaScreen assay
Agonist activity at human FXR assessed as SRC1 peptide interaction with receptor ligand binding domain by FRET assay relative to GW-4064
Agonist activity at Gal4-fused human FXR by luciferase reporter gene transactivation assay
Agonist activity at FXR (unknown origin) by coactivator recruitment assay
Agonist activity at human FXR LBD assessed as SRC1 peptide recruitment by FRET assay
Agonist activity at human FXR ligand binding domain assessed as induction of biotinylated SRC1 peptide recruitment at 4 uM by coactivator recruitment assay

Agonist activity at FXR (unknown origin) assessed as ligand-mediated interaction of the SRC1 peptide with protein LBD by FRET assay
Agonist activity at GST-tagged human FXR LBD assessed as recruitment of biotinylated SRC-1 peptide after 30 mins by AlphaScreen assay
Agonist activity at human GST-fused FXR LBD assessed as coactivator interaction with receptor ligand binding domain by Alphascreen assay
Agonist activity at human FXR assessed as SRC1 coactivator peptide recruitment by cell free FRET assay
Agonist activity at human GR by transactivation assay relative to standard compound
Agonist activity at human GR by transactivation assay
Agonist activity at human PPAR gamma by GAL4 transactivation assay
Agonist activity at PPAR-alpha (unknown origin) by luciferase reporter gene assay
Agonist activity at human PPAR delta by GAL4 transactivation assay relative to L-796449
Agonist activity at human PPAR delta by GAL4 transactivation assay
Agonist activity at PPAR-gamma (unknown origin) by luciferase reporter gene assay
Agonist activity at human PPAR alpha by GAL4 transactivation assay relative to WY-14643
Agonist activity for Human PPAR alpha receptor in transcriptional activation assay; IA means inactive at 10 uM
Agonist activity for Human PPAR gamma receptor in transcriptional activation assay
Agonist activity for Human PPAR alpha receptor in transcriptional activation assay;IA means inactive at 10 uM
Agonist activity for Human PPAR delta receptor in transcriptional activation assay
Agonist activity at PPAR-delta (unknown origin) by luciferase reporter gene assay
Agonist activity for Human PPAR alpha receptor in transcriptional activation assay; IA means inactive at 10 uM
Agonist activity against human PPAR-delta by transactivation assay relative to standard compound
Agonist activity at human PPAR gamma by GAL4 transactivation assay relative to rosiglitazone
Agonist activity at human PPAR-delta by transactivation assay
Agonist activity for Human PPAR delta receptor in transcriptional activation assay; IA means inactive at 10 uM
Agonist activity for Human PPAR delta receptor in transcriptional activation assay at 100 uM; IA means inactive
Agonist activity at human PPAR alpha by GAL4 transactivation assay
Agonist activity for Human PPAR alpha receptor in transcriptional activation assay
Agonist activity at PPAR-delta (unknown origin) by transactivation assay
Agonist response against human PPAR gamma in transactivation assay
Agonist activity at human PPAR alpha by FRET assay
Agonist activity for Human PPAR gamma receptor in transcriptional activation assay
Agonist activity at PPARgamma ligand binding domain (unknown origin) using fluormone Pan-PPAR green tracer by TR-FRET assay based competitive ligand binding method
Agonist activity for Human PPAR delta receptor in transcriptional activation assay;IA means inactive at 10 uM
Agonist response against human PPAR alpha in transactivation assay
Agonist activity for Human PPAR delta receptor in transcriptional activation assay; IA means inactive at 10 uM

Agonist activity at PPAR-alpha (unknown origin) by transactivation assay
Agonist activity at human PPAR delta by FRET assay
Agonist activity at human PPAR gamma by GAL4 transactivation assay
Agonist activity at PPAR-alpha (unknown origin) by luciferase reporter gene assay
Agonist activity at human PPAR delta by GAL4 transactivation assay relative to L-796449
Agonist activity at human PPAR delta by GAL4 transactivation assay
Agonist activity at PPAR-gamma (unknown origin) by luciferase reporter gene assay
Agonist activity at human PPAR alpha by GAL4 transactivation assay relative to WY-14643
Agonist activity for Human PPAR alpha receptor in transcriptional activation assay; IA means inactive at 10 uM
Agonist activity for Human PPAR gamma receptor in transcriptional activation assay
Agonist activity for Human PPAR alpha receptor in transcriptional activation assay;IA means inactive at 10 uM
Agonist activity for Human PPAR delta receptor in transcriptional activation assay
Agonist activity at PPAR-delta (unknown origin) by luciferase reporter gene assay
Agonist activity for Human PPAR alpha receptor in transcriptional activation assay; IA means inactive at 10 uM
Agonist activity against human PPAR-delta by transactivation assay relative to standard compound
Agonist activity at human PPAR gamma by GAL4 transactivation assay relative to rosiglitazone
Agonist activity at human PPAR-delta by transactivation assay
Agonist activity for Human PPAR delta receptor in transcriptional activation assay; IA means inactive at 10 uM
Agonist activity for Human PPAR delta receptor in transcriptional activation assay at 100 uM; IA means inactive
Agonist activity at human PPAR alpha by GAL4 transactivation assay
Agonist activity for Human PPAR alpha receptor in transcriptional activation assay
Agonist activity at PPAR-delta (unknown origin) by transactivation assay
Agonist response against human PPAR gamma in transactivation assay
Agonist activity at human PPAR alpha by FRET assay
Agonist activity for Human PPAR gamma receptor in transcriptional activation assay
Agonist activity at PPARgamma ligand binding domain (unknown origin) using fluormone Pan-PPAR green tracer by TR-FRET assay based competitive ligand binding method
Agonist activity for Human PPAR delta receptor in transcriptional activation assay;IA means inactive at 10 uM
Agonist response against human PPAR alpha in transactivation assay
Agonist activity for Human PPAR delta receptor in transcriptional activation assay; IA means inactive at 10 uM
Agonist activity at PPAR-alpha (unknown origin) by transactivation assay
Agonist activity at human PPAR delta by FRET assay
Agonist activity at PR (unknown origin) by luciferase reporter gene assay
Agonist activity at human PXR at
Agonist activity at recombinant human PXR at 3.16 uM by co-factor recruitment assay relative to control

| |
|---|
| Agonist activity at human PXR up to 50 uM by transactivation assay |
| Agonist activity at GST-tagged human FXR assessed as binding of receptor to cofactor by TRF method |
| Agonist activity at human alpha2C AR assessed as intrinsic activity |
| Agonist activity at human alpha2B AR assessed as intrinsic activity |
| Agonist activity at LXR in human myotubes assessed as upregulation of SCD1 expression at 1 uM after 4 days by qPCR analysis |
| Agonist activity at LXR in human myotubes assessed as upregulation of SCD1 expression at 10 uM after 4 days by qPCR analysis |
| Agonist activity at LXR-beta in human whole blood assessed as ABCG1 gene induction by measuring ABCA1 mRNA level after 4 hrs by SYBR-Green dye-based Q-PCR analysis relative to pan agonist 2-(4-(5-(5-cyano-1-(2,4-difluorobenzyl)-6-oxo-4-(trifluoromethyl)-1,6-dihydropyridin-2-yl)thiophen-2-yl)-3-methylphenyl)acetic acid |
| Agonist activity at LXR-beta in human whole blood assessed as ABCG1 gene induction by measuring ABCA1 mRNA level after 4 hrs by SYBR-Green dye-based Q-PCR analysis |
| Agonist activity at LXR-beta in human whole blood assessed as ABCA1 gene induction by measuring ABCA1 mRNA level after 4 hrs by SYBR-Green dye-based Q-PCR analysis relative to pan agonist 2-(4-(5-(5-cyano-1-(2,4-difluorobenzyl)-6-oxo-4-(trifluoromethyl)-1,6-dihydropyridin-2-yl)thiophen-2-yl)-3-methylphenyl)acetic acid |
| Agonist activity at LXR-beta in human whole blood assessed as ABCA1 gene induction by measuring ABCA1 mRNA level after 4 hrs by SYBR-Green dye-based Q-PCR analysis |
| Agonist activity at recombinant His-tagged human FXR ligand binding domain assessed as SRC-1 coactivator recruitment after 4 hrs by luminescence analysis relative to GW4064 |
| Agonist activity at recombinant His-tagged human FXR ligand binding domain assessed as SRC-1 coactivator recruitment after 4 hrs by luminescence analysis |
| Agonist activity at human GR assessed as dissociation half life |
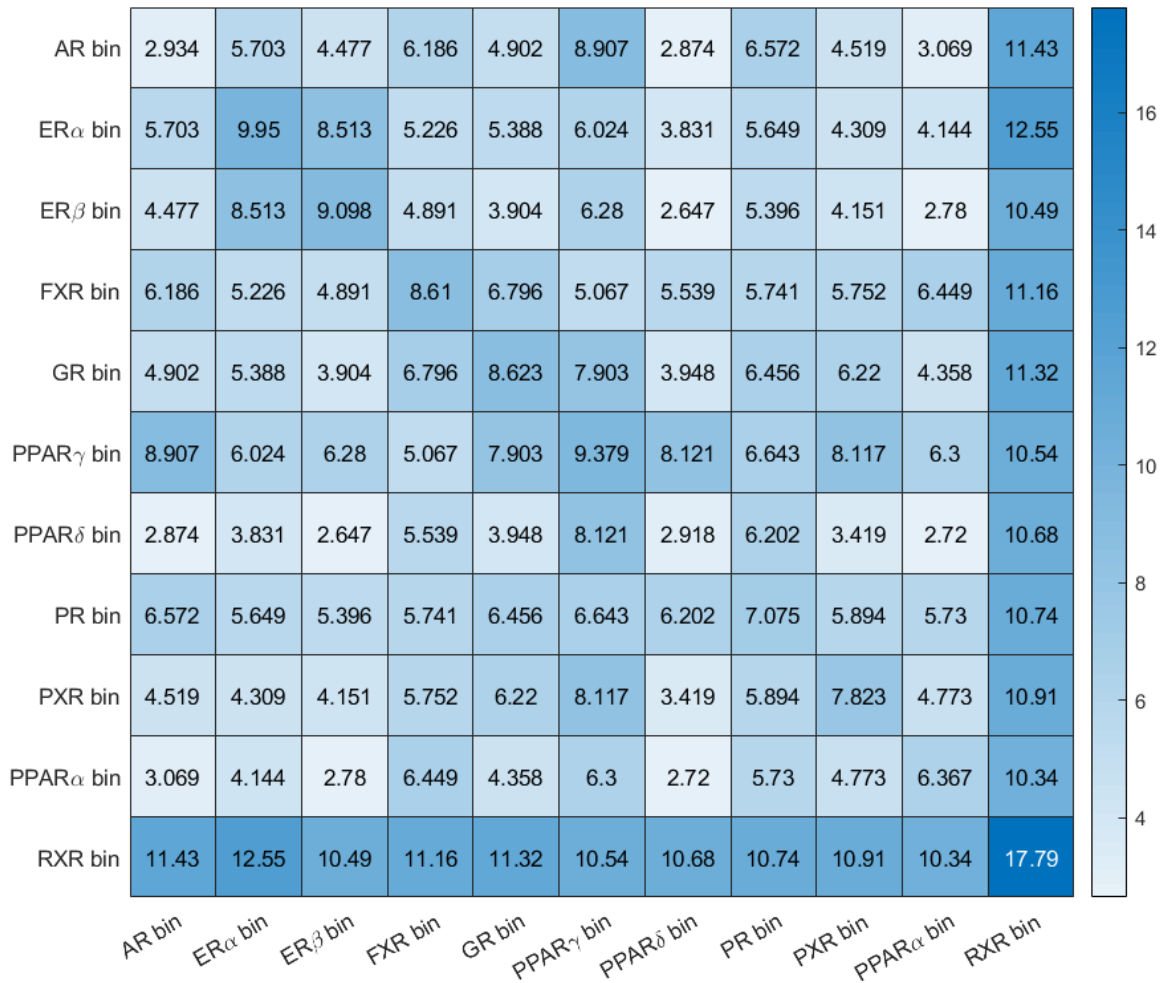
Figure S1. Heatmap of the standard deviation of the PMscores for each pair of targets, the darker the blue the higher the PMscore.
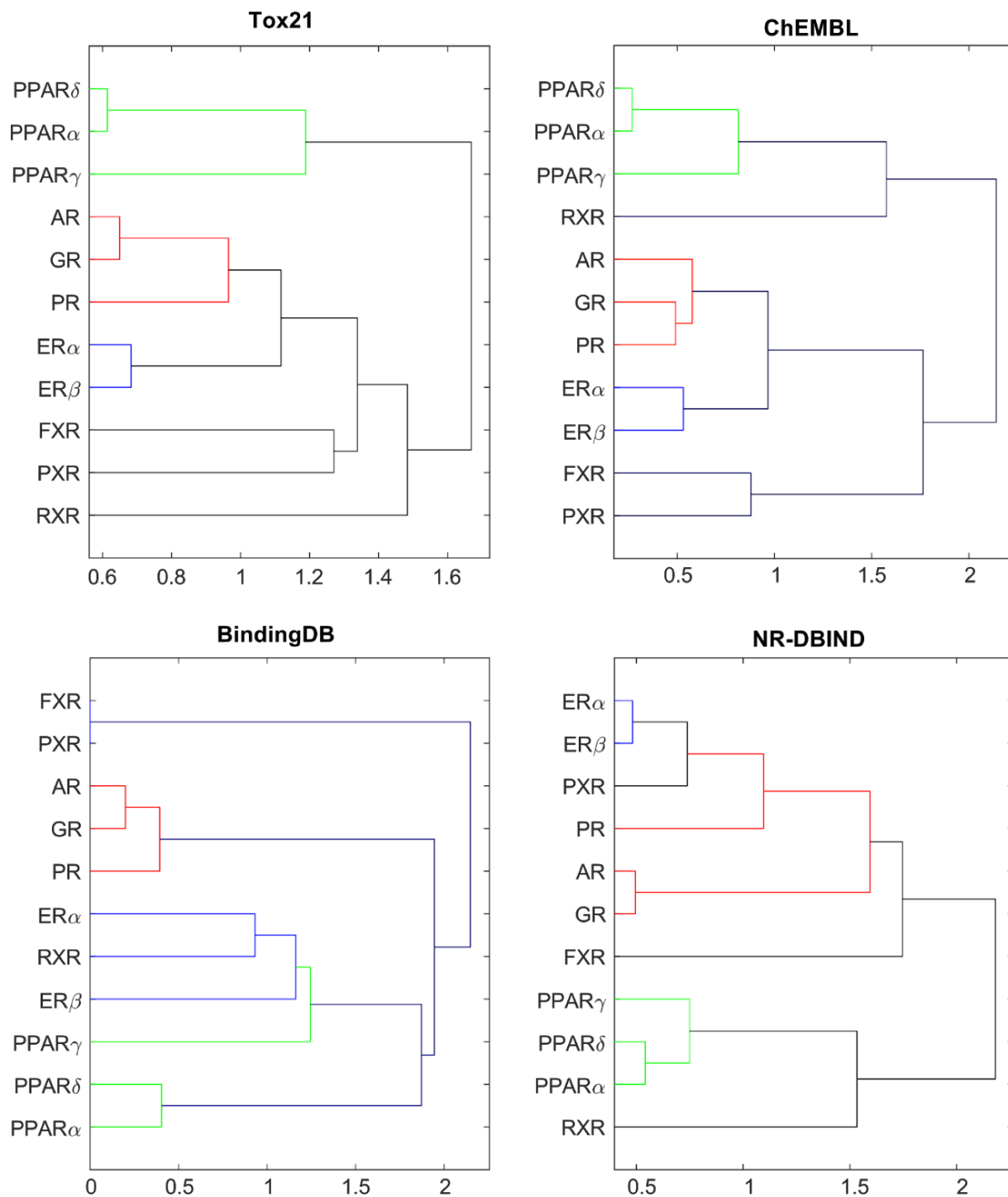
Figure S2. Ligand-based similarity between the analyzed nuclear receptors, depicted as dendrograms, on: (A) Tox21, (B) ChEMBL, (C) BindingDB and (D) NR-DBIND data.